This article was downloaded by:
On: *17 January 2011*
Access details: *Access Details: Free Access*
Publisher *Taylor & Francis*
Informa Ltd Registered in England and Wales Registered Number: 1072954 Registered office: Mortimer House, 37-41 Mortimer Street, London W1T 3JH, UK

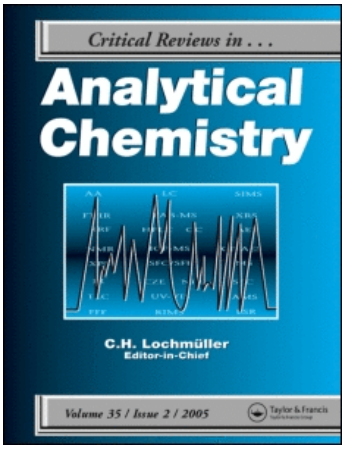

Critical Reviews in Analytical Chemistry
Publication details, including instructions for authors and subscription information:
http://www.informaworld.com/smpp/title~content=t713400837

Nuclear Magnetic Resonance of Biological Samples

Philip W. Kuchel; I. D. Campbell

To cite this Article Kuchel, Philip W. and Campbell, I. D.(1981) 'Nuclear Magnetic Resonance of Biological Samples', Critical Reviews in Analytical Chemistry, 12: 3, 155 — 231
To link to this Article: DOI: 10.1080/10408348108542746
URL: http://dx.doi.org/10.1080/10408348108542746

PLEASE SCROLL DOWN FOR ARTICLE

Full terms and conditions of use: http://www.informaworld.com/terms-and-conditions-of-access.pdf

This article may be used for research, teaching and private study purposes. Any substantial or systematic reproduction, re-distribution, re-selling, loan or sub-licensing, systematic supply or distribution in any form to anyone is expressly forbidden.

The publisher does not give any warranty express or implied or make any representation that the contents will be complete or accurate or up to date. The accuracy of any instructions, formulae and drug doses should be independently verified with primary sources. The publisher shall not be liable for any loss, actions, claims, proceedings, demand or costs or damages whatsoever or howsoever caused arising directly or indirectly in connection with or arising out of the use of this material.

NUCLEAR MAGNETIC RESONANCE OF BIOLOGICAL SAMPLES

Author: **Philip W. Kuchel**
Department of Biochemistry
University of Sydney
New South Wales, Australia

Referee: I. D. Campbell
Department of Biochemistry
University of Oxford
Oxford, England

TABLE OF CONTENTS

Downloaded At: 15:58 17 January 2011

Downloaded At: 15:58 17 January 2011

I. INTRODUCTION

A. Preamble

Nuclear magnetic resonance (NMR) spectroscopy is the only physical technique currently available that can potentially measure the concentration of free metabolites deep inside structurally and functionally intact biological samples. Consequently, the explosion in its application to the study of chemical events in, and structural properties of, many differing microorganisms and tissues is not surprising. The use of NMR for the study of biological systems has only really developed over the past 10 of the 35 years since the experimental demonstration of the NMR phenomenon.[1,2]

Because of the high water content ($\approx$55 mol ℓ^{-1}) in most biological samples the NMR signal from the water is readily detected. Therefore it was not unexpected that the first NMR studies of various tissues using the low resolution instruments of the time were directed at gaining insight into the properties of "biological" water.[3] Only recently, with the advent of high resolution spectrometers, has the technique been applied to the study of the chemical species, of low concentration, involved in cellular metabolism; this began with the ^{31}P NMR studies of whole human erythrocytes.[4]

The technological developments that have led to the present high resolution spectrometers are the advances in computers (both hardware and software), in high radio frequency electronics and microcircuitry,[5] and in high field super conducting magnets.

Downloaded At: 15:58 17 January 2011

B. Scope of the Review

This review surveys the literature pertaining to those investigations where NMR has been applied to large scale (in terms of complexity) chemically heterogeneous biological samples; it therefore does not discuss those studies on isolated purified proteins and isolated biological compounds such as plant natural products. Models of biological structures such as synthetic membranes and vesicles are discussed only where the methods used have possible applications to whole cells or organelles. The presentation contains an analysis of NMR studies of whole organs, intact tissue fragments, mammalian cell suspensions, and more primitive (phylogenetically) cells like yeast and bacteria. Also included in the review are discussions of work on subcellular organelles such as mitochondria and secretory vesicles.

NMR theory that has been used for the analysis of the data from experiments on biological systems is generally only outlined and not developed *in extenso*. The reader will be directed to various appropriate references.

Although protons are the predominant nuclear species in biology, the spectra from ^{1}H NMR studies of biological samples are correspondingly complex and often difficult to interpret. So, apart from studies on water, the majority of biological NMR work has used the less preponderant ^{31}P nuclide. Other nuclides studied frequently include ^{1}H and ^{13}C, but all nuclides that have been used in biological experiments are discussed.

Among the many reviews of biological NMR that have appeared recently, some have significant bearing on what is written here. They include one on cellular metabolism in general,[6] ^{31}P NMR studies in biology,[7] the structure of biological water,[8] and another devoted to experimental techniques in biological NMR.[9]

Before proceeding with a discussion of NMR, it is worth considering other physical techniques that yield useful information on cell structure and function; by so doing the relative contributions of NMR techniques to knowledge in biology should be more readily assessed.

C. Continuous Monitoring in Biological Chemistry

The dynamics of molecules in membranes, or metabolites in whole cell systems, can be

investigated by several physical techniques. The most common methods make use of radioactive tracer compounds or spectroscopy. Since biological samples are often in short supply, it is convenient to use methods in which one sample is monitored continuously; radiotracer methods generally involve discrete sampling. Most spectroscopic methods, including NMR, allow continuous monitoring of specific chemical changes in small samples of material.

The various branches of spectroscopy rely on the interaction of electromagnetic radiation with matter. The electromagnetic radiation (propagating, oscillating, electrical, and magnetic fields) interacts in an elastic (retransmitted at essentially the same frequency) or inelastic (retransmitted after a variable time interval at a different frequency) manner. Inelastic electrical field interactions of light and matter are measured in UV-, visible-, and IR-absorption and UV-, visible-, fluorescence-Raman, and UV-circular dichroism spectroscopies.

Circular dichroism has been used in the study of membrane preparations from erythrocytes and Ehrlich ascites tumor cells, but little specific information was forthcoming because of the relatively featureless spectrae, the result of many contributions to the spectrum from the heterogeneous mixture of proteins constituting the samples.[10,11]

The fluorescence of subsurface pyridine nucleotides and flavines has been measured in the following whole tissues: lung,[12] heart,[13,14] kidney,[15] and liver.[16] Anoxia was shown to cause a depression in pyridine nucleotide and an increase in flavoprotein-fluorescence indicating, to the authors, an alteration in the redox state of the cells. Studies of this type are severely limited to a few naturally fluorescent molecules and, of course, do not yield information on conditions deeper within the structure. Destructive sampling techniques, employing fluorescence spectroscopy after freezing tissue in liquid nitrogen and then sectioning, have also been used.[13] It is worthwhile noting, however, that the pyridine nucleotides are difficult to measure in whole tissue by any other method including NMR, because of their low concentrations.

Downloaded At: 15:58 17 January 2011

Raman spectroscopy relies on retransmission of photons from the light-matter interaction. The emitted photons have a frequency which is independent of the excitation frequencies, and can yield information on energy transmutations characteristic of molecular vibrations and rotations.[17] Energy transduction in bacterial purple membranes and vertebrate retinal rods has been studied by Lewis's group.[18-20] The chromophore retinal in the membrane is linked via a Schiff base to a lysine of the protein opsin. The Raman spectra indicate that the chromophore cycles between two energy states resulting in a transport of protons across the bacterial membrane.[19] The retinal pigment in live albino rabbits was also studied by laser Raman spectroscopy.[20] The Raman spectra were correlated with electroretinogram signals and the author has interpreted the results as indicating a protonation-deprotonation of the Schiff base of retinal occurring during visual transduction.[20]

The fluorescence of 1-aniline-8-naphthalene sulfonate (ANS) bound to membranes is sensitive to the polarity and fluidity of membrane-aqueous interfaces. IR absorption spectra are sensitive to hydrogen bonding and vibrational motion of water, membrane, protein, and lipids. Combined, these two techniques provided evidence of increasing rigidity and/or reduced polarity of the membrane-aqueous interface on removal of water. In one study, the IR spectra showed prominent hydration-dependent changes in what is possibly cholesterol (vinyl CH bend, OH stretch), proteins (amide A, II, V), and bound water (OH stretch).[21] However, little further work has been done using these techniques.

The applicability of UV and visible absorption spectroscopy is severely limited in studies of cells or membrane suspensions, due to elastic light scattering of incident radiation, that is, scattering of photons at nontransition (absorption) frequencies. The

physical explanation of this scattering phenomenon was considered by Rayleigh[22] in 1871. He described a classical model of oscillating dipoles (the electrons of a molecule) interacting with the electrical field component of light. The formulations show that the intensity of a light beam emerging from a solution of molecules whose radii are less than the wavelength of the incident beam varies inversely as the fourth power of the wavelength:

$$\frac{i_s}{I_o} = \frac{16\,\pi^4\,\alpha^2\,\sin^2\theta}{\lambda^4\,r^2} \qquad (1)$$

where i_s is the emergent beam intensity, I_o the original intensity, θ the angle of the emergent beam with respect to the axis of entry, λ the wavelength of light, r the distance from the sample to the detector, and α the polarizability of the particles. The polarizability is the proportionality constant that relates the magnitude of the electronic dipole moment, p, to the electrical field strength ϵ:[23,24]

$$p = \alpha\epsilon \qquad (2)$$

The polarizability in Rayleigh's simple model is frequency dependent and given by:[24]

$$\alpha = \frac{e^2}{m4\pi^2\,(\nu_o^2 - \nu^2)} \qquad (3)$$

where ν_o is the absorption frequency of the system, ν the radiation frequency, m the electron mass, and e the electronic charge.

Several studies have been performed using laser-light scattering, and formulation based on Equation 1, in order to measure particle motion inside whole biological systems. Doppler shifts in light scattered from particles in cytoplasmic streams in the fresh-water alga *Nitella flexilis* gave a uniform velocity profile for the particle streams.[25] Other scattering methods using neutrons and X-rays give rise to useful diffraction patterns from some biological structures. Both synthetic and natural membranes have been studied using X-ray diffraction; one example was from frog retinal membrane which gave a diffraction peak intensity indicative of chemical group spacings of 0.42 nm. The scattered peak intensity shifted to a spacing of 0.46 nm and a broadening of the distribution, on raising the temperature from 4.5°C to 42.5°C,[26] indicating that the hydrocarbon chains lose their rigidity at higher temperatures. Again, for obvious reasons such studies are virtually impossible to perform on whole cells.

Elastic scattering of light by matter yields information on particle size (molecular weight) and the organization and spacing of molecules in the matter. However, it is the inelastic (absorption) spectroscopies that yield information on energy transitions that are characteristic of molecular structure and environment.

The phenomena discussed so far have all involved electronic interactions with electromagnetic radiation. One further electronic phenomenon worth noting here is electron spin resonance (ESR). This technique has been of great value in the study of biological membranes, especially in relation to the mobility of the lipid components. Indeed, the application of this method to biological systems has been well discussed elsewhere.[27]

In common with ESR, NMR is a phenomenon in which energy transitions occur in states imposed upon the system by an external magnetic field. NMR like ESR also relies on the absorption of electromagnetic radiation, but it is of longer wavelength — in the radiofrequency domain (usually 25 to 600 MHz).

Equation 3 demonstrates that electronic polarizability is virtually independent of ν

Downloaded At: 15:58 17 January 2011

when it lies in the radiofrequency domain. This situation occurs because ν_o, the absorption frequency for electronic transitions, usually lies in the visible and UV regions of the spectrum. In other words, radiofrequency radiation fails to polarize the electronic configuration of atoms. The nucleus also is a relatively rigid structure (in classical-mechanical terms) and therefore is scarcely polarized by interactions with electrostatic fields. Therefore Equation 1 shows that since λ is relatively large in NMR studies the degree of elastic scattering by the sample is minute. Therefore a suspension of cells, which may be opaque due to the inelastic scattering of radiation in the UV and visible parts of the spectrum, will not be so to off-resonance radiofrequency radiation. For this reason alone NMR has great potential for application to intact biological samples. However, this happy situation is marred to a certain extent by the inherent insensitivity of the NMR technique.

Like other spectroscopic methods, NMR is used for the detection and identification of chemical compounds. Furthermore, the technique can be enhanced to yield information on the spatial distribution of nuclear spins in a sample. This has lead to recent developments in the use of NMR for one-, two-, and three-dimensional imaging.[28]

In summary, NMR like other forms of spectroscopy is noninvasive and can yield information on chemical structure and mobility inside undisrupted cell suspensions and organs.

Since a major aim of cell physiologists is an understanding of the *modus operandi* of whole integrated cells and organs, NMR is uniquely placed to furnish much new insight for a description of cell function in terms of well-defined physical properties of matter such as viscosity and diffusion coefficients, chemical reaction rate constants, and concentrations or activities.

Downloaded At: 15:58 17 January 2011

II. THEORY OF NMR RELEVANT TO THE STUDY OF CELLS

A. Basic Concepts

Abragam's book[29] is the ultimate authority on many aspects of NMR theory; other texts which are more accessible to the less mathematically tutored are also available.[30,31] Monographs focusing on biological applications of NMR have been written,[32-34] together with some others on specific aspects, such as the nuclear Overhauser effect[35] which has important applications in biology. Nevertheless, for the sake of clarity, some basic NMR theory pertinent to biological studies will be outlined.

We begin with the assertion that certain classes of chemical nuclei possess nonzero spin. This led Pauli in 1924 to describe the existence of a magnetic moment, μ, in spinning nuclei.[35] The nuclei which carry a net positive charge behave like current loops, which, according to a classical electromagnetic description, generate the dipolar field. Application of a uniform external magnetic field to an ensemble of spins causes them to not simply align with the field, but precess at a characteristic frequency. The precession is like that of a gyroscope; an increase in the magnetic field strength increases the torque applied to the nuclei. However, the torque does not incur a change in the tilt angle but instead leads to an increase in the frequency of precession. This phenomenon is summarized in the Larmor equation:[29]

$$\omega = B_o\gamma \qquad (4)$$

where ω is the precessional (Larmor) frequency (rad sec^{-1}), B_o the magnetic field strength (Tesla; 10^4 $ampere^{-1}$ $meter^{-1}$), and γ the magnetogyric ratio of the nuclei; this is the ratio of the magnetic and gyroscopic moments and has a specific value for the nucleus of a given element.

Table 1
PROPERTIES OF SOME MAGNETIC NUCLEI USED IN BIOLOGICAL NMR[9,33,71]

Nucleus	Spin quantum number (I)	Electric quadruple moment (Q) ($\times e \times 10^{-24}$ cm^2)	Natural abundance (%)	Approximate "biological" shift domain (ppm)	Relative sensitivity for equal number of nuclei at constant field	Magnetogyric ratio[a] (λ) ($\times 10^{-7}$ radians Tesla^{-1} sec^{-1})
^{1}H	1/2	—	99.9844	15	1.000	26.75
^{2}H	1	2.77×10^{-3}	1.56×10^{-2}	15	9.65×10^{-3}	4.1064
^{3}H	1/2	—	$<10^{-16}$	—	1.21	28.5336
^{7}Li	3/2	−0.1	92.57	—	0.294	10.40
^{13}C	1/2	—	1.108	200	1.59×10^{-2}	6.7263
^{14}N	1	7.1×10^{-2}	99.634	—	1.01×10^{-3}	1.9324
^{15}N	1/2	—	0.365	400	1.04×10^{-3}	−2.7107
^{17}O	5/2	-4×10^{-3}	3.7×10^{-2}	—	2.91×10^{-2}	−3.6266
^{19}F	1/2	—	100	—	0.833	25.17
^{23}Na	3/2	0.1	100	—	9.25×10^{-2}	7.08
^{31}P	1/2	—	100	30	6.63×10^{-2}	10.8290
^{35}Cl	3/2	-7.9×10^{-2}	75.4	—	4.70×10^{-3}	2.62
^{39}K	3/2	0.07	93.08	—	5.08×10^{-4}	1.25

[a] $B_o = 2\pi \times \nu/\gamma$, where B_o is the external field and ν the Larmor frequency.

Downloaded At: 15:58 17 January 2011

If an electromagnetic field oscillating at the precessional frequency is applied orthogonal to the external field, then nuclear resonance will occur, i.e., absorption of energy. The energy states are quantized and the number of these is given by the relationship $2I + 1$, where I is the fundamental spin quantum number and an immutable property of a given type of nucleus (see Table 1). The different (quantized) energy levels available to a nuclear spin are given by the relationship:

$$\Delta E = -\mu B_o \qquad (5)$$

where μ ($= m_I \gamma \hbar$) is the component of the nuclear magnetic moment parallel to the uniform field B_o and $\hbar$ is Planck's constant/2π:

$$m_I = I, (I-1), (I-2), \ldots, -(I-2), -(I-1), -I.$$

Therefore, protons which have a spin quantum number of ½ have only two spin-energy states and behave as spherical bodies with a uniform charge distribution. The charge distribution in nuclei with $I \geqslant 1$ must be described in a more complex manner such as on prolate or oblate ellipsoids; an index of the departure from sphericity is the electric quadrupole moment (Q) which of course is a function of I. Hence, with nonspherical nuclei the field experienced by an approaching charge will depend on the relative direction of approach to the nucleus. For example, the ^{2}H nucleus ($I = 1$) has a significant quadrupole moment (Table 1) which greatly affects the rate and mode of transfer of its spin energy to adjacent nuclei. So unlike ^{1}H NMR, ^{2}H NMR studies can yield information on orientation of, for example, perdeuterated hydrocarbon lipid chains in biomembranes. The energy levels between the quantized spin states are given by Equation 5, and this taken together with the Bohr equation ($E = h\nu$) enables the determination of the irradiation frequency necessary to invoke a transition between the states. These spin states are distributed according to Boltzmann's law which for an $I = ½$ nuclear system has the following specification:

$$\frac{N_{upper}}{N_{lower}} = \exp - (h\nu/kT) \quad (6)$$

where N_{upper} and N_{lower} are the population numbers of upper and lower energy states, respectively, and k is Boltzmann's constant. For ^1H nuclei with the ω ($\omega = 2\pi\nu$) values typical of modern NMR spectrometers with thermal equilibrium at room temperature, there is a *preponderance* of only about 15 low energy spins per total of a million. Since net absorption of radiation depends on a preponderance of low energy spins, it is readily seen why NMR is very insensitive compared with other branches of spectroscopy.

Another important feature of NMR spectroscopy arises because of the different electronic environments of nuclei in different types of molecules; an effect known as shielding. The result of the slight differences between *local* magnetic fields is differences in resonance frequencies (ω_o), depending on intramolecular environment. The frequencies are usually compared with a standard reference compound and the difference normalized with respect to the operating frequency of the spectrometer to yield an expression called the chemical shift (δ; expressed in parts per million):

$$\delta = 10^6 \times (\nu_{ref} - \nu_1)/\nu_o \quad (7)$$

where ν_1 is the resonance frequency of the nuclei in question, ν_{ref} that of the reference compound, and ν_o the operating frequency of the spectrometer. An example from biology is the [2-H] protons of the histidyl residues of hemoglobin; all 12 are presumably in slightly different intramolecular environments and these have chemical shifts that span a range of $\approx$1 ppm in whole erythrocytes. Typical ranges of δ for the various nuclei are given in Table 1; note in particular the small range for ^1H compared with those of ^{13}C and ^{31}P.

In addition to the effects of its orbiting electrons on the magnetic field experienced by a nucleus in a given molecule, there are effects on the field produced by other adjacent nuclei in the molecule. The interaction between the two nuclear spins is called *spin-spin coupling* and results in multiplet structure of an otherwise single resonance in the spectrum. The spin of the valence electron associated with a nucleus interacts electromagnetically with it so that when two atoms are involved mutually in a chemical bond the valence electron of the other atom interacts with the nucleus in question (and vice versa). Therefore there is an interaction path between the two nuclei involved in the bond via the valence electrons, which by the Pauli exclusion principle must have opposite spins. Therefore any change in the spin state of one nucleus will alter the spin energy of the adjacent nucleus giving rise (in the case of spin ½ nuclei) to a symmetrical splitting of the resonance of that nucleus. The separation between the two lines is called the *coupling constant* (J) and is expressed as a positive number of Hz. An important property of this splitting is that it, unlike the chemical shift, is independent of the external magnetic field.

The value of J between two nuclei generally depends on (1) the nature of the bonds between them, (2) the relative geometries of the bonds, and (3) whether or not the nuclei are directly bonded and the effect tends to decrease nonuniformly as the number of intervening bonds increases. In general, for a nucleus coupled to any equivalent spin ½ nuclei, there will be (n + 1) lines of relative intensity given by the binomial coefficients, e.g., 1:2:1 for a triplet, 1:3:3:1 for a quartet, etc. Spectra in which $J \ll \delta$ are called first order spectra, but clearly complications arise in the analysis of spectra when J becomes large compared with chemical shift differences between coupled nuclei. It should, however, be clear that it is at least theoretically possible to produce first order spectra by increasing the field strength.

The effects of spin-spin coupling on spectra will not be further elaborated here and reference to standard texts is recommended for further details. However, it is essential for

Downloaded At: 15:58 17 January 2011

the interpretation of spin-echo spectra (Section IV.C in particular) that the concept of spin-spin coupling be recalled.

Two other *through-space* or secondary effects which influence the local magnetic field at a nucleus are important. The first arises from a field perturbation due to a nearby aromatic ring, an effect known as *ring current shifts,* and this is due to the delocalized π orbital electrons which circulate in aromatic rings and give rise to a dipole that opposes the applied field. The second effect is due to paramagnetic ions which also perturb, via a relatively long range effect, the local field at a nucleus. The physical basis of these effects will not be discussed here but the topic has been admirably considered by, among others, Dwek.[32]

B. Relaxation Processes

Relaxation is the phenomenon which occurs when energetically excited states pass on their energy to other components of the system. In other branches of spectroscopy spontaneous emission is a common means of relaxation, but this is not the case with NMR. This is because the probability of such an event is proportional to the energy level differences in the transition and these are minute in the case of nuclear spins. Likewise, spin relaxation by molecular collision is unlikely because of the mechanical-type shielding afforded by electron clouds.

Downloaded At: 15:58 17 January 2011

For spin-half nuclei such as ^{1}H, ^{31}P, and ^{13}C the only relaxation mechanisms are magnetic in nature and are due to inductive coupling with fields which fluctuate at the Larmor frequency (see Equation 4) of the nuclei in the surrounding environment (frequently known as the lattice). These fields are dipolar; thus a given nucleus may experience the field of another moving past it. The local field B_μ set up by such a nucleus can be described by the simple dipole model:[33]

$$B_\mu = \pm \mu\,(3\,\mathrm{Cos}^2\theta - 1)/r^3 \qquad (8)$$

where μ is the dipole moment, θ the angle, and r the distance from the center of the dipole axis to the point of measurement. Random molecular motion will produce temporal changes in r and θ that can lead to periodic fluctuations in the field B_μ with a frequency equal to the Larmor frequency of an adjacent nucleus, a process known as modulation.

The rate constant assigned to this process of dipolar fluctuation is the reciprocal of τ_c, the correlation time; τ_c which is clearly an index of molecular mobility will be discussed later at greater length in Section III.A.

Another relaxation process is that invoked by chemical exchange, where an atom detaches from a binding molecule and the replacement atom possesses a nuclear spin which is the reverse of that of the previous occupant. This leads to a reversal of the field B_μ (Equation 8). If the field reversal occurs at the Larmor frequency ($1/\tau_{exchange} = \omega_o/2\pi$), relaxation of nuclear spins in the binding molecule may occur.[36] It should be noted that this is a special case of the frequently encountered phenomenon of chemical exchange. The latter involves the exchange of spins between two or more electrical and magnetic environments in which the spin-relaxation characteristics are different. This topic is discussed further in Sections II and III.

One other obvious contributor to local dipolar-field fluctuation is relative diffusional motion of molecules. Thus, diffusion, random molecular motion and rotation, and chemical exchange all contribute to spin relaxation; many mathematical relationships have been developed in an attempt to relate experimentally determinable parameters to interpretations of molecular events that occur even inside cells.[29-34] The mathematical relationships, definitions such as *relaxation times,* and special techniques will be introduced later where experimental results pertinent to the particular analyses are discussed.

C. Sensitivity

Biological experiments, where the survival times of samples are often short, or the half-life of metabolic processes under study are short, place stringent requirements on the sensitivity of instruments. Accordingly, only since the advent of high-field NMR spectrometers have many studies been possible. Clearly from Equation 6 an increase in the ratio N_{upper}/N_{lower} will increase sensitivity. This can be obtained by reducing temperature and, in addition, is dependent on ν which from Equation 4 is dependent on γ and B. The higher fields increase the spread of chemical shifts and thereby enhance resolution and lead, potentially, to the resolution of fine splittings and the generation of first order spectra from previously more complex ones. The signal to noise ratio (S/N) is clearly dependent on sample volume, but has been improved further by use of signal averaging with pulsed spectrometers employing Fourier transformation; the S/N is proportional to $\sqrt{n}$, where n is the number of transients accumulated. Quadrature detection enhances S/N by a factor of $\sqrt{2}$,[5,37] and the use of solenoid receiver coils coupled with concomitant cooling of the preamplifier to liquid nitrogen temperatures can positively improve signal to noise by a factor of 2.5[9] (the solenoid tends to occupy a greater space so wider bore magnets are more suitable for their use). Low temperature studies, which also involve cooling of the sample, are of course of no value when near-to-life conditions are required.

Additional signal-to-noise enhancement can be achieved by exploiting the nuclear Overhauser effect (nOe). This phenomenon is observed as the change in the integrated intensity of an NMR resonance line obtained from a nuclear spin system when the absorption of another adjacent spin system is saturated[34] (i.e., irradiated continuously at its Larmor frequency, thus preventing depopulation of the high-energy spin state). The other spin can be hetero- or homonuclear. In ^{13}C and ^{31}P studies the process results in a situation where dipole-dipole interactions of ^{1}H spins with the heteronuclear spin normally cause splitting (i.e., two adjacent resonance lines in the spectrum arising from one nuclear environment) of the latter spins.

Broad-band proton irradiation gives rise to heteronuclear decoupling with removal of the line multiplicity that arises from the coupling. In addition, S/N enhancement is obtained which is proportional to the following expression:

$$nOe = \gamma_s/2\gamma_I \qquad (9)$$

where γ_s is the magnetogyric ratio of the observed nuclei and γ_I that of the irradiated nuclei.[34] Quite apart from its practical utility in enhancing S/N in ^{13}C and ^{31}P NMR spectroscopy, the nOe can be studied in whole cell systems and the results interpreted in terms of molecular mobility inside the cells (Section VIII.B).

In relation to the previous comment about improving resolution by the use of higher magnetic fields, it is worth noting that a complicating factor in these attempts is the phenomenon known as chemical shift anisotropy (CSA). In this situation the chemical shift of a nucleus varies with the direction of the applied field, so that molecular motion produces a field which can fluctuate at the resonance frequency of the nuclear spin. This can give rise to relaxation of that spin. The effect increases in proportion to the square of the applied field.[33] CSA is prominent in ^{19}F,[32] and to a lesser extent ^{31}P nuclear relaxation. However, to date the effect has had little bearing on studies of whole cell systems.

III. DIFFUSION STUDIES

A. Introduction

The motions of small molecules inside cells are of special interest in mathematical

Downloaded At: 15:58 17 January 2011

descriptions of the kinetics of metabolic sequences, although to date no adequate general consideration of the influence of diffusion on these events has appeared in otherwise complex simulations.[38-40] The diffusional motion of a molecule can be detected if some means exists for tagging (or labeling) it. In the past, after considerable effort, success has been achieved in measuring the rate of diffusion of tritiated water into erythrocytes using a steady-state flow tube apparatus.[41,42] The excitation of nuclear spins, which then diffuse to a new location to relax, can be visualized as being akin to radioactive nuclei, except that the half-life, in this case of the high-energy spin states, is very short.

The mathematical theory necessary to account for the results is accordingly more complex but the NMR method of measuring diffusion of molecules inside cells has profound advantages over other methods, and these will hopefully become apparent in what follows.

B. Spin Echo

Hahn was the first to recognize the importance of the so-called spin-echo technique in measuring self-diffusion coefficients.[43] An outline of the spin-echo phenomenon will be given as it forms not only the basis of NMR techniques for measuring diffusion coefficients but is fundamental to the successful application of ^{1}H NMR in studies of erythrocyte metabolism; the reasons for its use there will be discussed in Section VI.B. Apart from the textbooks, several clear accounts of the spin-echo experiment[44] have also recently appeared in journals.[45-47]

As noted in Equation 4 nuclear spins in a uniform field B_0 precess at the Larmor frequency ω_0. Although each precessing moment vector can be resolved into a static component parallel (or antiparallel) to B_0, in the z-direction, and a component rotating with frequency ω_0 in the xy-plane, there will in general be no net magnetization in the xy-plane. This is due to the random phase of precession of each moment. Additionally, field homogeneity is rarely perfect and this results in a spatial distribution of precessional frequencies with respect to the field B_0. The spin-echo experiment is performed by applying, through a tuned coil (see Figure 1), a circularly polarized RF field, B_1, at the frequency ω_1 in the xy-plane; the circularly polarized field can be resolved into two orthogonal components of strength B_1. If the magnetization vector M is viewed from a frame of reference rotating at a frequency ω_0 about the z-axis, it appears stationary until the RF field (B_1) causes it to nutate about the direction of B_1, i.e., the rotating x-axis. The angle of nutation is determined by the relationship

$$\theta = \lambda B_1 t_p \qquad (10)$$

where t_p is the time-length of the RF pulse. Important values of θ for the present discussion are $\pi/2$ and π.

After a $\pi/2$ pulse the groups of magnetic moments (also known as spin isochromats) precess about the direction of B_o in the xy-plane and will be in phase initially, thus inducing an RF voltage in the detector coil. See Figure 2 for a description of the whole spin-echo process. (Because the spin-echo pulse sequence as described here is one of a general class that was described later by Carr and Purcell it is often called the CP pulse sequence.)

The rate at which the phase coherence between individual spin isochromats is irreversibly lost can be characterized by a transverse (because it is expressed in the xy-plane) relaxation time T_2.

Relaxation of the magnetization vector of a spin isochromat detected in the z-direction can be characterized by a time T_1, known as the longitudinal relaxation time. Both processes occur predominantly via dipole-dipole interactions (Section II.B) but the transverse relaxation occurs principally between neighboring spins, whereas longitudinal

Downloaded At: 15:58 17 January 2011

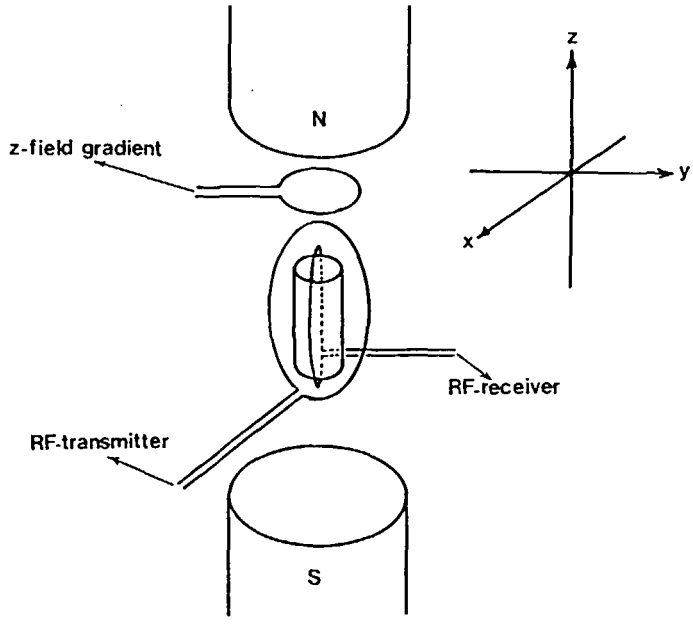

FIGURE 1. NMR spectrometer. A simplified scheme of a NMR spectrometer equipped for spin-echo and diffusion experiments. The circularly polarized RF field B_1 oscillates close to the Larmor frequency of the nuclear spins of the sample. A second coil, perpendicular to the transmitter coil, detects the precessing spins via electromagnetic induction. In modern spectrometers a single transmitter-receiver coil is usually used under the time-sharing control of the computer on the instrument.

Downloaded At: 15:58 17 January 2011

relaxation is generally considered to be via interactions with the lattice (Section II.B).

Other factors affect the apparent value of T_2. Inhomogeneities in B_o broaden the distribution of precessional frequencies of spin isochromats and lead to a shortening of T_2 due to an increased loss of phase coherence. This phase loss, however, is reversible. Application of a π pulse at a time τ after the $\pi/2$ pulse causes rotation of the spin isochromats about the x-axis in the rotating frame. Reference to Figure 2 will illustrate that just after the π pulse those spin isochromats rotating at a rate greater than ω_0 appear behind the slower rotating isochromats. Therefore at a time 2τ after the first pulse, phase coherence again occurs and an echo in the voltage of the detector coil ensues.

However, the presence of relaxation processes ensures that the echo amplitude is less than that evidenced just after the $\pi/2$ pulse. This echo decay process, in biological solutions, is usually described by an exponential decay with a single relaxation time T_2. However, in real systems, molecular diffusion also occurs. Therefore each spin isochromat will randomly change precessional frequency as it moves into regions of differing B_0. This random change will not in general be the same for the interval τ between the $\pi/2$ and π pulses and in the subsequent τ. The outcome is a reduction in the number of spins coming into phase at time 2τ after the $\pi/2$ (the first) pulse, thus leading to a reduction in the echo amplitude.

With improvements in magnetic field homogeneity, effects due to diffusion in spin-echo experiments can be significantly reduced. Certainly a multipulse sequence like that of Carr-Purcell-Meiboom-Gill (CPMG)[30] can be used to eliminate these diffusion effects, and a good demonstration of this has recently been given with glycine in suspensions of human erythrocytes.[48]

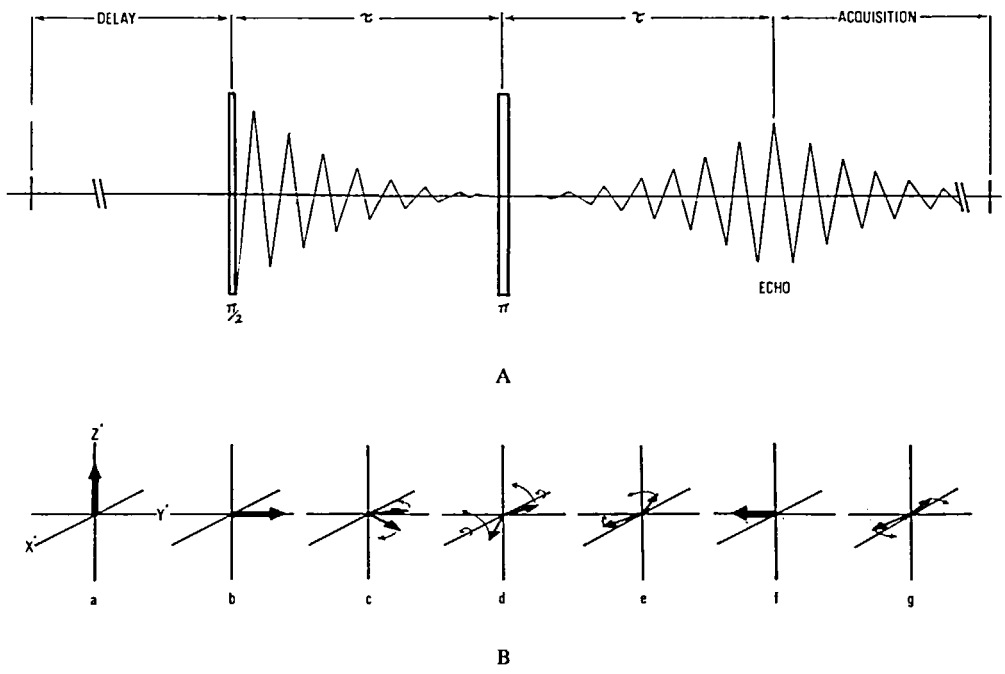

FIGURE 2. Spin echo. (A) The spin-echo pulse sequence. (B) The behavior of the outer components of a spin isochromat during the spin-echo sequence. Note: (a) Initially the net magnetic vector is in equilibrium parallel to the strong magnetic field B_o. (b) The RF field B_1 is applied for a short duration along the x-direction. As viewed from the rotating frame, the net magnetic moment nutates about the x'-axis into the x'-y' plane. (c) During the relatively long period following the removal of B_1 the spin vectors fan out, i.e., lose phase coherence. (d) At time $t = \tau$ the RF field B_1 is again applied for just long enough to nutate the spin vectors 180° about the x'-axis. Therefore the spin vectors again lie in the x'-y'-plane but with the faster precessing spin vector "behind" the slower vector. (e) The spin vectors begin to recluster. (f) At $t = 2\tau$ the vectors will have completely reclustered; thus a maximum signal will be induced in the detector coil at $t = 2\tau$. (g) Acquisition of the signal continues for any chosen time, whereupon follows a delay before the next sequence.

Downloaded At: 15:58 17 January 2011

C. Pulsed Field Gradients

The essence of NMR techniques for measuring diffusion is the application of a linear magnetic field gradient, usually in the direction of B_0, coupled with the spin-echo pulse sequence.[44] A great improvement in the accuracy of determining D in solutions was obtained when pulsed field gradients (PFG) were introduced in preference to continuous gradients.[49] In these experiments a strong linear gradient is pulsed on at a well-specified time after the $\pi/2$ pulse for a very short interval (a period δ sec) and again after the π pulse (see Figure 3). The principal reason for the refined accuracy of the PFG method is the improved ability to specify the time of diffusion, the time between the leading edges of the pulses (specified as Δ sec). The general expression for the spin-echo amplitude 2τ sec after the $\pi/2$ pulse ($S[2\tau]$), can be obtained by the solution of the differential equations describing spin relaxation (Bloch equations). The expression is[44,50]

$$S(2\tau) = S(0) \exp \left\{ -\frac{2\tau}{T_2} - \frac{2D\gamma^2G^2\tau^3}{3} \right\} F(J) \qquad (11)$$

where S(0) is the signal amplitude at $\tau = 0$, D the diffusion coefficient of the molecules, G the field gradient (Tesla m^{-1}), and F(J) a term which accounts for the signal modulation if there is homonuclear spin-spin coupling in the system. For a singlet $F(J) = 1$,

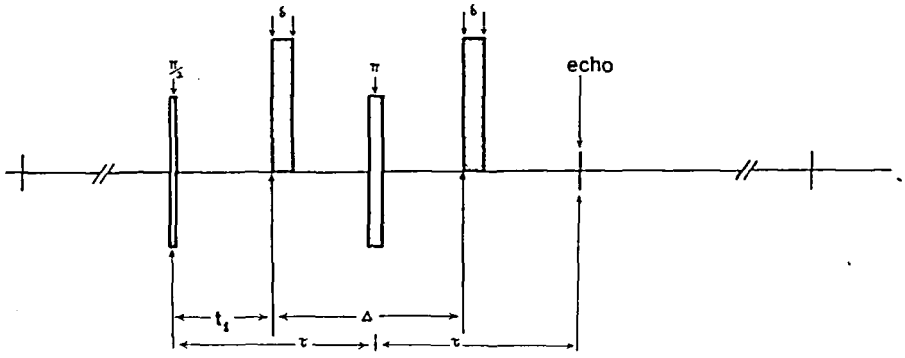

FIGURE 3. Spin-echo pfg. Pulsed field gradient spin-echo sequence for the measurement of self-diffusion of molecular nuclear spins: $\pi/2$ and π are the usual spin-echo pulses, δ is the time interval during which the linear field gradient is applied, and Δ is the time between the leading edges of the two pulses.

Downloaded At: 15:58 17 January 2011

but for a doublet $F(J) = \cos(2\pi J\tau)$ where J is the coupling constant of the doublet of spins.[51] A major assumption in the above-mentioned derivation is that the diffusion is isotropic and unbounded and described by Fick's laws.[44] The expression for the attenuation (R) of the echo amplitude in a PFG experiment is[49]

$$R = \ln[{}^*S(2\tau)/S(2\tau)] = -\gamma^2 D\delta^2(\Delta - \tfrac{1}{3}\delta)\, G^2 \qquad (12)$$

where the parameters are as specified for Equation 10 with ${}^*S(2\tau)$ as the signal amplitude in the presence of the PFG. Further simplification of the expression is possible if $\frac{1}{3}\delta \ll \Delta$ while ensuring that G is large, so that $G\delta$ is finite.[49] Consequently, a plot of the left-hand side of Equation 12 vs. the known, or experimentally established, parameters in the expression $\gamma^2\delta^2(\Delta - \frac{1}{3}\delta)\, G^2$ gives a line with a slope of $-D$.

A procedure that allows the more accurate determination of small values of D relies on prolongation of the inter-PFG time Δ, by superimposing the PFG on a CPMG sequence. This is achieved by applying a series of π pulses spaced at intervals of τ sec with the PFG being applied between $t = M\tau$ and $t = (M + 2)\tau$ and $t = (M + N + 2)\tau$ and $t = (M + N + 4)\tau$; where M is odd and $N = 4(i - 1)$, $i = 1,\ldots,n$.[52] The method was applied to studies on water in apple flesh and the accessible values of Δ were increased by a factor of 10.[52]

The motional behavior of biological water, or indeed other molecules, can only at best be described as undergoing isotropic bounded diffusion or at worst anisotropic bounded diffusion. In the case of the latter in any one region three diffusion coefficients are required for, at least, each of the three orthogonal axes. In the case of simple cellular systems, if the diffusion measurement is made over a time interval, t, such that $t > a^2/2D$ where a is the mean *free* path of the molecules, then it is likely that the diffusing molecules will meet an impenetrable barrier (e.g., membrane) during the time of measurement. The path of the molecule will be folded back and consequently the molecules will *appear* to have reduced translational diffusion coefficients. Theoretical consideration has been given to describe the diffusion behavior of molecules (nuclear spins) in isotropic media bounded in laminar systems,[53,55] a two-phase isotropic system,[56,57] near an attractive center,[58] and perhaps what is most relevant to biological systems, in cylindrical and spherical cavities.[54,59] Some of these analyses have been used in conjunction with data obtained with PFG techniques to estimate diffusion coefficients inside tissues.

D. Biological Studies

Yeast cells are almost spherical and growth conditions can be adjusted to give relatively uniform sizes. The total moisture content of compressed cells is ≈ 65% with ≈ 17% being extracellular. Data analysis from PFG experiments using the mathematical expression for isotropic diffusion between laminar boundaries (because the expression was relatively simple compared with that for the spherical case) yielded a value of D for water, at 25.5 ± 0.5° C, of 6.8×10^{-6} cm^2 sec^{-1}; this value is about 1/3 the value for pure water under the same conditions.[53] Furthermore, from the same analysis the average cell diameter was estimated to be 5.3×10^{-4} cm, a value in good agreement with that measured microscopically (6×10^{-4}cm).[53] Apple tissue, with its more variable but larger cell sizes, gave an average cell diameter of 4.3×10^{-3} cm and a diffusion coefficient of 1.81×10^{-5} cm^2 sec^{-1}, just less than the 2.3×10^{-5} cm^2 sec^{-1} of pure water. For tobacco pith with its large uniform cells protons appeared to move as freely as in pure water ($D = 2.37 \times 10^{-5}$ cm^2 sec^{-1}), an observation which is consistent with the low (3%) solid content.[53]

The self-diffusion of water protons in endosperm tissue of wheat grain has been measured, using a model that confines water molecules to a randomly oriented array of capillaries of diameter < 100 nm. The diffusion coefficients varied from 1.8×10^{-6} cm^2 sec^{-1} to 1.2×10^{-5} cm^2 sec^{-1}.[60]

The self-diffusion of water in human erythrocytes has also been studied; the exchange between external and internal water in whole blood significantly modifies the estimate of D obtained if a simple theory is applied. Therefore, the data were analyzed using an equation which describes heterogeneous diffusion in two domains, each with a different diffusion coefficient and with differing mean lifetimes (τ_i, i = 1, 2). A key assumption in the development of the equation was that the exchange rate between domains is much greater than $1/T_2$. D for the intraerythrocyte water was 1.16×10^{-5} cm^2 sec^{-1} with an exchange rate τ between the intra- and extracellular spaces of 17 msec. Cells treated with parachloromercuribenzoate (PCMB), which is known to significantly reduce water exchange in erythrocytes, gave a new D of 7.75×10^{-6} cm^2 sec^{-1} and τ of 48 msec.[61]

A recent publication presents a useful summary of estimates of diffusion coefficients for water and a few other biological compounds (K^+, Na^+, SO_4^{2-}, sucrose, ATP^{3-}, Ca^{2+}, urea, and glycerol) in muscle from various sources.[62] The new estimates of D for water in frog *(Rana pipiens)* muscles agree with older measurements on gastrocnemii from other species *(Bufo marinus)* and in mollusc *(Balanus nigrescens)* depressor muscle.[63] It is interesting to note that in a range of cells the ratio of diffusion coefficients (with the inter PFG time Δ extrapolated to zero so as to minimize the effects of impenetrable barriers) to those in free solution was ≈ 0.7 for water, ≈ 0.5 for sucrose and the ions, except Ca^{2+} with a value of 0.02; this is consistent with substantial binding of this ion to the contractile muscle proteins. Glycerol and urea had enhanced diffusion in barnacle muscle but the physical explanation is far from clear.[64]

It is clear from all the above-mentioned studies that biological water at least is freely mobile in many tissues, from plants to mammals. The attenuation of diffusion is only of the order of 0.7 in the fully enclosed complex muscle cell or the erythrocyte laden with hemoglobin, an observation that is, perhaps, quite surprising in view of the high protein concentrations.

E. ^{7}Li NMR

Li^+ transport across erythrocyte membranes is a slow process; therefore the diffusion of Li^+ inside the cell and across the membranes was able to be measured using a technique which exploits the fact that the *apparent* D of a molecular species inside a closed

Downloaded At: 15:58 17 January 2011

compartment decreases with the size of Δ in the PFG experiment.[65] If the observed spins undergo slow exchange between two sites A and B, the attenuation of the spin-echo amplitude is given by[56,65]

$$R = P_A \exp(-k D_A) + P_B \exp(-k D_B) \quad (13)$$

where $k = \gamma^2\delta^2G^2(\Delta - \frac{1}{3}\delta)$ and P_A and P_B are the fractions of nuclei at sites A and B with diffusion coefficients D_A and D_B, respectively. Choice of suitable values of δG and Δ in the experiments enabled elimination of the term ascribed to extracellular water (P_A), and a study of the intracellular Li^+ component. Furthermore, any net movement of molecules to the inside of the cell was measured by changes in the residual echo amplitude with time. The $t_{1/2}$ for Li^+ transport under the conditions used was 7½ hr, a value similar to that for choline,[66] which is thought to compete with Li^+ for transport.

Finally, it is worth noting that this method is only successful with systems with long T_2 ($\approx$5 to 20 sec) because this ensures an observable echo after long diffusion times. Furthermore, if this is the case, T_2 for the encapsulated species can also be measured.[65]

F. Flow Measurement

Since spin-echo amplitudes are sensitive to phase distributions of the resonating nuclei in fluid, the phase distribution is also dependent on flow. The translational and rotational diffusion and chemical exchange processes already mentioned are examples of incoherent molecular motion, whereas laminar flow is an example of coherent motion. Diffusion attenuates the spin echo whereas uniform flow merely shifts the phase; this is the essence of spin-echo methods for measuring flow rates.[67-69] Mathematical expressions that relate spin echo amplitudes to velocity distribution functions have been developed[69] and used to anlayze flow rates of blood in human fingers using detection of the water resonances at 10.5 MHz. The flow velocities ranged from 0 to 0.7 cm sec^{-1} with $\approx$80% of the spins flowing at less than 0.4 cm sec^{-1}. The method has yet to attain wide acceptability for physiological studies presumably because of the technical and analytical complexities. However, it does represent another valuable noninvasive blood flow measuring method. In addition, unlike Doppler flow meters, it does not need to operate on large vessels.

IV. BIOLOGICAL WATER

A. Introduction

The molecular organization of water most probably plays a key role in the function of all cells. It clearly influences the structure of organelles and the rates of enzyme catalyzed reactions by binding to proteins and affecting their conformations, by binding to ions, and simply by being the medium through which most reactants must diffuse. The physical behavior of water in biological systems was discussed in relation to translational diffusion in Section III.C, but many other studies directed at establishing different characteristics have been undertaken. Several reviews on this topic have appeared elsewhere.[8,33,70]

The physical behavior of water can be studied using the NMR of four different nuclei: the three isotopes of hydrogen (^1H, ^2H, and ^3H) and one of oxygen (^{17}O). ^1H, understandably, has been the most extensively studied with only limited attention given to ^2H and ^{17}O. NMR studies of biological water using the ^3H nuclide have yet to be reported but there is now a certain interest among chemists in this more recent NMR technique[71] since it is very sensitive (see Table 1). The motion of water molecules can be described, at least partially, by two parameters known as the rotational (τ_r) and translational (τ_l) correlation times: the first is defined simply as the mean time taken for a molecule to

Downloaded At: 15:58 17 January 2011

rotate through one radian, and the second is the mean time taken for the molecule to traverse one molecular diameter. More compex physical descriptions of molecular motion in fluids resort to the use of distributions of correlation times expressed in continuous form as correlation functions.[33] In some more complex situations coupling of rotational and translational processes must be accounted for.[72] However, more important for the present discussion is the fact that mathematical expressions exist that relate the readily (and commonly) obtained NMR parameters T_1, T_2, and $T_{1\rho}$ to molecular correlation times. (T_1 and T_2, the longitudinal and transverse relaxation times, were defined in Section II.B, and experimental means for their determination are well established.[30,33] $T_{1\rho}$ is a relaxation time equivalent to T_1, but is measured with a special pulse sequence,[32] designed so that the spin isochromat under study is orthogonal to B_0 and rotates with, and relaxes in, the weaker field B_1 (the usual RF pulse field).)

The most frequently used relationships were developed with the assumption that molecular motion is not involved in intramolecular spin relaxation and that one correlation time applies. The expressions are[33,73-75]

$$\frac{1}{T_1} = 2C\left\{\frac{\tau}{1+\omega_0^2\tau^2} + \frac{4\tau}{1+4\omega_0^2\tau^2}\right\} \tag{14}$$

$$\frac{1}{T_2} = C\left\{3\tau + \frac{5\tau}{1+\omega_0^2\tau^2} + \frac{2\tau}{1+4\omega_0^2\tau^2}\right\} \tag{15}$$

$$\frac{1}{T_{1\rho}} = C\left\{\frac{3\tau}{1+4\omega_1^2\tau^2} + \frac{5\tau}{1+\omega_0^2\tau^2} + \frac{2\tau}{1+4\omega_0^2\tau^2}\right\} \tag{16}$$

where ω_o is the Larmor frequency, ω_1 the frequency of the rotating frame, C is a constant given by γ^4 h I(I + 1) $r_{jk}^{-6}/2\pi$ for protons, and r_{jk} the internuclear distance. A similar series of expressions exists for deuterium relaxations in which C contains a term for the nuclear quadrupole.[76] The value of using different nuclides for the study of water stems from the intrinsically different relaxation properties and hence the possibility of measuring different inter- and intramolecular processes.

The spin relaxation of protons is influenced by inter- and intramolecular dipolar interactions whereas the relaxation behavior of ^2H and ^{17}O is dominated by quadrupolar interactions which clearly influence any measured T_1.[77] In water, deuteron nuclei relax 10 times faster than protons while ^{17}O nuclei relax at a rate $\approx$ 100 times that of deuterons. In other words, the fast relaxation rates of ^{17}O nuclei in water satisfy the so-called, *slow-exchange condition* ($1/\tau < 1/T_1, 1/T_2$), but in general ^1H and ^2H nuclei satisfy the *fast exchange condition* ($1/\tau \gg 1/T_1, 1/T_2$),[78] features important for theoretical analysis.

The T_1 of ^2H nuclei in ^2H_2O is governed completely by rotational times of individual ^2H_2O molecules; as a result ^2H NMR readily and usefully detects anisotropic motion (of water) in membranes and other biological systems.[76] On the other hand, the dipolar interactions of water protons are sensitive to rotational and translational motion, proton exchange, and the presence of paramagnetic centers[32] (Section II.B). Therefore, since the magnitude of quadrupolar interactions is greater than dipolar interactions,[29,33] small changes in nuclear environment more severely affect deuteron spin relaxation, but unfortunately the sensitivity of ^2H NMR is poor (Table 1) in the absence of isotope enrichment.

^1H NMR studies of "model" systems, such as solutions of purified proteins, have been numerous and have provided a lot of insight into the interpretation of complex NMR relaxation data; the interpretations were usually based on identifying domains or phases of water in various mole ratios from an analysis of relaxation times.[8,33,70] The

Downloaded At: 15:58 17 January 2011

techniques used are directly applicable to studies of biological tissues. A reasonably consistent observation from water protons in various tissues is that, compared with pure water, there appears to be (1) an overall reduction of T_1 by a factor of 4 to 5, (2) a reduction in T_2 by a factor of about 50, and (3) a reduction in the diffusion coefficient (Section III.C) by about 0.7 to 0.5.[79] Since many of the earlier studies of biological water were undertaken on muscle, these will be discussed first.

B. Muscle

The early investigations of muscle water were directed at discriminating between two opposing views of the nature of cellular water. One view was held that the water, which constitutes ≈ 80% by weight of the cells, is in a physical state similar to bulk water with only a small proportion affected by interactions with cellular components. The other view was that water is highly ordered (i.e., possesses a high degree of geometrical, translational, and rotational correlation) with extensive hydrogen bonding to cellular proteins, etc. resulting in the exclusion of ions from the bonded areas. Here *bound* molecules are taken to mean those that have reduced ranges of frequencies covered by their mobilities (translational or rotational), possibly with increased anisotropy.

In one early study of water in frog gastrocnemius muscle, a reduction of temperature resulted in the loss of the multiexponential character of the free induction decay (FID). The data showed a linear-decreasing dependence of initial FID amplitude, over the temperature domain ≈ −10 to −40° C and extrapolation of the line gave 20% as the estimate of the mole fraction of this phase of water present at +10° C. By "curve peeling" the multiexponential decay curves, three relaxation times were obtained, suggesting that at least three distinct water compartments exist in muscle; they are operationally if not physically or structurally distinct.[80] In other words, these data and those from similar systems can be described by the following expressions:

$$S(t) = \sum_{i=1}^{n} S_i(t) \qquad (17)$$

$$S_i(t) = S_{0i} \exp\{-t/T_{1i}\}$$

where S(t) is the amplitude of the FID at time t, S_{0i} are the corresponding zero time values, and T_{2i} (or indeed T_i) is the appropriate relaxation time for the ith component.[79,80] The shortest relaxation time which was evident in 20% of the water protons was identified with the "unfrozen" protein-bound water. The intermediate relaxation time which was associated with 65% of the protons was ascribed to bulk intracellular water, while the longest T_2 representing 15% of the total protons was taken to be extracellular.[80] Hazelwood et al.[79] also described three water fractions in rat gastrocnemius muscle; 8% of the water was slowly exchanging and thought to be bound to macromolecules, while 82% of the water had a T_2 of 45 msec (a 40-fold reduction compared with a physiological electrolyte solution) and was assigned to the myoplasm. The remaining ≈ 10% with a T_2 4 times that of the myoplasm was thought to be in the extracellular space.

Questions relating to the possible causes of the enhanced spin relaxation will now be discussed. Theoretical considerations showed that the reduction of T_2 of the myoplasmic water could neither be accounted for by fast exchange (e.g., theory of Carver et al.[36]) between protein-bound and free water, nor by diffusion of the water across local magnetic field gradients, which could conceivably arise from microheterogeneities in the magnetic susceptibilities in the sample.[79] Other calculations confirmed this deduction.[81] However, experimentally the invariance of T_2, at 25 MHz and 50 MHz, was valuable

Downloaded At: 15:58 17 January 2011

evidence in favor of no significant spin-echo attenuation being due to field gradients; the strength of induced field gradients should vary as the square of B_0; therefore, according to Equation 11, T_2 would change if the gradients were of significant magnitude.

The contribution of paramagnetic ions to relaxation is in general, related to γ^2.[32] The γ^2 for protons is 42.4 times larger than the value for deuterons (Table 1) so if paramagnetic relaxation contributes significantly to the reduction in the value of T_1 or T_2 of tissue water, the effect should be less for deuterons. In fact, the T_2 for deutrons is 10 times *shorter* than for protons.[79,82] Therefore, it can be concluded that paramagnetic centers are responsible for little of the spin relaxation of water nuclei in cells; the major enhancement of relaxation is probably due to cellular organelles (e.g., membranes) and/or the convection of cellular water.

In a further extension of studies on muscle water, the analytical procedures developed for the study of water (T_1 and T_2) in agarose and gelatin samples[83] were applied to data obtained at three frequencies (2.3, 8.9, and 30 MHz) from toad muscle. The T_1 data were analyzed in terms of a distribution of proton correlation times $p(\tau)$:

$$p(\tau) = \begin{cases} X \frac{A}{\tau} \left(\log_{10} \frac{\tau}{\tau_2} \right)^a & \tau'' > \tau > \tau' \\ (1 - x)\, \delta\, (\tau - \tau_2) \text{ otherwise} \end{cases} \qquad (18)$$

where $A = \int_{\tau'}^{\tau''} [\log_{10} (\tau/\tau_2)]^a \, d\tau/\tau = 1$, τ_2 is the proton correlation time in bulk water, x the fraction of protons in the modified state, and τ'' and τ' are the upper and lower limits of τ for the modified states; in addition $\tau'' > \tau' > \tau_2$ was assumed. The analysis revealed, among other things, that not more than 2% of the observed protons were in a state with $\tau > 10^{-9}$ sec.[84] The correlation times were $\approx 10^5$ times smaller than in ice and not more than $\approx$ 10 times larger than in bulk water (recall that τ in bulk water is $\approx 10^{-11}$ sec),[84] so the authors, in contradistinction to earlier workers who did not look at relaxation at different ω_0 values, concluded that there was little evidence for ice-like ordering of cellular water.[84]

In order to demonstrate how a completely different interpretation can be placed on the NMR relaxation data derived from tissue, consider the following: water in various mouse tissues (C3HBA implanted mammary carcinoma, spleen, and normal and neoplastic muscle) was described as undergoing exchange, molecular rotation, and diffusion with the respective correlation times 7×10^{-6}, 2×10^{-8}, and $< 10^{-10}$ sec.[75] The correlation times were derived from an analysis of T_1, T_2, and $T_{1\rho}$ values, obtained at 17 to 45 MHz and 10^3 to 10^5 Kz and in which data were fitted to a general expression for the relaxation rate:

$$R_{TOTAL} = R_{ex} + bR_{rot} + (1 - b)R_{diff} \qquad (19)$$

where R_{ex} is the relaxation rate due to exchange, R_{rot} that due to rotation, R_{diff} that due to diffusion, and b is the fraction of bound water. It was, however, acknowledged that the data could, equally well, have been analyzed by fitting it to a correlation function with a continuous distribution of correlation times (e.g., Reference 84).[75]

Yet another type of analysis was applied in studies of the frequency and temperature dependence of T_1 for both ^1H and ^2H nuclei in water of mouse liver and muscle. Some water remained unfrozen down to $-70°C$; it had a frequency-dependent T_1 and was described by a distribution of correlation times. It was visualized as being in the immediate vicinity of membranes and macromolecules. The remaining volume of the water

Downloaded At: 15:58 17 January 2011

had a T_1 independent of frequency, relaxed like pure water, and froze at −8° C. Finally, a hybrid model was used, for the analysis, with two compartments, one containing "bound" water described by a distribution of correlation times and the other behaving like bulk water.[76]

The comparative studies, at different frequencies, of T_1 from ^1H and ^2H in mouse muscle have been continued[85] in order to characterize better the mechanisms of spin relaxation in muscle water. The $1/T_1$ for ^1H nuclei increased monotonically with decreasing frequency down to 10^4 Hz, whereas for ^2H nuclei the value leveled off for frequencies (ν) below 10^5 Hz. However, the T_1 for bulk water shows no such frequency dispersion at 25° C; thus for $\nu \rightarrow 0$, $T_1(^1H \text{ bulk})/T_1(^1H \text{ muscle}) > 100$ and $T_1(^2H \text{ bulk})/T_1(^2H \text{ muscle}) \approx 16$. Similar measurements have been made in solutions of purified proteins of a series of molecular weights,[86,87] and ratios around 10.0 were obtained but they increased in proportion to an increase in the molecular weight. The overall conclusion then is that the major relaxation mechanism for protons in muscle water is via intermolecular dipolar interactions with the protons of macromolecules and hydration layers, for deuterons relaxation is predominently via the small fraction of water molecules directly hydrogen bonded to macromolecules.[85]

The continuous wave (CW) ^1H NMR spectra of frog striated muscle displayed a dependence of T_2 on the angle of orientation of the samples; in fact orientation at 180° to the long axis of the muscle resulted in splitting of the H_2O resonance. Broadening but not splitting was seen also under similar conditions using CW ^2H NMR.[89] These data suggested a preferential orientation of water molecules in muscle fibers and represent a conclusion that clearly accords with the microanatomical appearance of muscle.[89]

Finally, despite this gross ordering of water in muscle, the previously discussed studies on spin relaxation in muscle seem to exclude the possibility of there being a significant amount of water with a long correlation time of $\approx 10^{-5}$ sec akin to that of ice. The important development that has allowed clear resolution of the question of the presence or absence of ice-like ordering of muscle water has been the study of relaxation times as a function of frequency; the previous work from which ice-like ordering was suggested[89-93] had not made use of the methodology.

C. Erythrocytes

Pulsed ^1H NMR carried out at different frequencies and temperatures on solutions of albumin suggested the existence of three phases of water in the system: water that is free; $\tau \approx 10^{-11}$ sec near 0° C; translationally bound with $\tau \approx 10^{-9}$ sec; and irrotationally bound with $\tau \approx 10^{-8}$ sec.[94] As an aside, it is interesting to note that analysis of the data using a model similar to Equation 17 indicated the presence of less than 300 water molecules tightly bound per albumin molecule; this value agrees with the available charged and dipolar sites therein.

In another study, attention was focused on the relaxation behavior of the protons of the protein.[95] Only a single T_1 (0.16 sec) was obtained for the protein protons (presumably virtually all hemoglobin) in packed human erythrocytes. The overall relaxation curve was "peeled" of its $^2HO^1H$ component using a T_1 of 0.6 sec leaving the protein part. However, since the albumin study[94] showed a triphasic water relaxation, it is this type of curve that should have been "peeled" from the raw data. Nevertheless the qualitative conclusions which followed probably still hold,[95] and it is indeed surprising that hemoglobin proton relaxation in cells can be accounted for by a single T_1. The results suggested to the authors[95] that dipolar coupling between spins is stronger than the coupling to the lattice. Hence, the protein spins equilibrate (thermally) rapidly among themselves and relax more slowly to the lattice temperature as a single unit. The fact that in proteins $T_2 << T_1$ is a necessary condition for this.

Downloaded At: 15:58 17 January 2011

Table 2
T_2 OF WATER PROTONS IN ERYTHROCYTES AND HEMOGLOBIN SOLUTIONS[98]

	T_2 (msec)					
	4°C		37°C		T_2 (37°C)/T_2 (4°C)	
	Oxy	Deoxy	Oxy	Deoxy	Oxy	Deoxy
Sickle cells	183 ± 48*	117 ± 38	282 ± 48	68 ± 19	1.57 ± 0.13	0.60 ± 0.08
HbS	180	185	277	125	1.54	0.67
Normal cells	162 ± 47	144 ± 43	302 ± 74	260 ± 81	1.88 ± 0.01	1.84 ± 0.01
HbA	198	187	285	267	1.44	1.43

* 1 SD calculated from the data of Table II from Cottam, G. L., Valentine, K. M., Yamaoka, K., and Waterman, M. R., *Arch. Biochem. Biophys.*, 162, 487, 1974. With permission.

Addition of Mn^{2+} to an erythrocyte suspension introduced a biphasic relaxation profile for the protein protons;[95] this can be interpreted as due to a reduction of water T_1 to the millisecond range in which cross relaxation is no longer sufficient to equalize spin temperatures thus showing two components. Since Mn^{2+} does not freely penetrate erythrocytes and therefore does not make contact with intracellular hemoglobin, the enhanced protein-proton relaxation detected was interpreted as having been due to spin transfer via water.[95] Two possible flaws arise in relation to the interpretation: (1) Mn^{2+} does slowly, but significantly from the point of view of relaxation phenomena (see Section IV.C) penetrate erythrocyte membranes — but control experiments can be designed to subtract the effect and (2) Mn^{2+} may invoke a more complex water proton relaxation process than merely a single exponential one, so that the enhanced protein-proton relaxation may in fact be due to water protons, whose contribution to the curve has not been subtracted.

Isolated sickle cell hemoglobin (HbS) at a concentration of ≈250 mg $m\ell^{-1}$ forms a gel at 37° C which liquifies at 4° C or upon oxygenation.[97] Furthermore, deoxygenation at 37° C of sickled blood greatly increases the number of sickle shaped cells, but the number is reduced on cooling to 4° C. Therefore this biological system has been seen as a good one to use for the development of a means for detecting macromolecular aggregation inside cells using NMR.[98,99] The T_2 of water protons in cells containing hemoglobin A (HbA) and HbS, and in solutions, were measured and the anticipated (based on studies of agar and gelatine gels[83]) reduction of T_2 upon gelation of the HbS was detected in both systems.[98] Table 2 gives the ratios of T_2 values obtained at 37° C and 4° C for the cell suspensions and solutions of Hb. The ratio for normal cells and solutions scarcely altered on deoxygenation but was reduced 2.6-fold in sickled cells; other, confirmatory, studies of T_1 and T_2 have been reported.[100-102] Clearly, more careful analysis of data from this system should reveal more than one T_2 value for the water protons (e.g., Section III.B), but this does not degrade the value of this interesting finding from the point of view of using it to follow the sickling process inside intact erythrocytes.

Further work has shown that T_1 values of cellular water in sickle cells do not alter in the manner of T_2, on deoxygenation. Furthermore it was shown, by reducing cell volumes using hyperosmolar media, that the ≈10% reduction of cell volume that results from sickling of erythrocytes affects little the T_1 and T_2 values.[99] Finally, from an analysis of the temperature dependence of the relaxation times it was inferred that the aggregation of HbS is mediated via hydrophobic bonds, and that ≈0.4 g of water binds per gram of HbA or HbS.[99]

Downloaded At: 15:58 17 January 2011

Downloaded At: 15:58 17 January 2011

D. Neoplastic Tissues

The values of T_1, T_2, and $T_{1\rho}$ of water protons in a diverse array of tumorous tissues have been shown to be higher than in the corresponding normal tissue. Whether this observation will be useful in diagnosis or therapy is yet to be decided, despite some early exuberance.[103]

Damadian was the first to report altered T_1 and T_2 values for water in neoplastic tissues.[89] The results were followed by others[104] that showed that values of T_1 and $T_{1\rho}$ of water in many tissues (spleen, kidney, heart, muscle, intestine, stomach, skin, and lung) in mice afflicted with a hind leg tumor were considerably increased compared with normal mice. Similar results have been obtained for T_1 values for water in nonneoplastic tissues in humans with tumors.[105] The T_1 values for water in mouse liver, spleen, and kidney showed the same effect, but in addition the slowly growing (well-differentiated) tumors resembled normal tissue.[105] This finding has been confirmed using Morris hepatoma and several murine tumors.[106]

The T_1, T_2, and D values of water protons in mammary tumors of mice were found to increase monotonically with the transition from normal tissue, to small dysplastic nodules, to tumor. However, the correlation with tissue hydration was not strict.[107,108] The findings clearly indicate the need to evaluate the dependence of the NMR parameters on intra- and extracellular fluid but it seems clear that intracellular hydration is higher in tumors.[109] T_1 measurements of blood serum and liver homogenates were determined at various times after the inoculation of mice with live or dead Ehrlich-Lettré ascites tumor cells. One day after either live or dead cell inoculation T_1 of serum water was elevated $\approx$17%. In mice in which the tumors developed the T_1 of serum water was elevated again $\approx$17% above the controls after 3 to 5 days.[110] It was decided that the most likely cause of the effect was increased hydration in the tumorous, or otherwise diseased (e.g., immunologically perturbed) animals.[110]

In spite of variable correlation with water content, T_1 and T_2 for water protons in tumors appear to be consistently longer than corresponding normal tissues. In the study of mouse mammary glands,[107] T_2 appeared to be a better indicator of pathology than T_1. Furthermore, the authors claimed that by using the two relaxation times, the mammary tissue could be classified as normal, fibrocystic, or neoplastic according to the following rules: fibrocystic if $T_1 \leqslant 792$ and $T_2 \leqslant 58.1$ msec, or neoplastic if $T_1 > 792$ and $T_2 > 58.1$ msec.[107] Other experiments showed a clearer correlation between T_1 and water content in HeLa and ovary cells.[109]

Another interesting observation is that the *difference* in T_1 between normal and tumorous tissue is, significantly, frequency dependent, the difference being greater at the lower frequencies.[93] This finding has prompted the definition of detection resolution (r) as:

$$r = \frac{T_1\,(\text{tumorous}) - T_1\,(\text{healthy})}{T_1\,(\text{tumorous})} \tag{20}$$

$$= \frac{(1/T_1 - R_f)\delta b}{(1/T_1)\quad b} \tag{21}$$

where b is the proportion of bound water, $R_f = (1 - b)\,(1/T_1)_{\text{free } H_2O}$, and δb is the alteration in the fraction of tissue water from normal to neoplastic samples.

Resolution is greatest at 2 MHz and zero at $\approx$100 MHz. This observation of the frequency dependence of the T_1 and T_2 of water protons in whole cells has been found also in human erythrocytes and exploited in studies of metabolism, at 400 MHz, in situations where otherwise water signal suppression would be required.[112]

$$M = \frac{T_1}{T_1(\text{normal})} + \frac{T_2}{T_2(\text{normal})} \qquad (22)$$

(where T_1 and T_2 are the relaxation times of water protons) has been used and shown to enable discrimination between malignant and normal tissues in all of 36 colon samples, 22 out of 23 breast samples, and 26 out of 29 lung samples.[113] In 102 specimens of human gastrointestinal tissue from 87 patients, the mean and standard deviations of M for normal and malignant tissue were 2.004 ± 0.342 and 3.266 ± 0.642, respectively. Histologically normal tissue adjacent to the neoplasms also had elevated values of M.[113,114]

Unfrozen water (Section IV.B) is less in tumorous than in normal muscle; the difference is thought to be due to an increase in the water/solid ratio or an increase in K^+ concentration. Below −8° C the T_1 for unfrozen water was essentially the same in both classes of tissue, although the amount of unfrozen water in tumorous tissue was less.[115] The conclusion, again, is that there is relatively more free water in tumorous cells rather than, as previously suggested, an alteration in water structure.[82,89]

The effect of prolonged water proton T_1 and T_2 compared with normal tissues is not unique to neoplasia. Many inflammatory conditions, such as pneumonia[116] and others,[108,119] influence the results; further examples will be noted in Section X.C. Drug therapy can also produce spin-relaxation changes in some organs that are similar to those found in neoplasia; antithyroid drug treatment produced an elongation of T_1 similar to that seen in neoplasia of the same tissue.[118] In another study, nonmalignant samples of thyroid tissue in all but a few cases had a water proton $T_1 < 700$ msec, while most malignant samples had $T_1 > 700$ msec. However, a well-differentiated but metastasized papillary carcinoma had a water proton T_1 of 500 msec, and some necrotic tissue had values above 700 msec. Oxygenation or treatment of homogenized tissue with N_2 had little effect on the estimates of T_1, suggesting that the shorter relaxation times in normal tissues were not due to paramagnetically enhanced relaxation incurred by better oxygenation of normal tissue. Rather, in keeping with previously mentioned work, it was concluded that the effect was one of increased water content in the neoplastic tissue.[119]

It is to be expected that in the future low resolution NMR will be used to measure water proton T_1 and T_2 values and to assist the histopathologist in making a diagnosis regarding the malignancy or inflammatory derangement of tissue samples. It is unlikely that is will replace histopathology as the final arbiter in such decisions,[120] but will be useful in screening studies and to provide guidance in therapy, as well as giving evidence of the extent of dissemination of the disease.

E. Plants and Viruses

Bačic et al.[121] studied the effect of varying LiCl and KCl concentrations on the T_1 of water protons in roots of *Zea mays*. With both alkali metals a minimum in the plots of T_1 vs. salt concentration (20 m*M* for LiCl, 1 m*M* for KCl) was found to correspond with a minimum in cellular water content (or volume). The values of $1/T_1$ were interpreted in terms of a three-compartment model (Equation 17) with water said to be bound, associated with ionic shells, or free. A high Li^+ concentration, it was suggested, increased abstraction of water from the cellular macromolecules which have shorter T_1s than the free or coordinated water.

The T_1 for water in the fresh water alga *Nitella* was found to be a minimum when the extracellular Li^+ concentration was 3.0 m*M*.[122] The effect was rationalized by noting the fact that algal cells incubated in a range of Li^+ concentrations demonstrate a dependence of the ratio $[Li^+]_{inside}/[Li^+]_{outside}$ on $[Li^+]_{outside}$. For *Zea mays* roots the ratio 1.0 occurs at $[Li^+] = 1.85$ m*M* and for the alga *Nitella chara* it is 4.0 m*M*. Therefore on the low $[Li^+]$ side the higher T_1 could be attributed to increased cellular hydration due to an osmotic

Downloaded At: 15:58 17 January 2011

effect ($[Li^+]_{inside} > [Li^+]_{outside}$), whereas with high $[Li^+]_{outside}$ the total Li^+ uptake by the cell is large and more likely to disrupt the order of macromolecule-water interactions.[122]

The extension of this type of study to mammalian systems may prove useful in settling certain questions relating to the dependence of NMR relaxation parameters on tissue transformation. Indeed, an example of an NMR study on acute cell transformation will now be given.

The T_1 of water protons in suspensions of laryngeal epidermoid carcinoma (HEP-2) cells was determined using pulsed NMR, both before and after infection with Polio type 1 virus.[123] For uninfected cells the concentration (cells per milliliter) dependence of $1/T_1$ at 4°C was linear but varied between cell populations; the domain of cell counts was 0.25×10^6 to 8×10^6 cells $m\ell^{-1}$ and range of $1/T_1$ was 0.075 to 0.165 sec^{-1}. Suspensions of cells were then inoculated with the virus for 1 hr at 37°C prior to being studied at 4°C. Shortening of T_1 correlated closely with the viral concentration, expressed as plaque forming units per cell.

The molecular basis of the above-mentioned changes has not been fully explained, but it can be interpreted loosely in terms of the models of water-cell interaction and structure discussed in the previous sections. Indeed, virus-host interactions of the type mentioned may be the basis of many of the inflammations, and indeed tumors, already discussed.

V. TRANSPORT STUDIES

A. Introduction

It has been suggested that the preferential permeation of the neutral form of catecholeamines leads to their accumulation in the chromaffin granules of the adrenal gland.[124] This occurs in response to a lowering of intravesicular pH. A similar conclusion has been drawn from studies using synthetic liposomes.[125] Because of the importance of these and other transport processes in biology the NMR-based methods which can contribute to the understanding of them will be discussed.

All experimental means of measuring the migration of a chemical species into cells or vesicles rely on some means of distinguishing between those molecules inside and those outside. NMR methods rely on the ability to detect differences in the fundamental NMR parameters between the two or more compartments, namely: (1) the chemical shift may depend on the pH, which can be made to differ between compartments, (2) different relaxation times in the two compartments (several examples have been given in Section IV.B), and (3) different apparent diffusion coefficients (examples are given in Section III.C).

B. Vesicles

The dependence of the ^1H chemical shift on pH of carboxylic acids has been exploited to monitor transport of these compounds into synthetic vesicles.[126] The time courses were followed over approximately 30 min. Single bilayer vesicles containing maleate were made by the sonication of egg yolk phosphatidyl choline (PC) and cholesterol in ^2H_2O at pH 7.0. The external medium was exchanged for iso-osmotic fumarate at pH 8.0, by Sephadex chromatography. The chemical shifts of the nonexchangeable olefinic protons of this cis-trans isomer pair are significantly different and vary over the pH range 2 to 7. Consequently, addition of ^2HCl to the external medium initiated a time-dependent growth of a high field shoulder on the fumarate (external) resonance; this was attributed to the internal fumarate.

The conclusion from this experiment was that the acid form of the anions (fumarate) is transported, because the reduction of extravesicular pH increases the concentration gradient of the acid form, thus facilitating the rate of transmembrane transfer.[126]

Downloaded At: 15:58 17 January 2011

In addition, various alternative experimental designs for measuring transvesicular migration rates have been discussed.[126,127] The effect of electrostatic coupling on transport in the PC-phosphatidyl ethanolamine (PE) vesicle system has been studied using maleate and K^+ ions in the presence of the ionophore, valinomycin.[127] The integrals of the maleate ^1H resonances in both compartments of this system were related directly to concentrations because of the equality of T_1s therein. This observation was used to quantitate intra- and extravesicular volumes and concentrations, and coupled with a knowledge of the size of the vesicles the permeation coefficients for maleic acid and maleate anion were calculated. The values obtained in the presence and absence of ionophore were 10^{-5} cm sec^{-1} and 10^{-10} cm sec^{-1}, respectively.[127]

The above-mentioned studies utilized changes in the NMR signal of the transported substance. An alternative procedure has been used to monitor carrier-mediated transport of Mn^{2+} ions across phospholipid vesicles. The method relies on observing the disappearance of the ^1H NMR signals of the cholines in the inner phospholipid layer due to the paramagnetic broadening effect of the translocated Mn^{2+} ion.[128]

A similar method has been used to study Pr^{3+} transport into phospholipid vesicles.[129] However, in this system line broadening was not linearly related to ionic concentration, and hence transport, because of the nature of the relaxation enhancement. Moreover some of the resultant signal broadening could have arisen from heterogeneity of the size of the vesicles, since it has been shown in a separate study that in the PC-PE system the hydrocarbon chain-proton line width is a simple monotonic function of vesicle size.[130]

In PC vesicles the polar head groups of choline are in contact with intra- and extravesicular bulk water. In the small vesicles the resonances of the methyl protons of the quaternary ammonium ions, on the inside, are shifted 0.02 ppm upfield compared with those outside. Addition of Mn^{2+} caused a concentration-dependent broadening of the low field (external) $-N^+(CH_3)_3$ resonance. Superaddition of the ionophore X-537A (Lasalocid-A) gave rise to a time-dependent broadening of the high field (internal) $-N^+(CH_3)_3$ line. After careful calibration of the $[Mn^{2+}]$ dependence of the broadening effect, it was shown that the rate of broadening depended on the *square* of the ionophore concentration. It was therefore concluded that the transported complex contained two ionophore molecules and one Mn^{2+} ion. Studies at different pH values led to the deduction that the predominant transported complex species was the uncharged form. The temperature dependence of the rate of transport indicated that the activation energy of the overall ionophore-mediated transport of Mn^{2+} was 22 ± 5 kcal mol^{-1}, a value similar to that found in biological systems.[128]

It appears that these methods are in general applicable to the investigation of chemical movements between biological compartments, although a means of calibrating the concentration dependences of the paramagnetic broadening produced by the transposed ion inside the compartments is required. The calibration is simple with synthetic vesicles since they can be made in the presence of various known concentrations of paramagnetic ion. Although cells can be resealed after lysis, it is impossible not to lose some of the contents into the extracellular fluid. Consequently, the value of the present methods for studying transport into cells is limited.

Fortunately, other means of studying transport using NMR have been developed recently and, in particular, applied to erythrocytes.

C. Erythrocytes

The general subject of transport of water in erythrocytes was reviewed[132] in 1971. Since then, NMR studies have added a lot of new understanding of the process and some of the work is discussed in Section III.D.

The diffusion of water through erythrocyte membranes can be measured using a

Downloaded At: 15:58 17 January 2011

technique in which the T_2 of the water protons on either side of the membrane differ. This has been achieved in several studies with the paramagnetic Mn^{2+} ion. The rate constant of spontaneous loss of phase coherence in water proton spins is of the order of 0.140 sec; this is much longer than the cell-plasma exchange time known from radiotracer means to be about 0.010 sec.[41] If the T_2 in plasma is greatly shortened with (24 m*M*)[133] Mn^{2+}, loss of phase coherence is dominated by the exchange process; water molecules leaving the cells dephase very soon after contacting the plasma, while those entering the cell are fully dephased. Conventional CP pulse sequences[30-33] gave data which demonstrated a double exponential character when echo amplitude was plotted vs. time; homogenization of the cells caused a disappearance of the second exponential component of the curve, indicating that the slower relaxation was due to intracellular water.[133] Incidentally, the proportion of the total sample volume that is intracellular is also available from the extrapolation of the second portion of the decay curve back to the ordinate. Therefore, by careful measurement of the cytocrit value, it is possible to infer the actual exchangeable water in the cells; one estimate using this method gave the fraction of the cell volume as 0.70 ± 0.05.[134] Complications can arise with this technique because Mn^{2+} slowly diffuses inside the cell leading to a progressive time-dependent decrease of T_2 therein. However, it has been reported that use of aged (7-day-old) solutions of $MnCl_2$ obviates this problem,[135] possibly due to the formation of colloidal aggregates of MnO_2 which, although paramagnetic, are too large to cross the membranes. In addition, in studies in which the cells are suspended in plasma or albumin solutions the Mn^{2+} binds to the proteins and thence becomes impermeant.[136,137]

The relaxation time for water efflux across the erythrocyte membrane (τ_a) was calculated from the NMR data to be 0.010 sec,[133] a value in exact agreement with that obtained from radiotracer studies.[41] By use of the same NMR technique it was shown that the permeability of erythrocytes to water is independent of osmolarity.[138] The osmolarity of the medium (300 to 1000 mOsm) was varied by the addition of the permeable solutes, urea, methanol, ethanol, and glycerol.[138]

Abnormally long water exchange times (τ_a = 47 msec) were recorded when erythrocytes from sufferers of epilepsy were subjected to the method. The prolongation of τ_a appeared to be independent of therapy and was evident in the interictal period as well as during a convulsion.[139] It should be noted that abnormalities in erythrocyte membranes could be indicative of generalized membrane defects in other organs, such as the brain.[66,139] For example, measurements of water transport through erythrocyte membranes, using NMR, indicated a 13 to 55% increase in rate in Gaucher's disease, essential hyperlipidemia, obstructive jaundice, chronic hepatitis, and the nephrotic syndrome.[136] These results suggest that environmental (plasma) factors as well as primary heritable membrane-protein defects can alter water translocation rates.

A slightly different and more detailed approach to the study of erythrocyte-water transport has been taken by Pirkle et al.[135] Their method is based on the nonlinear fit of CPMG-T_2 data from blood doped with 1.7 m*M* $MnCl_2$, to the generalized two compartment-exchange equation.[141,142] The relaxation rate of water exchange (τ_a) was 21 ± 0.6 msec at 23° C. Furthermore, the Arrhenius plot for τ_a was linear over the temperature domain 3 to 37° C and gave an activation energy of 4.79 ± 0.03 kcal mol^{-1}; the authors claimed that this value is not significantly different from bulk water flow.[135] The value agrees reasonably well with those obtained by other means: ^{17}O NMR (Section IX.B), pulsed field gradients (Section III.C), and isotope tracer methods.[41]

The advantages with this more complex data analysis[135] are that (1) the effect of the small amount of Mn^{2+} influx into the cells can be mathematically accounted for, (2) calculations are rapid once it is automated on a computer, and (3) the method requires small sample volumes (50 $\mu\ell$). Apart from τ_a values of high accuracy and reproducibility

Downloaded At: 15:58 17 January 2011

(±2% SE), in common with some other methods,[133] the ratio of cellular/extracellular water is also obtained.[135]

An even more complex analysis of water-relaxation data obtained from Mn^{2+} doped erythrocytes has been used by Fabry and Eisenstadt.[134] The extra complexity arises from the consideration of the effects of spin diffusion on the spin-lattice relaxation time of water in cells. The process of spin diffusion, which was discussed in Section IV.B,[95,96] is one which leads to a mixing of spins from protein and water, by spin exchange, in much the same way as water protons inside and outside the cell mix with water exchange.[138] The effect of not removing the spin diffusion contribution to the relaxation of water is to make the water lifetime appear short.

Use of the aforementioned analysis gave the permeability to water of erythrocytes in heparinized plasma as $2.1 \pm 0.2 \times 10^{-3}$ cm sec^{-1}, and permeant solutes such as urea had little effect on the value.[134]

A completely general approach to the measurement of transport of small (protonated organic) molecules into cells relies on the molecules having different specific intensities on either side of the membrane. The intensity difference arises from altering the magnetic susceptibility between the two compartments, coupled with the use of the spin-echo (CP; Section III.B) technique.

The simple two-pulse ($\pi/2$-τ-π-τ) CP sequence gives rise to an echo in signal intensity 2τ sec after the $\pi/2$ pulse. The echo amplitude is given by Equation 11. The physical meaning of the term involving τ^3, γ^2, and D is that the spins are not properly refocused if the molecules diffuse to a region of different applied field during the time 2τ (see Section III.B). With a homogeneous sample in a precisely uniform field (such as in modern high field NMR spectrometers) this term is negligible for τ values even over 100 msec. However, with large values of τ or D this term in the equation predicts a rapid decay of the signal.[29,30]

The effect of the $2\gamma^2DG^2\tau^3/3$ term can be reduced by applying many π pulses between the $\pi/2$ pulse and data acquisition; τ is thence kept small and minimizes the term. The CPMG sequence with $\tau = 1$ msec is suitable for this purpose and ensures that the amplitude decay is dominated by the T_2 term. An example of this effect is given in Figure 4. A solution of glycine in ^2H_2O Ringer solution was studied using the simple CP and also the CPMG sequence. Data analysis gave a $t_{1/2}$ for the decay of the α-CH_2 spins equal to 1.5 sec in both cases. In a suspension of erythrocytes (cytocrit 0.8) the observed $t_{1/2}$ for added glycine, obtained from the simple pulse sequence, was much smaller ($\approx$0.1) than that from the CPMG sequence.[48] Therefore it was concluded that with the simple CP sequence the observed decay in the echo amplitude is dominated by the τ^3 term, an effect due to field gradients (G) in the extracellular space.[48]

The field gradients arise because of magnetic susceptibility differences between the medium and the cells. For the special case of spheres it has been shown that these gradients arise only outside. Experiments conducted with glass beads lead to a formula that relates field gradient to distance from the center of the sphere.[143]

$$G(r) = K(B_0)\,\Delta_\chi\, r_0^2 / [(r_0^2 + r_0 r + r^2)r] \qquad (23)$$

where K is a constant, Δ_χ is the difference in magnetic susceptibility between inside and outside, r_0 is the radius of the spheres, and r ($r > r_0$) the distance from the center of the sphere to the point at which G is measured. Figure 5 illustrates the situation diagrammatically and highlights the fact that since erythrocytes are not spherical, there could be some intracellular gradients.

Information regarding cell shape may also be obtained from extensions to this type of analysis. In addition, the presence of paramagnetic centers, such as vesicles with ingested

Downloaded At: 15:58 17 January 2011

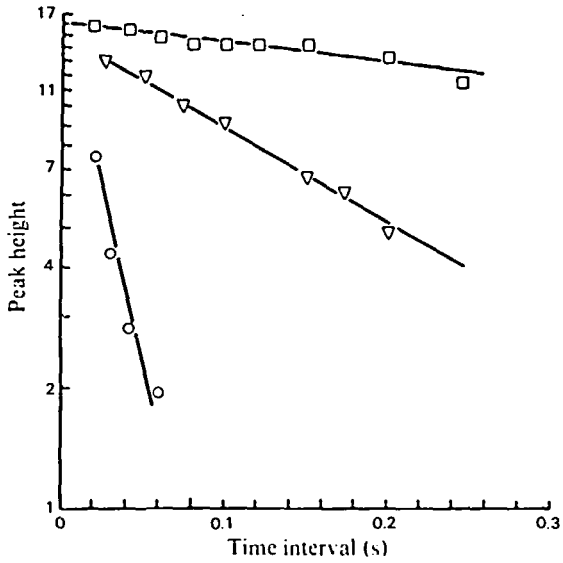

FIGURE 4. Effect of diffusion on spin-echo amplitude. The height of the CH_2 resonance of glycine observed in spin-echo experiments as a function of the time interval between the $\pi/2$ pulse and the start of data acquisition. The experiment is arranged so that essentially all the glycine is outside the erythrocyte. Other conditions were temperature, 293 K; haematocrit, 84%; $[glycine]_{out}$, 75 m*M* O, simple $\pi/2-\tau-\pi-\tau$ sequence on the suspension of cells ($[Dy\text{-}DTPA]_{out}$ 0.15 m*M*); ∇, multiple-pulse sequence (Carr-Purcell-Meiboom-Gill) on the same sample; □, a control experiment on a cell-free solution of glycine (12 m*M*) and Dy-DTPA (0.15 m*M*) using a $90° - \tau = 180° - \tau$ sequence. (From Brindle, K. M., Brown, F. F., Campbell, I. D., Grathwohl, C., and Kuchel, P. W., *Biochem. J.*, 180, 37, 1979. With permission.)

Downloaded At: 15:58 17 January 2011

Mn^{2+} complex or colloidal Fe^{3+},[144] could disturb the simple picture given here and yield information on intracellular organelles and compartmentation.[48]

The Δ_χ across erythrocytes has been altered by use of complexes of Dy^{3+}-DTPA[48] and Fe^{3+}-desferrioxamine.[48,66] Also, since deoxy- and met-Hb are paramagnetic it is possible to alter Δ_χ from *within* the erythrocytes.

Alanine transport measured by this method indicated the expected marked stereospecificity; $t_{1/2}$ for D- and L-alanine under the conditions was 40 ± 2 min and 10 ± 0.5 min, respectively.[48] Pyruvate transport rates showed significant variability between blood samples from different donors, and lactate transport gave a $t_{1/2}$ of 60 ± 3 sec.[48]

Figure 6 shows the results of an experiment in which choline was added to a suspension of erythrocytes in ^2H_2O Krebs bicarbonate ringer. Super addition of Fe^{3+}-desferrioxamine caused a large reduction in the $-N(CH_3)_3$ proton resonance. The time course of choline influx to the erythrocytes was followed by elevation of the resonance over a 10-hr period; the data yielded a rate constant of 160 ± 30 $\mu mol\ell^{-1}$ cells h^{-1},[66] consistent with radiotracer methods.

The technique holds promise for the study of membrane transport defects that occur in such conditions as manic-depressive psychosis. The requirement for only 0.5 mℓ of cells, and a minimum of manipulations, make it an appealing clinical-chemistry method.[66]

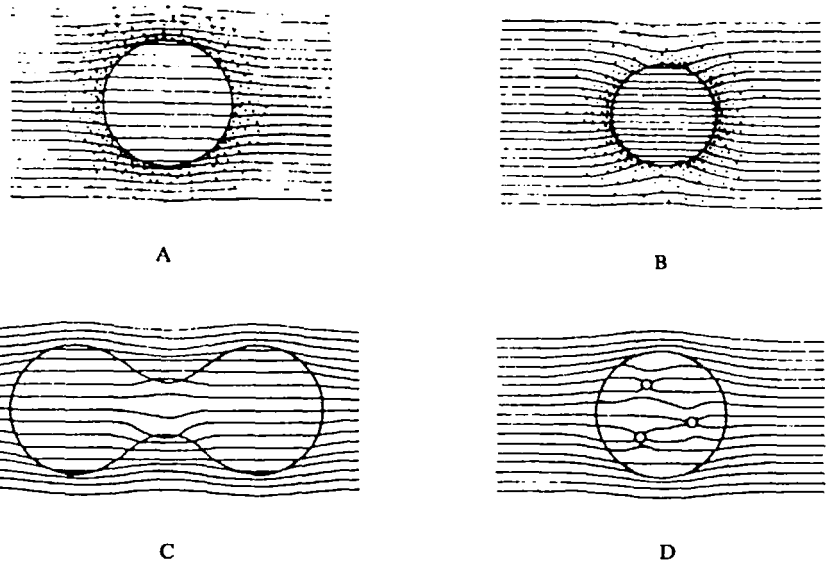

FIGURE 5. Magnetic field in particle suspensions. Illustration of the effects of different magnetic susceptibility on the lines of magnetic flux in different geometries: (A) $\chi_{in} < \chi_{out}$; (B) $\chi_{out} > \chi_{in}$; (C) Representations of lines of flux in the erythrocytes; (D) Representation of field within cell containing vesicles of different susceptibilities. (From Brindle, K. M., Brown, F. F., Campbell, I. D., Grathwohl, C., and Kuchel, P. W., *Biochem. J.*, 180, 37, 1979. With permission.)

Downloaded At: 15:58 17 January 2011

VI. ^{1}H NMR STUDIES OF CELL METABOLISM

A. Introduction

The ubiquity of ^{1}H nuclei leads to conventional ^{1}H NMR spectra of whole cell samples being rather featureless broad envelopes, due to overlap of a multitude of resonances.[145-147] Furthermore, the water in untreated samples is around 80% of the total mass ($\approx$44 *M*) and ensures that the water resonance is enormous in comparison with other substances. The integral of the water peak in untreated cells is $\approx 10^5$ that of metabolites. This often leads to the dynamic range of the data-storing computer being exceeded before an acceptable signal is detected from the small molecules.

Selective irradiation of water at its Larmor frequency can be used to, at least partially, saturate the water spins and reduce the peak in the spectrum.[9,148] The water suppression pulse is usually gated off during data acquisition. For cells in pure ^1H_2O media an excessive amount of RF power is required to totally eliminate the water peak. This region of the spectrum adjacent to the water is often severely distorted, so samples are often washed in media constituted from ^2H_2O.[48,66,145-147] However, the recently demonstrated anomalous, frequency dependence of T_1 and T_2 of water is particularly evident at 400 MHz; this ensures a small H_2O peak even in samples with no ^2H_2O,[112] at this frequency.

The procedures for the identification of unassigned resonances involve the use of model compounds which can be added to the sample and the number, multiplicity, and chemical shifts of the resonances noted. More detailed assignments have been made by studying CP spin-echo spectra as a function of τ and by double resonance methods.[146,147]

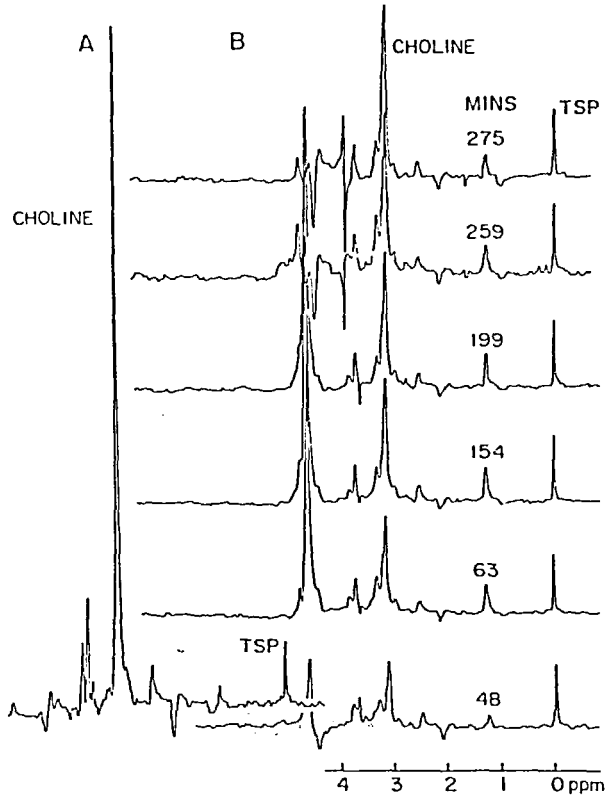

FIGURE 6. Choline uptake by erythrocytes. 0.5 mℓ of erythrocytes washed with ^2H_2O Krebs medium. Desferrioxamine-Fe^{3+} (0.317 μmol), glucose (5 μmol), and choline (6.0 μmol) were added to 0.5 mℓ of cells of cytocrit 0.92. 1024 transients were collected per spectrum. (A) The spectrum obtained before the addition of the desferrioxamine-F^{3+}; (B) The spectra obtained from accumulation of transients starting at the time of the addition of the desferrioxamine-Fe^{3+}. A sample of spectra in the time course is given here. (From Jones, A. J. and Kuchel, P. W., *Clin. Chim. Acta*, 104, 77, 1980. With permission.)

The chemical shifts of compounds have been given relative to tetramethylsilane (TMS), but since this is not water soluble, secondary standards such as 2,2-dimethyl-2 silapentane-5-sulfonate (DSS)[146] or sodium [2,2,3,3,-^{2}H] 3-trimethyl silylpropionate (TSP) have been used.[66] They have been used as internal standards in the solutions or externally in a coaxial capillary in the sample tube.

B. Erythrocytes

The erythrocyte epitomizes the differentiated cell. It has no nucleus or cytoplasmic organelles and yet it normally survives for a mean of 120 days in the circulation. Despite its structural simplicity it possesses a vast array of enzymic activities.[150] The most important for its survival are those of the anaerobic glycolytic pathway and the pentose phosphate pathway (PPP). The former produces a net 2 mol of ATP and lactate per mole of glucose metabolized. The ATP is used primarily to supply energy to maintain Na^+ and K^+ ion transport and cell shape. The PPP diverts glucose 6-phosphate via two redox reactions with the reduction of NADP. Glutathione reductase catalyzes the reduction of

Downloaded At: 15:58 17 January 2011

oxidized glutathione (GSSG) by NADPH to reduced glutathione (GSH). Because of its lower redox potential, GSH is involved in many reduction reactions in the cell, such as the maintenance of the active site -SH group of glyceraldehyde 3-phosphate dehydrogenase in the reduced form.[151-153]

A considerable amount of information has been collated on the steady-state concentrations of metabolites in erythrocytes, obtained by conventional biochemical techniques, and used in the development of computer simulations of erythrocyte-glycolysis.[154-157] NMR more than any other method has the potential to contribute to the understanding of the processes as they occur *in situ*. ^{31}P NMR spectra of human erythrocytes contain resonances due to 2,3-diphosphoglycerate (23DPG), ATP, inorganic phosphate (P_i), and sugar phosphate; the last is of such low concentration that quantitation from the spectra is not yet possible with current spectrometer sensitivities.

Thus, ^{31}P NMR alone does not provide very much information on erythrocyte glycolysis, although the data do relate to the intact system. ^{1}H NMR contributes a little more to matters directly related to the dynamics of the PPP and glycolysis.

Figure 7 shows a simple ^{1}H NMR spectrum of starved human erythrocytes washed in $^{2}H_2O$ Krebs Ringer solution at 37° C obtained at 270 MHz. Figures 7B and 7C illustrate the result of applying the CP pulse sequence; the broad envelope of resonances, attributed mostly to proteins, was eliminated when a delay, τ, of 60 msec was used. This occurs because the short T_2 values of the relatively immobile species ensure that the spin-echo amplitude at 60 msec is small (Equation 11). In addition, at this value of τ peaks arising from singlets and triplets (2n + 1-lets) of most of the small molecules are upright while doublets (2n-lets) are inverted.

A remarkable amount of detail is seen in the spin-echo spectra of human erythrocytes at 270 MHz,[48,146,147] and even more using the newer 400-MHz spectrometers.[158] All of the major resonances in the spectrum have been assigned,[146,158] and some of the details are given in Figure 8. The higher resolution seen in the later studies at 400 MHz enabled further assignments to be made in for example the $-N^{+}(CH_3)_3$ region just upfield of ergothioneine (3.2 ppm); the two resonances arise from choline[66] and carnitine[66a] and are in the expected ratios for plasma (although the cells were washed in Ringer solution).

The [2-H] and [4-H] histidyl resonances of hemoglobin are well resolved in the low field aromatic region of the ^{1}H NMR spectrum.[146] The relative amplitudes and chemical shifts are pH dependent and have been used to determine the intracellular pH. The pH was estimated to be 7.4,[146] using titration data obtained on purified human hemoglobin.[159] Anaesthetic gases interacted with hemoglobin and induced spectral perturbations that were seen also in whole erythrocytes.[159] This suggested that the hypotheses of anaesthetic action at a molecular level, based on in vitro studies, apply equally well to the intact cell.[159]

The time course of the glucose-dependent reduction of glutathione, after its oxidation by t-butylhydroperoxide, can also be monitored in erythrocyte suspensions. The reduction normally takes $\approx$30 min for completion and was detected by the reemergence of the dispersive [3-H] cystinyl resonance and a regrowth of the [2-H] glycyl line.[146]

The conversion of glucose to lactate has been followed in $^{2}H_2O$ Krebs medium by noting a decline in amplitude of the glucose resonances, with a concomitant growth of the [3-H] resonance of lactate. A similar experiment, but conducted in $^{1}H_2O$ Krebs medium, and employing high-power water suppression (Section VI.A), yielded a lactate resonance larger in amplitude but of opposite phase to the lactate in the $^{2}H_2O$ medium. In $^{2}H_2O$ medium, solvent exchange at the triose phosphate isomerase (TIM) and aldolase catalyzed reactions leads to deuteration of glyceraldehyde 3-phosphate (GA3-P) and thence to the aldehydic ^{2}H being introduced onto NAD^{+} at the glyceraldehyde 3-phosphate dehydrogenase (GAPDH) step. Ultimately, at the lactate dehydrogenase (LDH) step, the ^{2}H is transferred onto the C-2 of pyruvate to give deuterated lactate.

Downloaded At: 15:58 17 January 2011

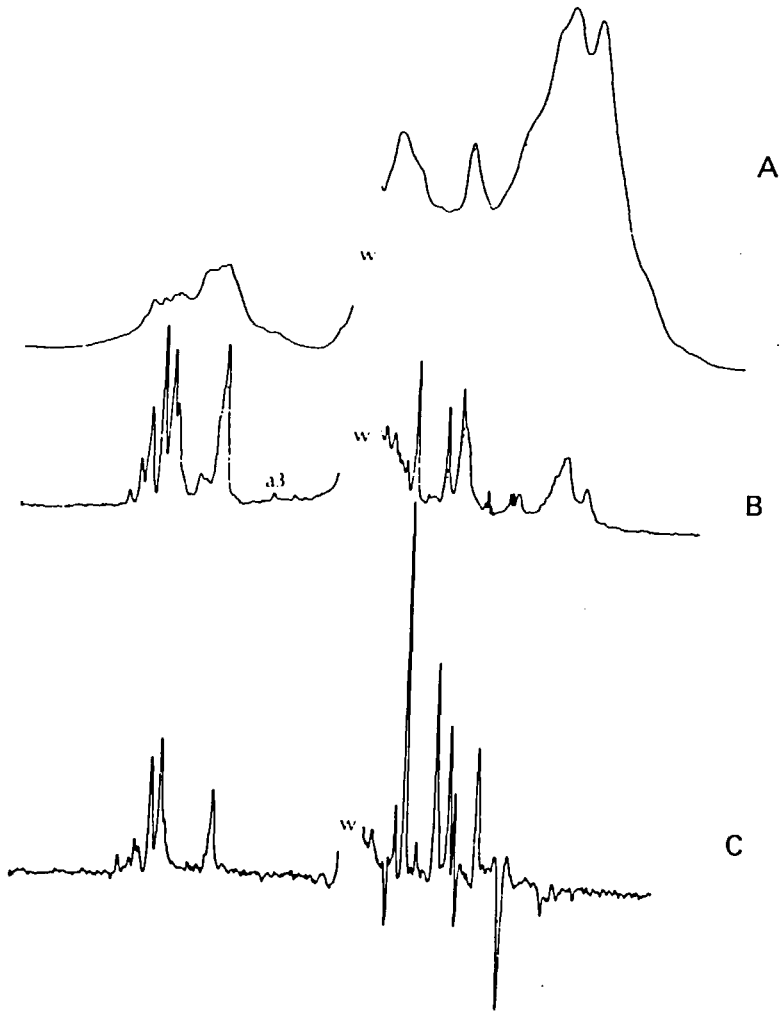

FIGURE 7. 270 MHz ^1H spectra of glucose-depleted erythrocytes at 37°C. (A) Normal Fourier transform spectrum; (B) spectrum obtained using a $\pi/2$-τ-π-τ spin-echo sequence with τ = 20 msec; (C) spin-echo spectrum with τ = 60 msec. (From Brown, F. F., Campbell, I. D., Kuchel, P. W., and Rabenstein, D. L., *FEBS Lett.*, 82, 12, 1977. With permission.)

In contrast, in H_2O medium the lactate is fully protonated with resulting homonuclear coupling between [2-H] and [3-H] lactate protons; this results in the doublet character of the [3-H] proton line, and at τ = 60 msec in the spin-echo spectrum gives an inverted peak.[47,146] In the ^2H_2O medium, with [2-^{2}H] lactate, no homonuclear coupling occurs and an upright singlet is seen. Furthermore, the reduced amplitude of the [3-H] lactate peak is due to some deuteration at the C-3 during glycolysis. Lactate assayed by conventional enzymatic means indicated approximately equal rates of glycolysis by human erythrocytes in both media, and the deuteration reactions can all be accounted for on the basis of known stereospecificity of the dehydrogenases involved.[146]

The resonance of protonated lactate added to a suspension of erythrocytes in ^2H_2O Krebs medium undergoes a 180° change in phase over a time course lasting 10 to 15 min. The reaction being followed is the LDH catalyzed deuteration of [2-C] of lactate via its reversible conversion to pyruvate in the presence of NAD(^{2}H)^{1}H, NAD(^{2}H)^{2}H.[148]

Downloaded At: 15:58 17 January 2011

Downloaded At: 15:58 17 January 2011

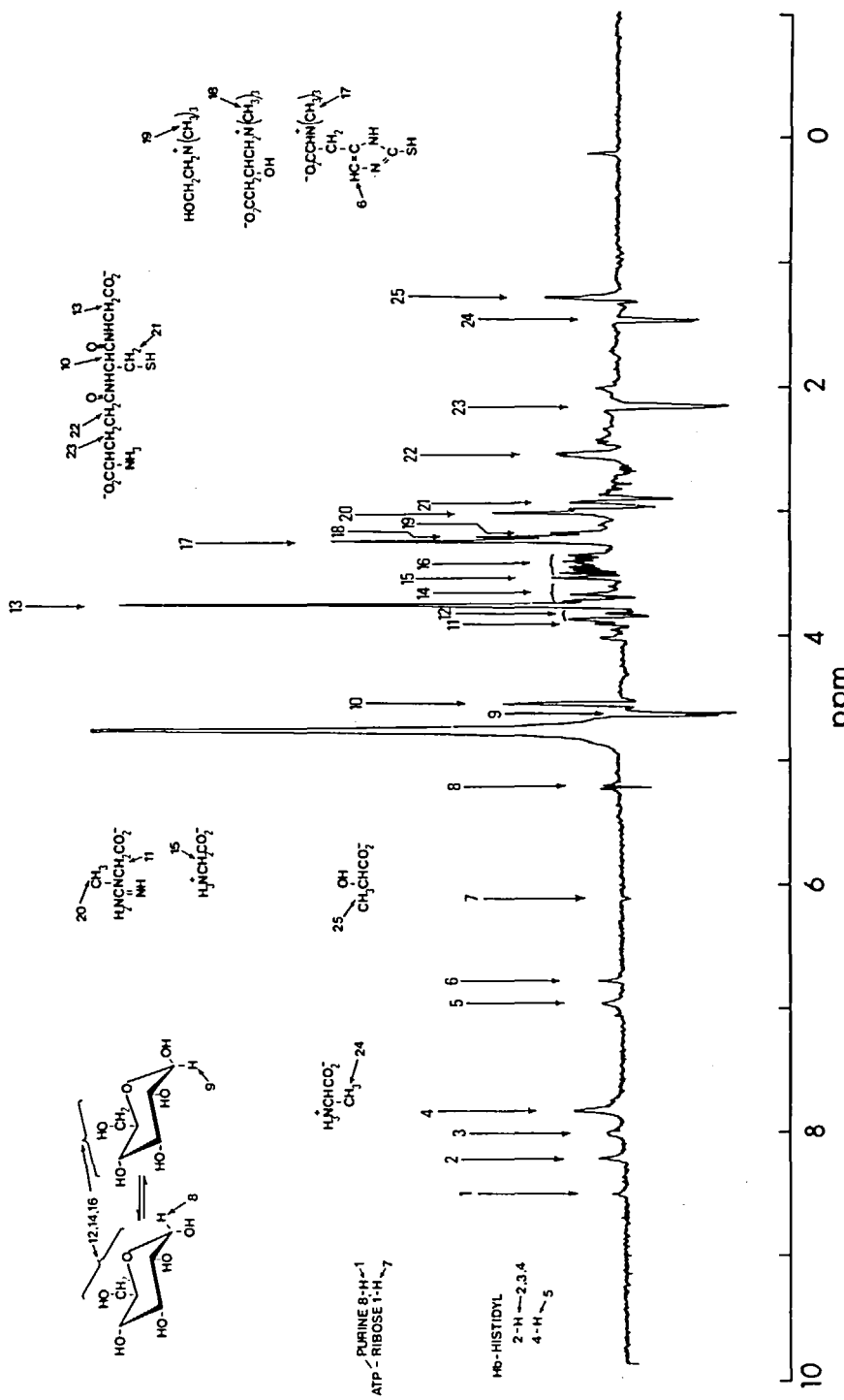

FIGURE 8. 400 MHz ^{1}H spin-echo (τ = 60 msec) FT NMR spectrum of intact human erythrocytes at 25°C. The packed cells were washed four times in ^2H_2O solution containing 0.154 *M* NaCl and 5 m*M* glucose. The chemical shift is referenced to TMS. The resonances in the spectrum have been assigned, as indicated in the figure and as discussed in the text, to the following compounds: alanine 24; ATP 1, 7; carnitine 18; choline 19; creatine 11, 20; ergothioneine 6, 17; glycine 15; glucose 8, 9, 12, 14, 16; glutathione 10, 13, 21, 22, 23; hemoglobin-histidyl residues 2, 3, 4, 5; lactate 25. (Basic spectrum kindly supplied by Professor D. L. Rabenstein.)

Clearly, this exchange process requires the reduction and deuteration of pyridine nucleotides by the GAPDH-TIM-adolase reactions. Thus, the *in situ* activity of LDH and the rate of NADH supply to LDH can be monitored using this methodology. Preliminary studies of erythrocytes from sufferers of heritable hemolytic anemia, with known enzyme defects, have been carried out in order to assess the value of the method for the detection of enzymic defects.[146a]

If erythrocytes incubated in ^2H_2O medium, with glucose, are allowed to deplete their substrate, then the [3-H] lactate resonance grows as expected, but then declines. This process is not one of lactate degradation (since assays for lactate confirm its presence) but of ^2H exchange at [3-C] of the lactate.[146,147,158] The chemistry of the reaction is still being investigated.

Dihydroxyacetone[160] and inosine[161] are alternative substrates for erythrocyte glycolysis and enter the main pathway via reasonably well-understood reactions. ^1H spin-echo NMR has been used to follow the decline of the well-resolved resonances of these chemical species and the subsequent emergence of a [3-H] lactate peak. For instance, metabolism of inosine is seen as a decline in the purine [8-H] peak and concomitant elevation of the [2-H] purine and [3-H] lactate peaks.[66a]

Turnover of the glutathione residues has been followed in human erythrocytes, at 25°C. Glucose and perdeuterated glycine (which is undetected by ^1H NMR) were added to the cells. Over a period of 14 hr the [2-H] resonance of glycine at 3.54 ppm increased in intensity, while there was a (slight) drop in the glycyl(α-CH_2) resonance of the glutathione. The inequality of changes in peak amplitude (growth and decline, respectively) was attributed to different attenuation of the resonances in the spin-echo experiment owing to different T_2 values.[158] A similar experiment was conducted with perdeuterated glutamic acid, and incorporation into glutathione was detected by a decline in the intensities of the β-CH_2 and γ-CH_2 resonances, with elevation in the free glutamate signals. In agreement with other non-NMR studies, this rate was considerably slower than that for glycine-glutathione exchange.[158]

^1H spin-echo NMR can be used to assay intraerythrocyte compounds and has been applied to the determination of choline concentrations in erythrocytes from psychiatric patients treated with lithium salts. The latter is one accepted form of therapy for manic-depressive psychosis and schizo-affective disorders and leads to an accumulation of choline in erythrocytes; its molecular mode of action is as yet unknown.[66] Figure 9 shows the $-N^+(CH_3)_3$ region of a series of spectra from nine psychiatric patients. It can be seen that the choline peak amplitudes bear little correlation with the serum lithium concentration. It is therefore interesting to speculate whether choline levels are not a better index of a likely successful therapeutic outcome than the lithium levels.

The ease and rapidity of assaying metabolites like choline using the ^1H NMR method which requires only 0.5 mℓ of cells is appealing to clinical chemists.

C. Other Tissues

^1H NMR studies of tissues and cells other than erythroctyes have not yielded the same detail in terms of kinetic information or identification of intracellular metabolites. Some of the earliest work focused on storage tissues and vesicles from them, because signals were readily obtained.[145,162]

The adrenal cortex from rats gave a simple spectrum from unsaturated fats with little evidence of the steroids that are supposed to be present.[145,162] In fact, 50% of the mass of the cortex is alleged to be cholesterol which must be relatively immobile compared with the unsaturated fats. However, a resonance at 0.7 ppm was assigned to the 18-methyl group of cholesterol.

Adrenal medullas from rat, pig, and sheep gave complex spectra, which were simplified and resolution-enhanced, by removal of the broad lines, using a computational (digital

Downloaded At: 15:58 17 January 2011

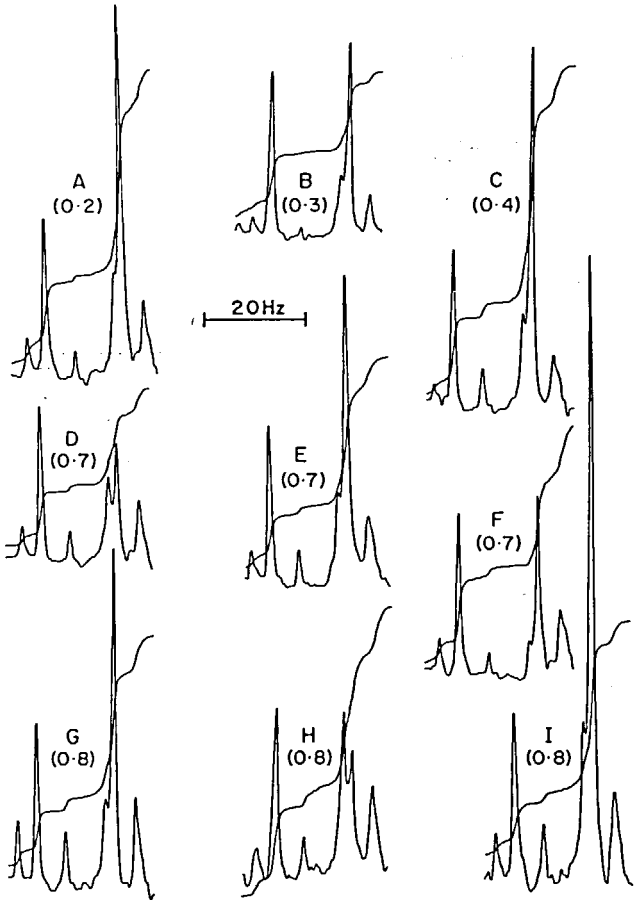

FIGURE 9. Erythrocytes from lithium-treated manic depressive patients. 0.5 mℓ of ^2H_2O washed cells with cytocrits of 0.90 ± 0.02; 1024 transients per spectrum. Only the region of the α-CH_2 peak of glutathione and that of the $-N^+(CH_3)_3$ of choline is shown. The serum lithium concentrations and estimates of intracellular choline were (m*M*): (A) 0.2, 3.9; (B) 0.3, 2.0; (C) 0.4, 3.8; (D) 0.7, 1.7; (E) 0.7, 3.3; (F) 0.7, 1.8; (G) 0.8, 3.6; (H) 0.8, 1.2; (I) 0.8, 6.5. (From Jones, A. J. and Kuchel, P. W., *Clin. Chim. Acta*, 104, 77, 1980. With permission.)

signal processing) technique known as convolution difference.[9] By comparison ^{31}P NMR spectra of adrenal medulla and chromaffin granules showed large amounts of ATP (Section VII.D) and other measurements indicated large amounts of catecholamines.

At 270 MHz using convolution difference ^1H spectroscopy, both of these compounds were detected: ATP resonances were [8-H] at 8.30 ppm, [2-H] 7.95 ppm, [1-H] 5.89 ppm, and the adrenaline resonances were -CH_2- 6.78 (broad) ppm, -CH_3 3.10 and 2.69 ppm. The spectra obtained from granules were identical with those from whole tissue, thus supporting the notion that the granule-isolation procedure was satisfactory.

Incubation of slices of adrenal medulla at 50° C caused a time-dependent elevation and sharpening of the aromatic and aliphatic adrenaline resonances, consistent with its release from the more rigid ordering inside the granules.[145]

Chromogranin A, a protein from chromaffin granules, has been isolated and purified and shown to be predominently in the random coil configuration in free solution. ^1H NMR spectra of the pure protein and of granules were shown to be the same. This

Downloaded At: 15:58 17 January 2011

observation together with the finding that the protein has similar T_1 and T_2 values for its resonances suggested that in vivo it is in the random coil form as well. The *in situ* random coil character of the egg phosphorous storage protein phosvitin was also confirmed using ^{1}H NMR.[145]

The salivary gland of octopus gave a ^{1}H NMR spectrum with a large resonance in the aromatic region (≈8.7 ppm) which was assigned, on the basis of its chemical shift and pH titration, to a nicotinamide species. Also, large -N-$(CH_3)_n$ resonances were detected in these screening studies but no further analysis was performed.[145] Brain slices, among other tissues, also showed a major group of signals at 8.0 ± 3.0 ppm thought to be due to nucleotides.[145]

In conclusion, it can be said that no detailed studies have developed using ^{1}H NMR to study tissues other than erythrocytes, but many interesting preliminary observations have been made.

D. Microorganisms

The ^{1}H NMR work on microorganisms is interesting from the point of view of the NMR technique that was first used to study them.[163] The technique known as correlation spectroscopy subjects the sample to a fast linear frequency sweep of RF power followed by Fourier deconvolution of the resulting signal. The deconvolution uses the signal obtained from a similar fast sweep of a substance with a single resonance, such as TSP.[164,165] Elimination of the water resonance, and in theory any other resonances, can be achieved by tailoring of the sweep to leave out the requisite frequencies. This, in fact, was the original stimulus for the development of the technique and the reason for its value in the study of aqueous suspensions of cells. Other methods of solvent suppression are now equally effective.[148]

Using the pH dependence of the chemical shifts and model compounds, the following metabolites were identified in *Escherichia coli* using correlation spectroscopy: succinate, pyruvate, acetate, lactate, ethanol, and formate. The concentrations detected ranged down to 0.1 m*M* and were followed in a time study that extended for 7 hr in which glucose was the substrate.[163]

No further ^{1}H NMR work on *E. coli* has come to this author's attention, but it appears that *E. coli,* and indeed other microorganisms such as yeast, could be studied using the somewhat simpler (in terms of set-up time and computation) but equally revealing CP spin-echo method.

VII. ^{31}P NMR STUDIES OF CELL METABOLISM

A. Overview

The first report of ^{31}P NMR studies of whole tissue was that of Moon and Richards,[4] on human erythrocytes. Since that time a large body of literature on the subject has appeared and recent reviews are numerous.[4,6,7,166-168]

The currently attainable sensitivity and resolution in studies on whole cells is exemplified by the work of Shulman's group on *E. coli* suspensions.[168,169] Improved sensitivity and S/N have been obtained as a result of a thorough understanding of the factors affecting these features, in particular, in the ^{31}P spectrometer[5] (Section II.C). Figure 10 is a typical ^{31}P NMR spectrum of *E. coli* and is indeed similar to those obtained from muscle of various sources.[149,170-175] Although the domain of chemical shifts for ^{31}P nuclei is large (600 ppm: for tables see References 27 and 176), the shift range of biological phosphorous compounds extends over only ≈40 ppm (Table 1); this is because the compounds are virtually all phosphate esters. The chemical shifts of phosphorous compounds identified in a diverse range of tissues have been tabulated,[9,167] and the most complete current list is given in Table 3.

Downloaded At: 15:58 17 January 2011

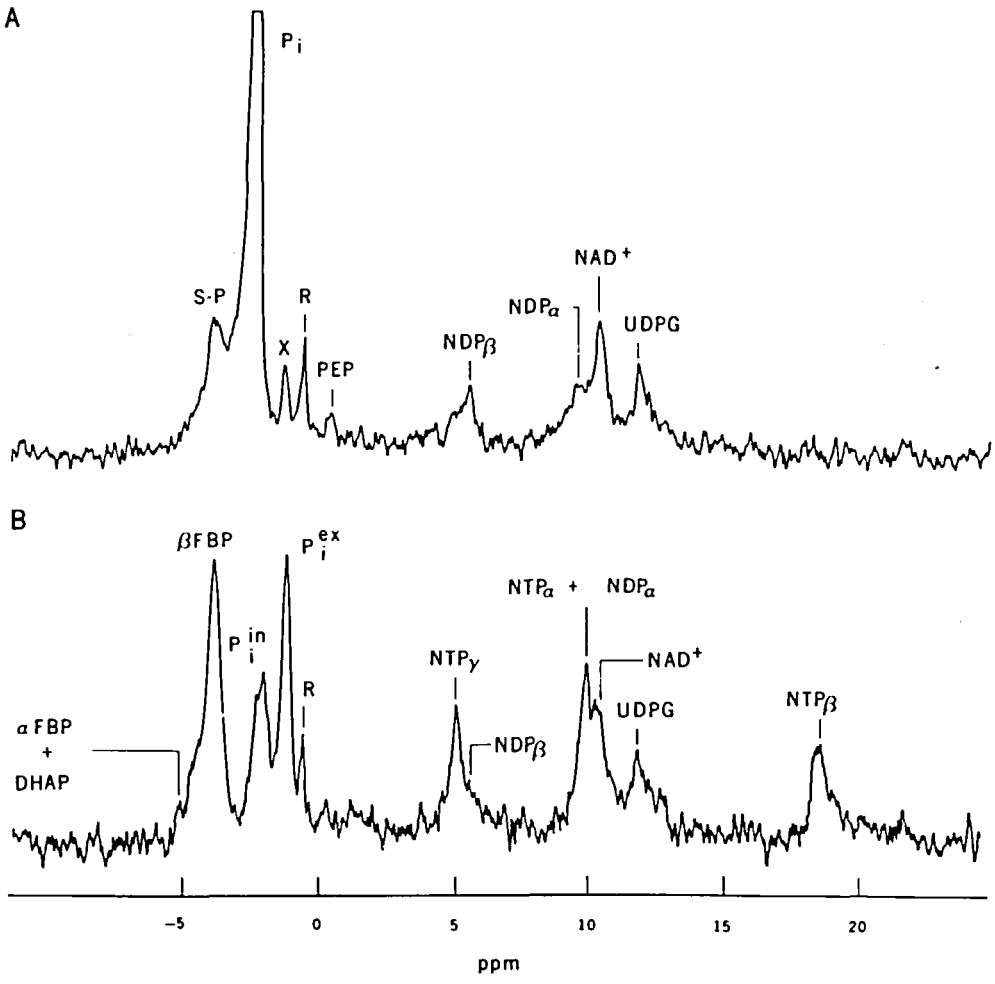

FIGURE 10. ^{31}P NMR of *E. coli*. ^{31}P NMR spectra at 145.7 MHz of an anaerobic *E. coli* suspension containing 5×10^{11} cells per milliliter (A) before and (B) 4 to 6 min after glucose addition. Each spectrum was the sum of 400 scans with a repetition time of 0.34 sec and a 45° RF pulse. Abbreviations: S-P, sugar phosphates; P_i, inorganic phosphate; P_i^{ex}, P_i^{in}, external and internal P_i, respectively; PEP, phosphoenolpyruvate; NDP, nucleoside diphosphate; NAD^+, nicotinamide adenine dinucleotide; UDPG, uridine diphosphate glucose; FBP, fructose 1,6-bisphosphate; DHAP, dihydroxyacetone phosphate; NTP, nucleoside triphosphate; and R is the reference signal from 0.1% orthophosphoric acid in 0.1 *M* HCl. X is unassigned. (From Shulman, R. G., Brown, T. R., Ugurbil, K., Ogawa, S., Cohen, S. M., and Den Hollander, J. A., *Science*, 205, 160, 1979. Copyright 1979 by the American Association for the Advancement of Science. With permission.)

The generally accepted ^{31}P reference compound is 85% inorganic orthophosphoric acid (H_3PO_4) but it, of course, must be used as an external standard in a glass capillary. There has been some discussion on the use of the very stable secondary standard, aqueous tetrahydroxy phosphonium perchlorate, because of its extremely narrow line, 0.067 ppm, upfield of H_3PO_4.[178] However, a common ploy, in muscle studies at least, is to use the endogenous phosphocreatine PC_r as the secondary reference; the pK_a of this phosphate is 4.6 and therefore not subject to significant chemical shift variation with the pH changes found in biological systems.[170,173]

Peak assignment can follow several paths[9] (Section VI.A), but one simple method has been to add a known compound to a perchloric acid extract of the tissue. Coincidence of the resonance line(s) of the added material and that of the signal from the sample is

Downloaded At: 15:58 17 January 2011

Table 3
CHEMICAL SHIFTS OF PHOSPHORUS METABOLITES IN WHOLE TISSUES AT pH ~7.0

Metabolite[a]	Chemical shift[b] (ppm)
Phosphonate in snail eggs	~22
DHAP	4.5
α-P of FDP	4.4
GAP and glucose 6-phosphate	4.2
β-P of FDP	3.8
AMP, IMP	3.7
PEt	3.4
3-P of DPG	3.3
PCh	3.1
2-P of DPG, F6P	2.6
P_i	2.2
Phosphoprotein in frog eggs	~1.0
GPE, GPS	0.4
GPC	−0.1
Sphingomyelin and phosphatidyethanolamine	−0.3
SEP	−0.4
Phosphatidylcholine and PEP	−0.9
PCr	−3.0
PArg	−3.5
γ-P of ATP	−5.7
γ-P of UTP	−5.8
β-P of ADP	−6.1
α-P of ADP	−10.4
α-P of ATP	−10.8
α-P of UTP	−10.9
NAD	−11.3
Unknown diphosphodiester	−11.5; −13.0
β-P of ATP (Mg bound)	−19.5
β-P of ATP	−21.2
β-P of UTP	−21.3
Polyphosphates (yeast)	>−22

[a] Abbreviations: ADP, adenosine 5'-diphosphate; AMP, adenosine 5'-monophosphate; ATP, adenosine 5'-triphosphate; DHAP, dihydroxy acetone phosphate; DPG, 2,3-bisphosphoglycerate (23DGP); FDP, fructose 1,6-bisphosphate (F16P); F6P, fructose 6-phosphate; GAP, glyceraldehyde 3-phosphate (GA3-P); GPC, sn-glycerol 3-phosphorylcholine; GPE, sn-glycerol 3-phosphoryl ethanolamine; GPS, sn-glycerol 3-phosphoryl serine; IMP, inosine 5'-monophosphate; NAD, nicotinamide adenine dinucleotide; PArg, phospho-arginine; PCh, phosphoryl choline; PCr, phosphocreatine; PEP, phosphoenol pyruvate; PEt, phosphatidylethanolanine; Pi, inorganic phosphate; SEP, serine ethanolamine phosphodiester; and UTP, uridine 5'-triphosphate.

[b] Chemical shifts are reported as downfield shifts with respect to 85% orthophosphoric acid.

From Burt, C. T., Cohen, S. M., and Bárány, M., *Ann. Rev. Biophys. Bioeng.*, 8, 1, 1979. With permission.

Downloaded At: 15:58 17 January 2011

usually sufficient to identify an unknown compound.[174,179] Alternatively, in regions of closely packed lines, such as in the hexose-phosphate and orthophosphate regions of the spectrum, the assignments have been reinforced by selectively shifting the resonance of interest with respect to other compounds by judicious adjustment of pH, or ionic strength or both, or by changing the counter cation.[173,180]

Having identified a chemical compound in a spectrum it is useful to determine its concentration and what follows is applicable to any nucleus. In ^{31}P NMR the S/N is improved if a large number of transients are collected in as short a time as possible. This can be achieved by using an RF pulse of a duration such that the tilt angle of the macroscopic spin vector is less than $\pi/2$. However, because many phosphorous compounds have a long T_1, of the order of 16 sec, the rapid pulsing causes partial saturation of the spins and therefore gives smaller peak areas than otherwise expected. Additionally, peak areas in spectra are only proportional to the concentrations of the metabolites if all resonances have the same T_1. Therefore, to obtain true concentrations correction factors that are dependent on T_1 values for each metabolite have been evaluated.[149,175] The values were obtained by using sample compounds and measuring the peak areas as a function of pulse-repetition rate. Extrapolation to long times gave the maximal peak area.[149,175,181]

A second method has been to insert a capillary containing a compound of known concentration and chemical shift into the sample. Assuming that the spin-relaxation characteristics in the tissue and the buffered sample are identical,[173] the peak area of the reference can be compared with that of the metabolite in the sample and with a similar sample tube containing a known concentration of the metabolite in a chemical environment similar to that of the tissue. From the ratios of the metabolite peak areas in the tissue and in free solution, normalized with respect to the signal from the reference capillary, the *in situ* concentration of the metabolite can be evaluated.[66,173]

Like the ^1H NMR method (Section VI.B), ^{31}P NMR has been used to determine noninvasively the intracellular pH;[4,170,173,183,184] other methods have relied on the distribution of weak acids,[185] bases, and microelectrodes[186] and they have agreed in general with the measurements made by NMR. The most commonly used ^{31}P NMR method relies on the facts that (1) the pK_a of the following reaction is 6.9, (2) insensitive to ionic strength (−0.1 pH unit in KCl domain 0.1 to 0.2 *M*):[187]

$$HPO_4^{=} + H^+ \rightleftharpoons H_2PO_4^-$$

(3) the chemical shift difference ($\Delta\delta$) between the two phosphate forms is 2.3 ppm,[175] and (4) the two forms are in rapid chemical exchange[9] on the NMR time scale. The Pi peak is then a weighted average of contributions from the two resonances and the position of its maximum ordinate is therefore an index of pH and is accurate to about 0.06 pH units.

A slightly different approach was used by Moon and Richards[4] who performed titrations on several phosphate metabolites and measured the intracellular pH of human erythrocytes using the relative shifts of the two phosphates of 23DPG (See Figure 11A and B). Erythrocytes contain high concentrations of 23DPG so this is a useful indication therein, but other tissues such as muscle have little of it so the Pi method is usually used.

B. Blood Components

The first ^{31}P NMR studies on human erythrocytes focused attention on the −4 to 2 ppm region of the spectrum wherein lie resonances of 23DPG Pi (two lines: one line due to intra- and the other extracellular Pi) and lipid phosphate.[4] The latter resonance has been assigned to serum phospholipids,[189] and not membrane phospholipids as was previously thought.[4] The time-dependent hydrolysis of 23DPG manifested itself as a decline in the

Downloaded At: 15:58 17 January 2011

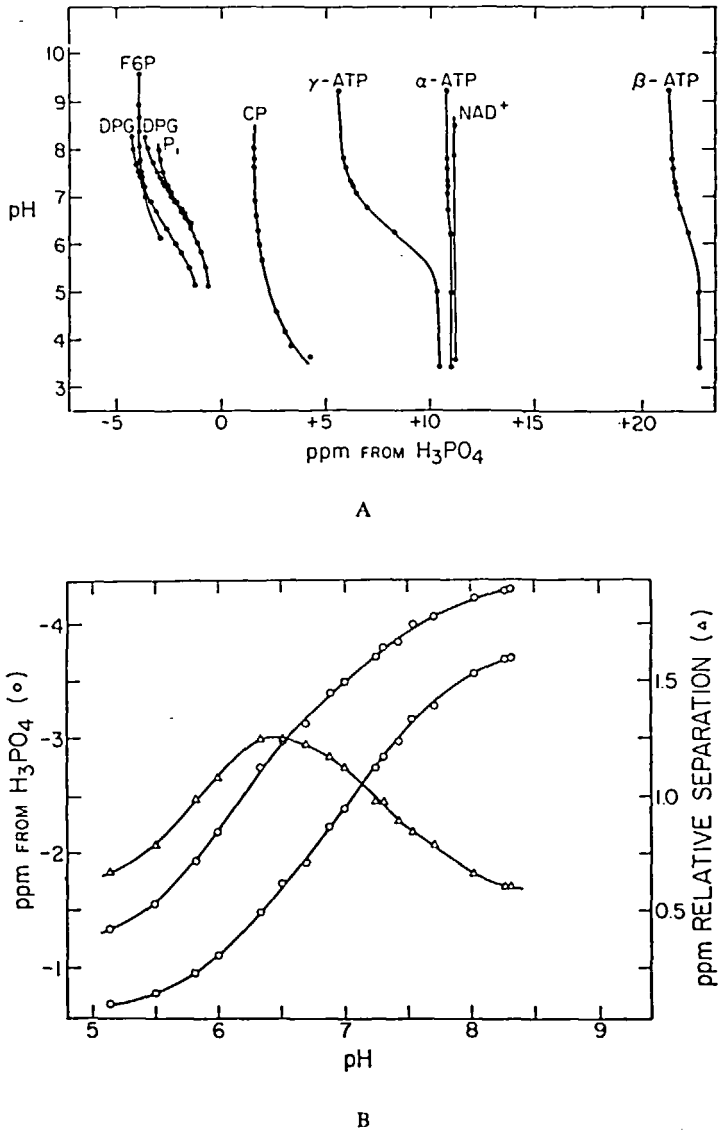

FIGURE 11. Chemical shift behavior of some biological organic phosphates. (A) Chemical shifts are reported relative to external 1.0 *M* phosphoric acid. F6P, fructose 6-phosphate; DPG, 2,3-diphosphoglycerate; CP, carbamyl phosphate. (B) The detailed pH-dependent chemical shift behavior of 2,3-diphosphoglycerate. Absolute shifts from external H_3PO_4 are indicated on the *left ordinate* while the relative separation of the ^{31}P resonances are shown on the *right*. The *upper* and *lower* titration curves correspond to phosphates at positions 3 and 2 of 2,3-diphosphoglycerate, respectively. (From Moon, R. L. and Richards, J. H., *J. Biol. Chem.*, 248, 7276, 1973. With permission.)

relevant resonances with a concomitant rise in the Pi peak over ≈26 hr at 25°C. Furthermore, incubation of the cells under conditions known to (1) enhance 23DPG levels (10 m*M* inosine, 10 m*M* phosphate)[191] or (2) decrease them (storage in acid-citrate-dextrose medium) indicated for the first time that ^{31}P NMR can be used to follow metabolic processes.[189]

A systematic comparison between the NMR method and biological (enzymatic) assays

Downloaded At: 15:58 17 January 2011

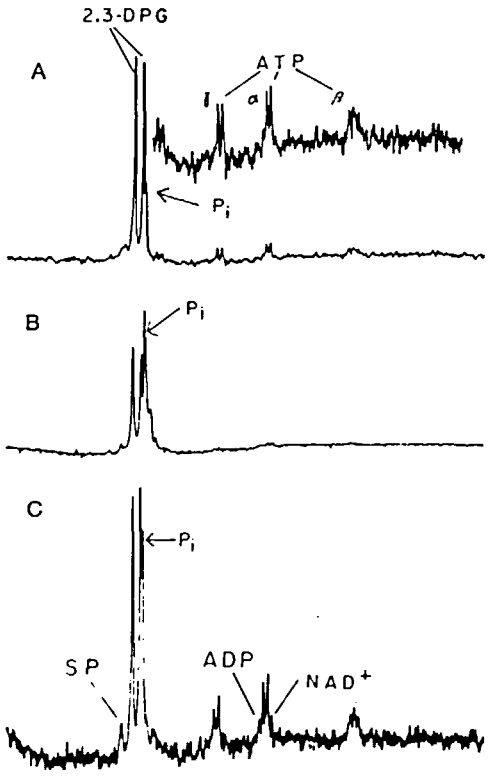

FIGURE 12. ^{31}P NMR spectra of rabbit erythrocytes. (A) Fresh intact cells stimulated to produce 23DPG with inosine and pyruvate. (B) Intact cells incubated without substrate for 16 hr. (C) Perchloric acid extract of fresh cells. The spectra A and B were obtained after ~ 1 hr of signal averaging, while C was obtained after ~ 10 hr. Broad band proton decoupling was used so the only multiplet structure seen is due to the P-P couplings in ATP. (From Labotka, R. J., Glonek, T., Hruby, M. A., and Honig, G. R., *Biochem. Med.*, 15, 311, 1976. With permission.)

of phosphorous metabolites in erythrocytes, reticulocytes, and platelets showed excellent agreement between the two approaches.[180,190] Some typical erythrocyte spectra are shown in Figure 12. The multiplet structure of the 3 ATP resonances is obvious. The β (19.4 ppm) peak is a triplet while the α (10.6 ppm) and γ (5.7 ppm) peaks are doublets. In addition, the high degree of multiplicity in the region of the α ATP resonance suggests the presence of NAD, immediately upfield, and ADP.[180] Greater resolution in this region of the spectrum has been obtained with other tissues and is discussed later (Section VII.D).

Reticulocytes which are more active metabolically have also been studied from the point of view of ATP stability. The natural decline of ATP levels was halted by ferricyanide with a consequent rise in the sugar phosphate peaks (−3.6 ppm) and even more so in the orthphosphate diester region; PEP at 0.9 ppm is at the high field end of this region. Other features of the spectra and estimates of metabolite concentrations were similar to erythrocytes.[180]

Erythrocytes from sufferers of sickle-cell anemia,[190] autoimmune hemolytic anemia,[190] and hereditary spherocytosis[192] have been subjected to ^{31}P NMR. The intracellular pH of

Downloaded At: 15:58 17 January 2011

the cells was measured using the Pi and 23DPG methods. Sickle cells had a pH of 7.14,[190] normal cells a pH of 7.29,[190] the autoimmune-anemia cells were even more acidic, and the hereditary spherocytes had an internal pH of 6.7 to 6.9.[192] The low values may have resulted from the long storage (24 hr) prior to the experiment. Levels of 23DPG were higher in the anemias, being 30% above normal in sickle cells, but this compound disappeared more rapidly during substrate-free incubation.[190]

The influence of pH on erythrocyte glycolysis is well established,[193] but equally complex is the regulatory effect on glycolysis of the state of oxygenation of hemoglobin. The regulation is mediated by the binding by hemoglobin of 23DPG and ATP,[195,196] but these compounds also bind Mg^{2+} which presumably modulates the regulation. Gupta and co-workers[196] calculated the free Mg^{2+} concentration in human erythrocytes to be 0.25 ± 0.07 m*M* and 0.6 ± 0.15 m*M* under aerobic and anaerobic conditions, respectively. From these values they were able to compute the distribution of the Mg^{2+}-complexes of ATP, ADP, and 23DPG. The basis of the experimental measurements is the fact that Mg^{2+} binding to ATP induces a change, in relative chemical shifts, of the α and β peaks ($\Delta\delta_{\alpha\beta}$ 10.8 ± 0.02 shifts to 8.32 ± 0.02 ppm), and of the coupling constants $J_{\overline{\alpha}\beta}$ (19.4 ± 0.1 goes to 15.4 ± 0.1 Hz) and $J_{\beta\gamma}$ (20.0 ± 0.1 goes to 15.0 ± 0.1 Hz): these values can be measured with an accuracy of 1% and 0.1%, respectively, giving a 5% accuracy to estimates of free $[Mg^{2+}]$.[196]

An estimate of intracellular ADP/ATP ratios can be made from a comparison of the integrals of the β and γ ATP peaks since ADP makes no contribution to the β resonance but does to the γ. The ATP/ADP ratio in fresh human platelets was accordingly found to be 1.32:1[180] and 19:1;[197] this vast difference is presumably due to the different incubation conditions.

Platelets possess two nucleotide pools, one in the cytoplasm which turns over rapidly, and the other representing 65% of the ATP and ADP which is enclosed in dense secretion granules.

NaN_3/H_2O_2 solution added to platelets depleted ATP as detected by ^{31}P NMR. However, perchlorate extracts indicated persistent large amounts of ATP, and stimulation of the platelets with thrombin, which is known to induce granule secretion, greatly enhanced the ATP resonances.[197] Along with evidence from studies at different temperatures the investigators inferred that the intragranular nucleotides have greatly reduced mobility. Indeed, calculations showed that the lack of contribution to the nucleotide signal was not due to paramagnetic metal ion broadening, and could be accounted for by spherical complexes of molecular weight 10^6D with rotation correlation times (τ_r) of $\gtrsim 1$ μsec.[197]

C. Microorganisms

Yeast and many other microorganisms produce polyphosphates and thus it was from *Micrococcus lysodeikticus* that "electrondense particulate structures" were found to contain a high concentration of polyphosphate.[180] The ^{31}P NMR spectrum of the particles was a single sharp resonance at 22 ppm and was similar to other added polyphosphates. The molecular weight of the substance was found to be $\approx$5000 by chromatography.[180] Salhany *et al.*[198] noted a similar nontitratable resonance at 23 ppm in yeast. In addition, the intracellular pH was measured, by the Pi method, and found to vary only 1 pH unit around 6.3, despite changes in the external pH ranging from 3.5 to 9.1. Several other nontitratable unassigned ^{31}P resonances were present in yeast, and little ATP was in evidence in these early studies.[198]

Much more metabolic information has been obtained in ^{31}P NMR studies of *E. coli*.[169,181,199,200] In an elegant application of the saturation transfer technique[201-203] to intact *E. coli*, the unidirectional rate constants for the ATPase reaction were calculated using a simple two-site formula ($P_i \xrightarrow{k} \gamma ATP$ $k = 0.6 \pm 0.15$ sec^{-1}; $\gamma ATP \xrightarrow{k} P_i$ $k = 5 - 15$

Downloaded At: 15:58 17 January 2011

sec^{-1}).[199] Partial saturation of the intracellular Pi spins by selective RF irradiation of the sample incurred a 50 to 75% reduction in area of the γATP resonance. Conversely, irradiation at the γATP resonance frequency resulted in a 20 ± 5% reduction in the intracellular Pi peak area. The ATPase inhibitor dicyclohexyl carbodiimide (DCCD) prevented the saturation transfer, indicating that the exchange pathway is dominated by the ATPase catalyzed reaction.[199] This work is an example of the great potential for NMR to study the *in situ* activities of enzymes even bound to membranes, on the 1-sec time scale.

By using computer-controlled synchronization of oxygenation of *E. coli* with the RF pulsing, and then using signal averaging, it was possible with the good S/N obtained to measure pH changes with time resolution down to 1 sec. The pH variation was monitored by noting the Pi chemical shift; the pH was stable at 7.5 ± 0.1 for several minutes after stopping oxygenation.[199] Under steady-state metabolic conditions, the ΔpH across *E. coli* membranes was also measured,[204] using the shift difference between the two Pi peaks.

With succinate as a carbon source and in an environment of N_2 the pH inside (pH_{in}) equaled the pH outside (pH_{ex}) the cells. Addition of glucose rendered $pH_{in} > pH_{ex}$, but this effect was prevented in some instances by the addition of DCCD. Other experiments with O_2 and DCCD showed $pH_{in} > pH_{ex}$, and in summary the results are consistent with the chemiosmotic hypothesis that a ΔpH can be created by reversal of the ATPase reaction and that protons are pumped during respiration.[204]

In further experiments the rate of glycolysis by *E. coli* cells was inferred from the ^{31}P NMR spectra by noting changes in the pH of the extracellular medium.[181] Furthermore, the rate was found to correlate closely with the intracellular pH, decreasing sharply at pH $< \approx 7.2$. The sensitivity and resolution obtained in this study (10-mm sample tubes, 145.7 MHz, 2-min accumulations, repetition rate 0.34 sec, and pulse angle 60°, or 0.68 sec and 90°) enabled good visualization of resonances due to DHAP, F16P, Pi and nucleoside tri-, di-, and monophosphates; in the presence of glucose approximately 90% of the overall sugar-phosphate intensity at −3.5 ppm was due to the β phosphate of F16P. The latter concentration was ≈13 m*M* in the presence of 25 m*M* glucose.

Time courses, extending over ≈½ hr, of the changes in metabolite concentration in *E. coli* were obtained in the presence and absence of DCCD and the uncoupler of oxidative phosphorylation p-trifluoromethylphenyl hydrazone (FCCP).[181] The total sugar-phosphate, nicotinamide triphosphate/nicotinamide diphosphate ratio, pH_{in}, pH_{ex}, and ΔpH were all recorded as a function of time.[181]

It is clear that since lactate and pyruvate, which are the end products of glycolysis, cannot be followed using ^{31}P NMR. ^{1}H spin-echo NMR, which can detect these in whole cells,[146] has distinct advantages over the indirect means of measuring glycolytic flux such as changes in pH_{ex}, necessary with the ^{31}P studies.[198] Ideally, of course, a combined time-shared NMR probe is needed.

D. Other Tissues, Cells, and Organelles

The concentrations of nucleotide triphosphates, Pi and the yolk proteins phosvitin and lipovitellin were monitored in the living embryos of the frog *Xenopus laevis* by ^{31}P NMR; [ATP] was estimated to be 3.4 m*M* and the internal pH was 6.8 ± 0.2.[205] The major component contributing to the spectrum from oocytes, unfertilized eggs, and early embryos was the yolk phosphoprotein resonance. During embryonic development, it was evident that of the yolk phosphates the protein phosphate disappeared more rapidly than did the lipid-phosphate but most striking was the rise in inorganic phosphate. Although the total phosphate was invariant during development that observed by NMR was only 40% of the total. It was argued that because of the quantity involved this apparent deficit could not be allocated totally to uptake of phosphate into nucleic acids. Also, by comparing titrations of ATP with and without Mg^{2+} present it was inferred that

Downloaded At: 15:58 17 January 2011

intracellular ATP in the embryos is complexed to a divalent cation (not Mn^{2+}). This observation has since been made in many studies of whole cells.[206,207]

Considerable success in assigning ^{31}P resonances to specific metabolites has been achieved with Ehrlich ascites tumor cells,[206] lymphoid cells, Friend erythroleukemia cells, HeLa cells,[207,208] and rat liver mitochondria[187] using perchlorate extracts of the samples and pure metabolites as comparisons. In the case of Ehrlich ascites tumor cells it was possible to assign resonances to F16P, DHAP, ATP, ADP, AMP, Pi, NAD^+, PCr, glycero-3-phosphorylcholine (GPC), glycerophosphorylethanolamine (GPE), and GA3-P using chemical shifts, pH behavior, and spin coupling. Even more impressive is the fact that only GA3-P was of such low concentration so as not to be detected in whole cells, at 147.5 MHz after 34 min of data accumulation.[206] The ATP/ADP ratio in whole cells was 0.8 while in extracts it was 5.0. The latter value, together with an estimate of [AMP] from the spectrum of the extract, gave an estimate of the equilibrium constant of the adenylate kinase reaction; the value was 0.9, which is close to the expected value of 1.0.[206] However, this estimate, obtained from data from cell extracts, needs further exploration before it can be accepted as the value *in vivo*, since it has been shown that significant amounts of ATP are bound in the cell.[207,208]

From the spectra of extracts from Ehrlich ascites cells relative intensities of F16P, DHAP, and GA3-P were 95:21:4 and the value for the overall ratio [DHAP][GA3-P]/[F16P] was $\approx$0.1 m*M*, which is in agreement with the reported equilibrium constant (0.1 m*M*) of this aldolase catalyzed reaction at 38°C. Though it has been argued before that the aldolase reaction is not a regulatory step in glycolysis,[209] caution must be exercised in extrapolating the extract data to the *in situ* situation, as argued above. To further illustrate the above-mentioned point, the DHAP/GA3-P ratio in the same study of extracts[206] was 5.2, a value quite different from the expected *in vivo* value of 20 for this rapid "equilibrium"[209] triose phosphate isomerase catalyzed reaction.

It should be noted, by way of contrast, that among the many phosphate metabolites that were not detected by ^{31}P NMR in ascites cells were glucose-6-phosphate, nucleotide monophosphates, $NADP^+$ or NADPH, and F6P.[206] Recall that much more detail was seen in *E. coli* spectra.[181] The resonances due to phospholipid metabolites, phosphoryl choline, phosphoryl ethanolamine, and their glycerol esters were all of relatively large magnitude although of differing relative proportions in the three mammalian cell lines,[208] Friend erythroleukemia, HeLa, and lymphoid. A single Pi resonance was seen despite incubation of the cells in a medium containing phosphate and in the presence or absence of O_2, thus indicating no ΔpH across the cell membrane.[208] Interestingly, a small resonance at 3.85 ppm due to phosphocholine increased in intensity in cells incubated with glucose; the metabolic significance of this is unknown.[208] Also, lymphoid cells showed comparatively smaller and slower changes in metabolite levels such as ATP, in response to glucose, than HeLa, ascites, and Friend erythroleukemia cells.[208] Furthermore, resonances from as yet unidentified diphosphodiester compounds at 10.77 and 12.4 ppm were prominent in Friend and HeLa cells but not in lymphoid and ascites tumor cells.

Evans[207] conducted a thorough study of HeLa cells in an attempt to explain the extensive broadening of phosphorus resonances in whole cells, compared with cell-free systems. The T_1 of ATP phosphates was reduced much more than other compounds when compared with free solutions. In addition, the nOe was smaller for intracellular metabolites with ATP affected the most; the nOe for ATP in cells was 0, and was 0.4 in free solution. Both of these effects could be, at least partially, attributed to selective paramagnetic metal binding by ATP but other factors could also contribute; magnetic field inhomogeneities in the cell suspensions and particularly tissues were considered but were excluded as being major contributors because this effect should be the same, in terms of chemical shift for a different nucleus (^1H) in the same magnet, but it was not.

Downloaded At: 15:58 17 January 2011

Some of the peak broadening could be attributed to binding of ATP to enzymes which have long correlation times and thus give rise to chemical shift anisotropy.[207] In this context it should be noted that only ≈30% of total cell phosphorus is acid extractable, the remainder being in RNA (≈18%), DNA (≈25%), phosphoprotein (≈9%), and phospholipids (≈20%)[210] which all have expected chemical shifts in the 0.2-ppm region of the spectrum and yet remain undetected, presumably due to very long correlation times.

Another study was directed at measuring T_1 of phosphates in tumors and normal tissue from mice in order to ascertain if ^{31}P NMR could be useful in detecting neoplasia. The resulting spectra were not presented, but presumably the T_1 measurements were made from the whole spectral envelope so the result is a weighted average of several signals; in spite of this, T_1 values for neoplastic tissues were at least twice those of normal tissue.[211]

In studies of brain, energy-related metabolites were "trapped" by "funnel freezing" the tissues *in situ* using liquid nitrogen.[212] The samples were inspected by ^{31}P NMR at −20°C to −10°C, and changes noted with continued incubation at these temperatures. Notable changes were a decline in PCr and evaluation of Pi with time.[212] Spectra obtained from a live mouse head, although containing poor S/N for the same number of transients, still displayed distinct differences depending on whether the mouse was made anoxic or normoxic. In particular, PCr and Pi were reversed in relative intensity between the two states.

Downloaded At: 15:58 17 January 2011

Further application of ^{31}P NMR to studies on cell metabolism exploited the chemical shift differences of Pi between mitochondria and the cytosol in order to monitor transmembrane (mitochondrial) ΔpH, in rat liver cells subjected to various drugs.[213] Valinomycin, which is known to enhance the ΔpH across the membranes of suspensions of isolated mitochondria, induced a splitting of the Pi resonance in isolated rat liver cells; it was shown that *little* Pi was present in the *extra* cellular medium. Likewise, the addition of pH 3.3 buffer to the cells increased the splitting of the Pi peaks whereas FCCP or withdrawal of O_2 reduced the splitting. The method indicated that the pH of the cytosol was in all cases less than or equal to that in the mitochondria, and simultaneous changes in ATP levels were also followed.

Spectra of whole adrenal glands have been obtained which show clearly in one example moderate ATP signals,[183,214] while in another only one resonance was seen in the NAD^+ region and several in the mono- and di-ester region.[215]

The chromaffin granules of the adrenal medulla accumulate adrenalin by a mechanism that appears to be coupled to a proton-translocating ATPase.[124,216] Since the concentration of ATP in the granules is 110 m*M* (catecholeamine is 0.5 M) a substantial ^{31}P NMR signal is obtained; however, the ATP chemical shifts are peculiar because of the interaction of ATP with the catecholeamines.[183] The intragranular pH was calculated to be ≈6, which is the pK_a of the γ phosphate of ATP, using a calibration curve of chemical shifts vs. pH obtained from a solution of ATP, catecholeamine, and other components designed to mimic the contents of the granules.[183] Thus, the chemical shift differences between cytosolic and intragranular ATP were used as a measure of transmembrane ΔpH. The NMR results were supported by experiments using radioactive methylamine distribution as an index of ΔpH.[184] Addition of ATP to the extragranular medium invoked a ΔpH drop of 0.2 to 0.5 units only if a permeant ion such as Cl^- was present. The effect was not evident in the presence of FCCP. The data therefore support the idea that the membranes of the granules possess an inwardly directed electrogenic proton pump.[184]

E. Muscle

The report of the first ^{31}P NMR studies of muscle showed spectra, obtained from rat hind leg, which demonstrated peaks that were assigned to sugar phosphates, Pi, PCr, and the three phosphates of ATP.[170] It was stated in this first report, and has been verified several times since, that the ATP is complexed to Mg^{2+} or some non paramagnetic

cation.[173,175] Even in the early studies, time courses over 2 hr were obtained from muscles incubated at 20°C; a progressive decline in the ATP resonances was seen, simultaneously with a decline in PCr and a shift in the Pi resonance, indicating a fall in pH.[170]

The ATP and Pi resonances in muscle were broader than expected and it was suggested that there exist several different chemical environments with a distribution of pH.[170] Field inhomogeneity could not account for all the broadening because the PCr resonance was quite sharp; in fact its chemical shift differs little even between samples.[149,217] The question of compartmentation was dealt with in further detail with HeLa[207] cells, and using intact white muscle from rabbits.[172] The line width of Pi in the rabbit muscles was also seen to increase with time after excision (50 to 200 Hz), and occurred in parallel with developing lactic acidosis.[172,175] In order to exclude a relaxation phenomenon as a major cause of the broad Pi line, the T_2 was determined: it was 0.1 sec and corresponded to a line width of only 3 Hz. Therefore, it was concluded that the Pi peak consists of many narrow and partially overlapping components resulting from a pH distribution of 6.6 ± 0.2.[172,175] The pH distribution may be intra- or extracellular, but since the signals are volume averaged further details will have to await study by techniques that selectively excite spins in well-defined small volumes (e.g., sensitive point zeugmatography, Sections X.B and C).

The development of mechanical energy by contraction in muscles is consequent upon ATP hydrolysis. However, the concentration of ATP in muscles does not change perceptably during normal contraction because of its rapid rephosphorylation from PCr by creatine kinase.[217] A puzzle remains, in that PCr hydrolysis accounts for only half of the heat released and work performed during contraction and the source of the energy deficit is unknown. Although the answer to this problem was not forthcoming, Dawson *et al.* constructed an elaborate ^{31}P probe system to study perfused muscles and simultaneously record their tension via strain gauges.[149,217] The weak ^{31}P signals were time averaged by repetitively collecting data over specified time intervals, in separate memory blocks of the computer, after electrical stimulation of the muscle. Elaborate measures were taken to estimate true concentrations of metabolites, a matter made more difficult by uncertainties in the value of the extracellular volume. Time courses taken of frog sartorius muscles at 4°C showed that PCr resynthesis is roughly exponential with a $t_{1/2}$ of 10 min; extrapolation of the curve back to the time of the electrical impulse (t_o) indicated that 20% of the PCr was hydrolyzed during a 25-sec stimulated contraction. In other words, $\approx 1\%$ of the PCr was broken down per sec of contraction.[149] Time courses with frog muscle showed that ATP levels remained unchanged until PCr was virtually depleted.[173]

Inhibitors of metabolism such as iodoacetate, cyanide, and anoxia (N_2) all had profound effects on the spectra obtained during time course experiments, especially in the appearance of large amounts of hexose phosphates identified mostly as F16P.[199] The spectra obtained from various sources of muscle showed considerable variation in their phosphorus profiles.[149,173] Differences were detected between vertebrates and invertebrates, different types of muscle (red or white) from the same animal, and between diseased and normal muscle. A compound, subsequently identified as glycerol-3-phosphorylcholine (GPC), with a resonance at 3.2 ppm, was seen in high concentration in toad muscle compared with frog.[172,174] It has also been observed in muscle from several other sources.[173] Also, serine ethanolamine phosphodiester (SEP) was first identified by use of ^{31}P NMR in the muscles of dystrophic chickens.[7,173] Perchlorate extracts of quadriceps muscle from sufferers of Duchenne muscular dystrophy displayed a tenfold decrease of GPC levels compared with equivalent normal muscle tissue.[7,218] One suggestion therefore is that this heritable disease is a primary defect in phospholipid metabolism. In another muscle disease, nemaline rod myopathy, the time dependence of phosphate metabolite changes on incubation showed that the PCr signal decreased and

Downloaded At: 15:58 17 January 2011

Pi increased significantly faster than normal. It was suggested that this indicates a primary defect in the muscle ATPase in this disease.

In conclusion, along with the solution to more fundamental questions, the possible use of ^{31}P NMR for assisting in the diagnosis of muscle and other diseases is clear.

F. Whole Organs

The whole heart of a young rat, excised and maintained at 0°C, showed the characteristic spectrum seen previously with skeletal muscle, sugar phosphate, Pi, PCr, and Mg-ATP resonances.[220] Warming the heart to 30°C was used to impose an "energy load" which resulted in short-term resumption of beating with a simultaneous decline in ATP, PCr, and intracellular pH, from 7.0 to 6.0.

A Langendorff perfusion system at 37°C enabled the maintenance of a metabolic steady-state in rat hearts, and ^{31}P NMR spectra accumulated over 20-min periods showed all the previously mentioned metabolites. The high values of the signal intensity ratios PCr/ATP $\approx$1.8 and ATP/Pi$\approx$0.56 were used as indexes of efficient cardiac respiration. Estimates of the true concentrations of metabolites were not made,[220] because of the previously mentioned difficulties with determining the volume of the extracellular space.[149]

Global ischemia in rat hearts at 37°C[221] and 30°C,[222] incurred by reduced perfusion rates, gave rise to raised sugar phosphate and reduced ATP signals consistent with accelerated glycolysis.

Beating perfused rabbit[223] and guinea pig hearts[224] have been subjected to regional ischemia by ligation of a coronary artery. The consequences for the ^{31}P NMR spectrum were a splitting of the Pi resonance into two components indicative of a high and low pH region in the system. Global ischemia resulting from reduced perfusion rates caused a coalescence of the two Pi peaks to one with an average chemical shift indicating a lower pH value. In the study of (23) guinea pig hearts, the intracellular pH was given as 7.0 and ischemia resulted in a drop to 6.6 $\pm$ 0.1 units.[224]

Rat kidneys perfused in ice cold buffer gave spectra quite different from those of heart and muscle. The most distinguishing features were a prominent AMP resonance and a previously unassigned phosphodiester resonance. The other resonances were the familiar ATP, PCr, and Pi ones, of which the latter was of highest intensity. The gradual depletion of ATP and PCr was able to be followed during the cold ischemia. By using a live "assist" rat thus simulating a renal transplant operation, the recovery of ADP initially and then ATP was monitored.[225] It was concluded, on the basis of these results, that ^{31}P NMR may be useful for evaluating procedures undertaken to enhance survival of organs prior to transplant, and indeed even after being placed *in situ*.[66]

VIII. ^{13}C NMR STUDIES OF WHOLE CELLS

A. Introduction

The sensitivity for detection of ^{13}C nuclear magnetic spins is about 1% of an equal number of ^{1}H spins in the same magnetic field (see Table 1). However, the natural abundance of ^{13}C is only 1.1% so the relative sensitivity is 1.8×10^{-4} that of ^{1}H. Therefore, in order to conduct successfully ^{13}C NMR studies of biological samples, signal enhancement is required. Several methods are now almost routinely used and they include, apart from pulse techniques, (1) hydrogen noise decoupling to remove ^{1}H-^{13}C spin-spin splittings (the RF irradiation of protons may also result in Overhauser enhancement[226] (Section II.C) of the ^{13}C resonances by a factor of up to three) and (2) ^{13}C enrichment.

Pulse methods have greatly reduced the time required for ^{13}C NMR data accumulation. For example, the natural abundance CW spectrum at 26 MHz of 17 m*M*

Downloaded At: 15:58 17 January 2011

hen egg-white lysozyme took 87 hr to achieve a S/N ratio of 5,[227] whereas use of a Fourier transform pulse method on a 20 m*M* solution of ribonuclease A gave a S/N ratio of 35 to 40 after 10 hr.[228]

The relative difference in mass between ^{12}C and ^{13}C is sufficiently small, compared with say ^{1}H, ^{2}H, and ^{3}H, so that the predicted primary isotope effects on the rates of enzyme catalyzed reactions is minimal.[229] This ensures that ^{13}C-enriched metabolites can be used to "trace" metabolic events in cells and yet still reflect the normal kinetics. Furthermore, because of the low concentration of ^{13}C in natural metabolites and polymers, the probability of two adjacent carbons being both ^{13}C is negligible; this ensures simple first order spectra in natural abundance ^{13}C NMR. However, with ^{13}C-substituted metabolites, the patterns of multiplicity of resonances yield direct information on carbon backbone mixing and hence on the pathway of synthesis.[230,231] This information could otherwise only be obtained by tedious extraction and isolation procedures followed by mass spectroscopy or ^{14}C radioactivity measurements.

The chemical shift range of ^{13}C nuclei is large, ≈300 ppm (see Table 1); in other words, the shifts are very sensitive to the chemical environments of the nuclei. The chemical shifts are referenced to TMS, but in earlier work CS_2 or benzene was used. Several comprehensive tables of shift data are available (e.g., in Reference 27). The ^{13}C chemical shifts presented here have been converted where necessary to the TMS reference: to convert shifts referenced to (1) benzene, −128 ppm was added, (2) methanol, −48.5 ppm, and (3) CS_2, 192.2 ppm,[27] and then by convention the negative sign was deleted.

Because the γ of ^{13}C is small (Table 1) the relaxation times are long, even for large molecules in viscous media.[232] Therefore its nuclear properties render ^{13}C a valuable probe for studies of the structure, dynamics, and metabolic events in biological systems. One drawback, however, is the high cost of ^{13}C-enriched chemicals, although a recent publication describes procedures for the synthesis of a large number of differently labeled triose-, tetrose-, and pentose phosphates. Several other sugar phosphates are also able to be synthesized from these precursors by use of specific enzymic reactions.[233]

A review which focuses on new ^{13}C NMR techniques, with particular emphasis on the study of proteins, has recently appeared.[234]

Downloaded At: 15:58 17 January 2011

B. Erythrocytes

In one early report using ^{13}C NMR to study dog erythrocytes the mobility of components of hemoglobin *in situ* was studied using cells exposed to ^{13}CO, $^{13}CN^-$ and $^{13}CO_2$.[235] The first two of these species bind tightly to the heme group. In the experiments with CN^- the ion was present as 0.1 *M* KCN, a concentration that almost certainly would have led to lysis of the cells and perhaps, therefore, altered the interpretation of the results. Still, the spectra that were obtained were indicative of several environments for the ion, presumably bound to hemoglobin as well as membrane proteins,[235] although it is questionable whether the latter would be detected because of the low concentration of membranes.

Exposure of the erythrocytes to 90% ^{13}CO gave rise to a substantial ^{13}C peak at 205.6 ± 0.2 ppm in the spectrum and a line width (at ½ height) of 55 ± 3 Hz. These two characteristics were identical, within experimental error, to hemoglobin from lysed dog blood and were similar to whole human blood and hemoglobin. It was therefore concluded that steric interactions and relaxation effects on the ^{13}CO moiety are not affected in the intracellular compared with the extracellular environment.[235]

The separate signals due to ^{13}CO on the α and β subunits seen in purified mouse hemoglobin [236] were not seen *in vivo* or in concentrated lysed cell solutions. However, dilution by a factor of ten, to give a solution of 2 m*M* hemoglobin, allowed the demonstration of two ^{13}CO-hemoglobin peaks separated by 0.4 ppm.[235]

Bubbling $^{13}CO_2$ into a suspension of erythrocytes gave a sample with a ^{13}C spectrum which contained prominent narrow lines assigned to $^{13}CO_2$ and $H^{13}CO_3^-$, neither of which were split as might have been expected to occur owing to the differences between intra- and extracellular environments.[235] Likewise, the permeant species ^{13}C-urea and acetate gave unsplit peaks.[235] Since erythrocytes contain a high concentration of carbonic anhydrase it is surprising that the $^{13}CO_2$ and $H^{13}CO_3^-$ resonances in whole blood were quite narrow, $\approx$10 Hz and $\approx$30 Hz, respectively. The relative line widths were in approximate inverse ratio of the population of the two sites, $\approx$3/1, suggesting that slow chemical exchange (on the ^{13}C NMR time scale) between HCO_3^- and CO_2 occurred.[235] Furthermore, the exchange rate was seen to be faster when carbonic anhydrase was in homogeneous solution rather than when localized within the erythrocytes; the ^{13}C NMR spectrum showed significant broadening of both the $^{13}CO_2$ and the $H^{13}CO_3^-$ peaks on addition of carbonic anhydrase to a suspension of erythrocytes, to lysed cells, and in free solution.[235]

Also in the $^{13}CO_2$ erythrocyte experiments an additional peak was evident;[235] it had a chemical shift the same as that of the carbamino complex of $^{13}CO_2$ with glycine (R = H) and alanine (R = CH_3)

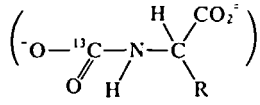

and presumably resulted from the formation of the same complex with the terminal valine residues of the α and β chains of hemoglobin.

The intensity of the specific carbamino resonance (at 164.4 ppm) has been used as a measure of the degree of saturation of hemoglobin solutions at pH 7.19 $\pm$ 0.2 by CO_2.[237] In contrast, it was observed that CO_2 binding to hemoglobin is cooperative and gives a sigmoidal binding curve with a Hill coefficient of 2.1. The effect does not appear to have been demonstrated *in situ* in erythrocytes, but there is no reason why the experiment could not be performed.

CNO^- ions stabilize the oxy- form of hemoglobin by binding to the N-terminal valines of the α and β chains in much the same way as CO_2. For this reason it is of interest in the treatment of sickle cell anemia since in this disorder, deoxyhemoglobin polymerizes more readily than normal and in so doing renders the cells sickle shaped.[238] Early studies of the ^{13}C NMR spectra, from ^{13}CO bound to purified hemoglobin (from the various sources: human, mouse, and rabbit), showed a great stability of the ^{13}CO-hemoglobin chemical shift over the pH range 6.5 to 7.5, and, more importantly for the present discussion, a lack of perturbation of the chemical shift by 23 DPG which is a known allosteric effector of hemoglobin.[236] In light of this finding, and since $^{13}CO_2$-hemoglobin displays no peak splitting, it is unlikely that $^{13}CNO^-$ will demonstrate any marked effects that will be useful for monitoring the intracellular binding behavior of hemoglobin; this is despite some early optimism that the reaction would be able to be followed *in situ*.[235]

T_1 measurements were made on ^{13}C in histidyl residues of hemoglobin in erythrocytes and lysates from mice fed for 12 days on a diet devoid of ordinary histidine but supplemented with [2-^{13}C] histidine.[232] The T_1 values (intracellular 114 msec, extracellular 138 msec) differed only by 25%, suggesting that the intracellular fluid is not substantially more viscous than lysates. Furthermore, calculations of the rotational correlation time suggested that the histidyl carbons are tightly locked into the hemoglobin structure and that the correlation time of the [2-^{13}C] histidyl resonances is that for the rotation of the whole hemoglobin molecule. By use of the Einstein-Stokes

Downloaded At: 15:58 17 January 2011

equation and a value of 5.5 nm for the molecular diameter of hemoglobin, the viscosities were calculated to be 1.94 and 1.56 cP before and after lysis. The viscosity increase above that of pure water can be attributed, not to any special ordering of water or protein molecules, but simply to the high concentration of the protein.[232]

Preliminary time-course experiments at 37°C in which [1-^{13}C] glucose was added to an erythrocyte suspension have been reported.[147] The preferential metabolism of the β anomer of glucose was evidenced by the decline of the peak at 98 ppm (α 1-^{13}C, $\delta = 94$ ppm). The label was incorporated into C-3 of 23 DPG (68 ppm) and finally a lactate C-3 resonance (13 ppm) appeared in accordance with ^{1}H NMR experiments done under the same conditions. Further reports on this type of work can be expected in the near future, because of the information that such experiments can yield on the cycling rate of the 23 DPG shunt. The cycling rate is generally assumed to be slow but definitive evidence is not yet at hand.[154,155]

C. Vesicles

Although a general aim of this review is to consider only NMR studies of whole cells or organelles, it is worth noting some work in which synthetic vesicles were used because of the general applicability of the method to whole cells. In the natural abundance ^{13}C NMR spectrum of lecithin vesicles, two resonances separated by 0.3 ppm have been assigned to the overlapping α and β chain carboxyl carbons of lecithin.[239] The low field line was broadened by the nonpermeant line-broadening and shift probes Yb^{3+} (the most efficient ^{13}C shift reagent), Ho^{3+} and Gd^{3+}, thus indicating that it corresponded to the lecithin in the outer layer of the membrane.

Addition of the major tranquilizer, chlorpromazine, to a suspension of vesicles resulted in significant broadening of the two lecithin lines.[240] This was interpreted as indicating restriction of motion of the membrane components as the drug molecules became incorporated in the membrane. Furthermore, the shift difference between the two lecithin resonances vanished, a result again attributed to the close proximity of the heterocyclic drug molecules to the carbonyls of the lecithin.

Addition of 20 m*M* Yb^{3+} to drug-free vesicles caused a splitting of the choline methyl peak into two; the "external" methyl peak was shifted upfield. Superaddition of chlorpromazine (110 m*M*) cancelled the splitting. This effect was interpreted as due to the drug displacing the Yb^{3+} ions from the polar $-N^{+}(CH_3)_3$ groups as a result of becoming intercalated in the membrane adjacent to the hydrocarbon chain near the carbonyls.

Clearly, simple ^{13}C NMR-based experiments can yield interesting information on the structural and fluid-dynamic effects of drugs in membranes and should be able to be used for the study of intact cells.

D. Plants and Microorganisms

^{13}C NMR (25.2 MHz) spectra have been obtained from suspensions of the yeast *Candida utilis* after growing the cells in a medium containing ^{13}C-enriched acetic acid and from cells grown in unenriched medium but then exposed to [1-^{13}C] glucose.[241] In the latter case, the α and β anomeric carbons were located at 92.4 and 96.2 ppm, whereas standard solutions of glucose 6-phosphate and glycogen showed resonances at 92.5 ppm (α), 96.3 ppm (β), and 100.0 ppm, respectively. Perchlorate extracts of the cells gave spectra that showed that many of the peaks in the complex spectrum from whole cells were small, mobile metabolites. Furthermore, among the many peaks were those due to terminal methyl resonances of the long chain fatty acids (11.5 ppm), the α-carbons of peptides (55.3 ppm), and a weak signal at 53.5 ppm was assigned to $-N^{+}(CH_3)_3$ groups of choline-phospholipids. During a 1½-hr incubation period the signal due to the isotopic carbons from C-1 of glucose disappeared, as expected, and the peak due to the C-2 of

Downloaded At: 15:58 17 January 2011

ethanol rose, accompanied by a small increase in an unassigned glucose metabolite signal.[241] It therefore can be deduced that the ability to observe high resolution spectra from cell suspensions using ^{13}C NMR is not strongly dependent on the mobility of the cellular components.

Another series of experiments involved the combined use of natural abundance ^{13}C and ^{31}P NMR to monitor the *in situ* phosphorylation of adenosine to ATP in baker's yeast.[242] The ^{13}C (25.2 MHz) spectra were obtained over a 30-hr period in 30-min (4000 transients) segments, with glucose and adenosine as substrates at 34°C. Among the peaks in the spectra were some readily identified as glucose, trehalose, F16P, glycerol, ethanol, ATP, and AMP and they were all followed as a function of time. After 7 hr the glucose was depleted while F16P was at its maximum. The ^{31}P NMR (40.5 MHz) counterpart of this experiment showed the high F16P at 7 hr with a corresponding minimum in Pi, and a maximum of ATP after 18 hr.[242]

^{13}C label was introduced into soy bean ovules by exposing portions of a plant to $^{13}CO_2$.[243] About 200 mg of $^{13}CO_2$ was fixed by the segment of plant in a 4-hr period. The fixed CO_2 is normally transported to the ovules as (heavily labeled) sucrose where it is used in the synthesis of fatty and amino acids and various insoluble substances. By taking note of the ^{13}C-^{13}C coupling in the lipid peaks, distribution of label within the lipids was able to be studied; this distribution is however complicated by the effect of recycling of hexose phosphates in the PPP. Therefore, the information concerning pairs of labels leads to a fast and simple means of estimating the amount of glucose in an intact ovule that was involved in the PPP relative to that utilized by other metabolic sequences. Among the peaks assigned were the olefinic carbons of the fatty acids at 130 ppm, the soluble sugars at 60 to 100 ppm, and methylene and methyl carbons of the fatty acid chains at 30 ppm. From the multiplicity and amplitude of the olefinic carbon peaks, it was argued that ≈30% of the sugar carbons, which ended up as these fatty acids, had been randomized in the sugar molecules of the PPP. (See also similar experiments noted in Sections VII.C and D). Comparison of spectra of the ovules at different times showed that 3 days after the $^{13}CO_2$ treatment most of the sugar signals had disappeared while the lipid signals were considerably larger.

The most detailed studies of metabolism in microorganisms using ^{13}C NMR have been undertaken by Shulman's group,[168,244] and these have been paralleled by similar investigations of isolated rat liver cells (Section VII.D).[168,245] Very important for data analysis from these experiments is that considerable effort has been expended in establishing assignments of resonances to metabolites.

The ^{13}C label of the β anomer of [1-^{13}C] glucose was seen to disappear faster than the α anomer, from a suspension of *E. coli* (strain MRE 600) at 20°C, in a 15.5 min time course, monitored by a 90.52-MHz spectrometer acquiring 200 FIDs in 2 min/spectrum.[245] However, this preferential utilization of the β anomer was not evident in three other strains of *E. coli,* which clearly possessed high anomerase activity. *E. coli* cells produce varying ratios of glycolytic intermediates and products depending on their growth environment. For instance, under one set of conditions the dominant product was lactate, with some succinate, malate, ethanol, and acetate also present. In addition, the F16P reached a high level (≈13 m*M* as estimated by ^{31}P NMR) after 1 to 2 min and remained that way until the glucose concentration was only 10% of the initial value. This F16P rise was clearly much more rapid than that seen in a similar study of yeast cells.[242]

The fact that the two virtually equal anomeric [1-^{13}C] peaks of F16P (65.8α, 66.6β) are well resolved in *E. coli* suggests that the two forms are in rapid equilibrium (on the NMR time scale). A large peak assigned to C-6 of β F16P was also evident in these spectra, thus indicating that the C-1 carbons of [1-^{13}C] glucose that was added as sole ^{13}C-substrate instead of passing directly to C-1 of F16P had become scrambled in the hexose carbon backbone.

Downloaded At: 15:58 17 January 2011

If it is assumed that the enzymes involved in this reaction are F16P-aldolase or transaldolase and triose phosphate isomerase and that the back and forth flux through these reactions is rapid in comparison with the total glycolytic flux, then the intensity of the ^{13}C-6 and ^{13}C-1 peaks would be identical. Alternatively, if reverse tracer flux was low, no C-1 to C-6 scrambling would occur. Therefore in spectra from whole cells the relative areas of ^{13}C-6 and ^{13}C-1 of F16P could give a measure of the relative flux rates in the relevant segment of the glycolytic pathway *in situ*.[168,244]

However, [6-^{13}C] glucose added to *E. coli* cells gave rise to almost no [1-^{13}C] F16P, whereas the degree of scrambling in yeast was much higher.[168] Therefore reversal of carbon flux through aldolase is slow in *E. coli* but clearly varies from species to species. In addition, the series of enzymic reactions, other than those mentioned above, must exist for the C-1 → C-6 scrambling in *E. coli*.

Among the ^{13}C peaks evident from *E. coli* cells incubated under anaerobic conditions with [1-^{13}C] glucose were three assigned to C-4, C-3, and C-2 of glutamate. From the known chemistry of the Krebs cycle a label entering it as the methyl of acetyl CoA will in the first turn of the cycle be incorporated into C-4 of glutamate. If it proceeds to succinate the label will be distributed equally between C-2 and C-3 of succinate. In the second turn of the cycle it will be incorporated into C-2 and C-3 of glutamate.[244] Therefore the observation that the estimates of C-2 and C-3 were less by a factor of ≈2 than C-4 indicated that the mean number of cycles, undertaken before passing on to other pathways, by any one carbon of glutamate was ≈2. Another interesting calculation was made from noting the rate of disappearance of the β anomeric peak of [1-^{13}C] glucose in *E. coli* suspensions. A Lineweaver-Burk plot consisting of the reciprocal of the rate of decline of the peak, vs. the reciprocal of the peak area (concentration estimate) gave a line which yielded an estimate of the (intracellular) Km for this process, ≈7 m*M*.

Studies similar to those discussed above have been followed by some on isolated rat liver which will now be considered.

Downloaded At: 15:58 17 January 2011

E. Liver

Figure 13 is a ^{13}C NMR spectrum obtained from isolated rat liver cells which had metabolized [1, 3-^{13}C] glycerol.[245] The heavy labeling of glucose at C-1, 3, 4, and 6 with only 1/10 of the intensity arising from C-2 and 5 was as predicted from a knowledge of the synthesis of glucose from glycerol.[246] In addition, the C-3 and C-4 peaks appeared as triplets. If a glucose molecule had been formed by the condensation of 2[1, 3-^{13}C] trioses then the resonances at C-3 and C-4 would have only been doublets, while if only one of the trioses were labeled then a singlet would have resulted. Thus, from a comparison of the area of the central peak with that of the two outer ones, an idea can be gained as to the relative contributions of labeled and unlabeled trioses to the glucose formed.[245] Furthermore, the equality of the C-3 and C-4 resonances suggested that the label flux from DHAP and GA3-P was equal, which is consistent with rapid equilibration of these two substances via triose phosphate isomerase (TIM). Also, the relative enrichment of C-6 of glucose compared with C-1, together with the demonstrated rapid equilibrium of trioses via TIM, can be viewed as a measure of the rate of loss of $^{13}CO_2$ from C-1 of 6-phosphogluconate in the formation of ribulose 5-phosphate in the PPP, i.e., it is an index of relative PPP activity compared with the glycerol to glucose flux.

The relative activities of the transketolase and transaldolase reactions were estimated from the distribution of labeling at C-3 and C-4 of glucose, but the details of the analysis, which involved several (reasonable) assumptions about the metabolic sequence,[245] will not be discussed further here. Isolated liver cells were also incubated with [2-^{13}C] glycerol and a different labeling pattern was observed for glucose and other metabolites. The C-2 and C-5 positions of glucose were labeled after ≈100 min of incubation at 25°C, and the peak intensities due to label at positions C-4 and C-6 of glucose were < 3% of the C-2 and

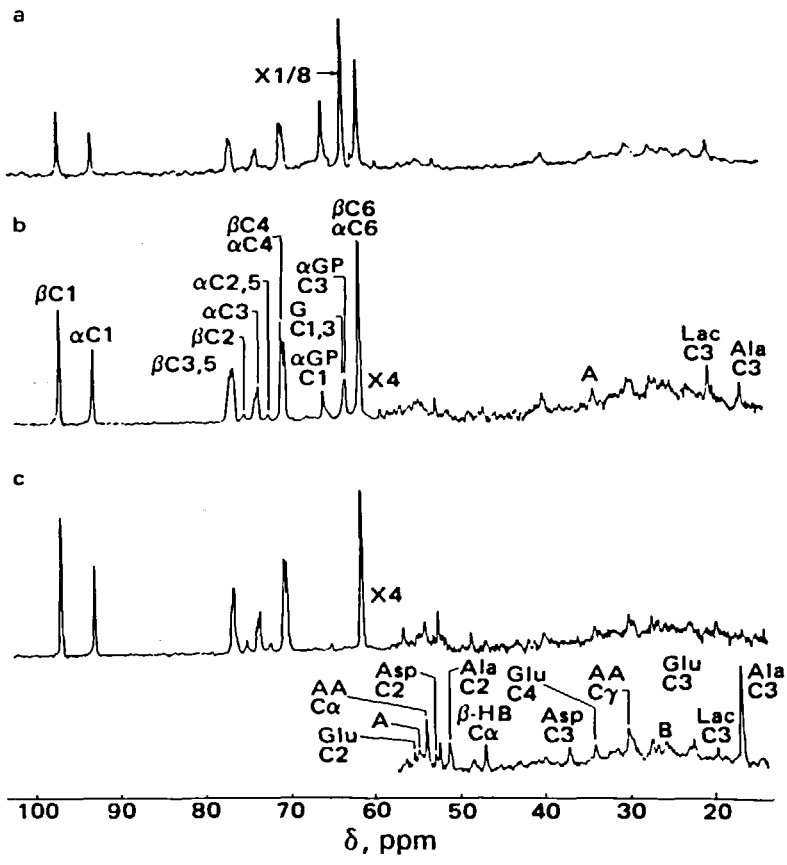

FIGURE 13. ^{13}C NMR spectrum of rat liver cells. Part of a sequence of spectra taken at 25° C after a suspension of liver cells isolated from a triidothyronine-treated rat was made 22 m*M* in [1,3-^{13}C] glycerol. (a) Accumulated during the period 0 to 17 min after the addition of substrate; (b) 35 to 51 min; (c) 85 to 115 min. The pulse repetition rate was 0.334 sec for spectra a and b and 2 sec for spectrum c. (Inset at bottom.) Upfield region of a similar hepatocyte sample made 16 m*M* in NH_4^+ recorded with increased vertical gain. Abbreviations are GCl, 3, glycerol C-1 and C-3; αGPCl, α glycerophosphate C-1; Glu C2, glutamate C-2; Asp C2, aspartate C-2; AACα, acetoacetate CH_2; β-HB Cα, β-hydroxybutyrate CH_2 AA Cα, acetoacetate CH_3; and Lac C3, lactate C-3. (From Cohen, S. M., Ogawa, S., and Shulman, R. G., *Proc. Natl. Acad. Sci. U.S.A.*, 76, 1603, 1979. With permission.)

C-5 peaks. In addition, the relative intensities of C-2 and C-5 gave an idea of the PPP cycling rate because in a second passage through the PPP, of what was originally [2, 5-^{13}C] glucose, the old C-2 has become C-1 and is then lost as $^{13}CO_2$.

Addition of NH_4^+ and [1, 3-^{13}C] glycerol to cells derived from rats treated with thyroxin caused the accumulation of metabolites that were identified from their chemical shifts to be lactate, alanine, β hydroxybutyrate, acetoacetate, glutamate, and aspartate.[245] The rates of glycerol uptake and glucose production were faster in the absence of NH_4^+ but alanine synthesis was slower. In corresponding spectra from euthyroid rats lactate, alanine and other amino acids and the ketone bodies were consistently below levels of detection. These results suggested to the authors[245] that in thyrotoxicosis the net increase in glycolytic end products is consistent with enhanced lactate dehydrogenase activity, whereas the increased glycerol uptake and glucose production is consistent with the known increase in mitochondrial α-glycerophosphate

Downloaded At: 15:58 17 January 2011

dehydrogenase.[246] In an equally elegant study with perfused whole mouse livers, a vast amount of information was forthcoming from adding [3-^{13}C] alanine, [2-^{13}C] ethanol, or both together.[247] The distribution of label into the various positions of glucose, glutamine, and glutamate was studied in detail, but a great deal of other information was present in the spectra.

For example, label distribution in C-3 and C-4 of glucose was equal, indicating rapid equilibration of the triose phosphate isomerase step *in situ*, a situation that pertained in the studies of rat liver cells and *E. coli*.[168,244,245] Perhaps the major finding of the work was that in the presence of ethanol *and* alanine the flux of label into glutamate from ethanol proceeded almost exclusively via acetyl CoA, while that from alanine flowed predominantly into the Krebs cycle via carboxylation of pyruvate. The data obtained and arguments for this conclusion will not be presented, but the conclusions are consistent with prior understanding of the complexities of liver ethanol and alanine metabolism; the conclusion is presented more to illustrate the sophistication of analysis available solely from a ^{13}C NMR experiment.

Other interesting results have been obtained in studies of mouse and rat liver metabolism, but what has been discussed has hopefully identified the major features of spectral analysis that will be useful in tracing ^{13}C-label distributions in other metabolic systems.

Downloaded At: 15:58 17 January 2011

F. Muscle and Other Tissue

Fung[248] used natural abundance ^{13}C NMR to study mouse skeletal muscle in order to determine whether water bound to macromolecules contributed significantly to the fast relaxing proton spin components seen in the studies of T_1 in which ^{1}H NMR (see Section IV.B) had been used. The ^{13}C NMR spectra contained three prominent resonances assigned to aliphatic (30 ppm), aromatic (130 ppm), and carbonyl (175 ppm) carbons with T_2 estimated from the half widths ($\Delta\nu_{1/2}$) of the peaks ($T_2 = \Delta\nu_{1/2}/\pi$), 1.6, 1.6, and 0.6 msec, respectively. Since relaxation times of protons are usually 2 to 5 times shorter than directly attached carbons, it was concluded that there are sufficient mobile aromatic and alipathic carbons with attached protons to account for a significantly large proton component with T_1 in the expected range of 1.6/5 msec. Simple calculations from a knowledge of protein and membrane composition suggested that 6 to 8% of muscle protons are in nonrigidly held organic residues. It was therefore concluded that nonrigid organic protons are responsible for, at least, a large part of the fast (millisecond) proton spin-spin relaxation seen in muscles. Furthermore, it was suggested that changes in the ^{1}H spin-echo decays that occur after cell death, and that give rise to nonexponential decays, could be attributed to protein conformational changes.[248]

In a (mammalian) Chinese hamster ovary cell line grown in the presence of [methyl-^{13}C] choline it was concluded that the ^{13}C NMR signal obtained was dominated by free phosphorylcholine and not membrane-bound species.[249] Therefore the T_1 value (546 msec, 6°C) was used in the calculation of the intracellular viscosity. It is interesting to note that the T_1 for the calcium salt of phosphorylcholine in water (0.386 *M*, pH 7.0, 7°C) was 660 msec. The ratio of viscosity inside the ovary cells to water was $\approx$1.20,[249] a value in close agreement with that obtained from studies of [2-^{13}C] histidine in the hemoglobin of mouse erythrocytes[232] (Section VIII.B).

Natural abundance ^{13}C NMR spectra have been obtained from dog sciatic nerve.[250] No resonances attributed to cholesterol, glycolipids, or sphingolipids were detected despite the abundance of myelin in this nerve. However, many of the resonances seen in a 1-pentanol extract were assigned to the above-mentioned substances. Therefore, it was concluded that these species are immobilized in the nerve cell, and much of the detail seen in the spectrum of the whole nerve could be accounted for by the triglycerides in associated fat cells.[251]

^{13}C NMR has also been used to gain information on the fluidity of virion membranes by incorporating ^{13}C into the membranes of host cells, and then measuring T_1 values of the ^{13}C in samples of the virions produced from the cells.[251] By incorporating [methyl-^{13}C] choline as a probe for the polar head group and [3-^{13}C] and [11-^{13}C] oleic acid and [16-^{13}C] palmitic acid for the hydrophobic region of the bilayer, T_1 measurements gave an idea of the fluidity as a function of depth in the membranes.[252]

The T_1 of the polar choline head group was ≈240 msec in virion membranes; those of the fatty acids were ≈130 msec, ≈170 msec, and ≈1500 msec. This led to the suggestion that the choline head groups are relatively immobile, with the lipid layer down to 15 nm being rigid also, but the inner layer being very fluid.

Other ^{13}C NMR studies of membranes have, of course, been undertaken but these studies on virions represent some of the first on biological membranes from intact systems.

Finally, spectra have been obtained from solid wood and ivory,[253] using natural abundance ^{13}C NMR coupled with cross polarization (CP)[254] and magic angle techniques.[255] In wood, signals due to the glucose residues of cellulose were readily discernible and the lowest field lines were from lignin. In ivory, the major organic component is collagen and approximately six lines were evident in the spectrum. These results are not very interesting to the biologist, but the implications of the NMR techniques employed are great for studies or packed biological membranes.

IX. BIOLOGICAL STUDIES USING OTHER NUCLIDES

A. ^2H NMR Studies

The ^2H nucleus is much less sensitive to detection by NMR than protons, principally because of its low γ value; its spin quantum number 1 indicates a magnetic quadrupole. Thus, via electrical interactions, its relaxation rates are enhanced in comparison with protons and this leads to broad resonances (Table 1).

Recent reviews on ^2H NMR have appeared[256-258] but most applications of the technique in biology have concentrated on studies of deuterated proteins and synthetic membranes. Since ^2H spin relaxations are dominated by interactions of the nuclear quadrupole with electrical field gradients, the relaxation rate is very sensitive to molecular mobility. Therefore, ^2H-labeled lipids have been used in order to deduce order parameters from quadrupolar splitting and relaxation times, as a function of acyl chain length, degree of saturation, and temperature in synthetic membranes.[259-263]

The molecular order in *Acholeplasma laidlawii* membranes has been studied using biosynthetically incorporated ^2H-labeled lipids.[263,264] In the first study,[263] perdeuterated lauric and palmitic acids were added to media in which the organisms were growing. The fatty acid chains were biosynthetically elongated to myristic and palmitic acids and then incorporated into membranes. The ^2H NMR (8 MHz) spectrum of the membranes was a very broad single envelope with a width at half height of 65 KHz. The spectra were interpreted in terms of a physical model and compared with spectra from pure lipids; it was concluded that the mobility in the membranes was similar to that in the gel state of dimyristoyl lecithin. In a second series of experiments,[264] palmitic acid ^2H-labeled at the terminal methyl group was biosynthetically incorporated into [16-$^2H_3$] lipids of the membranes of *A. laidlawii*. ^2H NMR [15.4 MHz] spectra contained more detail than the previous study, with the clear splitting in the broad envelope most obvious at 48°C, in the range 30 to 60°C.

The observation of this quadrupolar splitting implied that the lipids were oriented in an anisotropic way. The data were interpreted in terms of a line shape function which contained an order parameter (S, which characterizes the degree of orientation of the electric field gradient around the normal to the bilayer) for the C-^2H bond. The

Downloaded At: 15:58 17 January 2011

conclusions were that below 37°C the membranes possess lipid in both gel and liquid crystalline states. Above this temperature they demonstrate the existence of an entirely liquid crystalline membrane whose order parameter decreases rapidly with increasing temperature.[264]

[Methyl-$^2H_9$] choline was added to the media of mouse LM cells in culture and was incorporated biosynthetically into the cell membranes. The resulting ^2H NMR (33.8 MHz, 2048 FIDs spectra width, 5000-Hz recycle time, 0.11 sec) spectra of the membranes contained two types of signals. First, a sharp central line split by 56 KHz was attributed to natural abundance ^2H and free ^2H-choline. Second, there were two broad peaks assigned to the choline head groups with a quadrupole coupling constant of $\approx$1 KHz. This is characteristic of a spin 1 nucleus with a low asymmetry parameter. In addition,[265] rat liver slices and mitochondria from rats fed [methyl-$^2H_9$] choline gave similar ^2H NMR spectra. However, in neither case were the data analyzed in terms of a strict physical model containing order parameters. A more detailed analysis was made using data from mitochondria of rats fed [methyl-$^2H_9$] choline.[266] The analysis, which included a consideration of the order parameter (S), suggested that the degree of splitting of the ^2H-choline peak, which was less than expected for a simple bilayer, occurred because the choline head group was restricted to certain conformations by nearby membrane proteins.

With a view to reducing, substantially, the complexity of ^1H NMR spectra of the lactose repressor protein, bacteria were grown in media containing deuterated analogues of histidine, tyrosine, phenylalanine, and tryptophan.[267] ^1H and ^2H NMR spectra were obtained of the denatured protein and it was suggested that it may in future be possible to study the binding of *lac* repressor protein to DNA by noting the quadrupolar splittings of the deuterated protein.

Other interesting information has been obtained from studies of ^2H-substituted proteins by ^2H NMR. For example, 2,4-diacetyl hemin deuterated in the methyls of the acetyl moieties was mixed with sperm whale apomyoglobin.[268] The two ^2H-labeled methyl groups were then observed by ^2H NMR. The rotational correlation time of the acetyl groups was determined, by considering T_1 values and line broadening, to be $\approx$50 μsec. The important point to note is that ^2H NMR can readily monitor the behavior of chemical groups near paramagnetic centers (such as Fe in this case) where this is not often the case with ^1H NMR. This is due to the dominance of quadrupolar relaxation over that of the paramagnetic center effects in the case of the ^2H nucleus. Due to the problems of obtaining sufficient levels of deuteration in a given type of protein (such as hemoglobin) no similar measurements have been made on whole cells.

Another exciting development in NMR has been its use in detecting protein polymerization. In the case of ^1H NMR, the polymerization of hemoglobin that underlies the sickling process in sickle cell anemia was discussed in Section IV.C. A very recent report of the use of ^2H NMR to study protein-protein interaction has appeared,[269] and although on an *in vitro* system the possible application to whole cells warrants its discussion here.

Hen eggwhite lysozyme was prepared (by incubation in ^2H_2O at 37°C for 7 days) in which the C_ϵ position of the single HIS-15 residue was substituted for a deuterium atom. The ^2H NMR (41.4 MHz) spectrum in H_2O showed a broad resonance (500 to 1000 Hz) due to the ^2H-HIS and a sharp signal from residual $^2HO^1H$. The line width of the ^2H-HIS signal increased with pH reflecting the self-association of lysozyme which is known to involve this HIS. Correlation times calculated from T_2 measurements derived from the line widths indicated that the lysozyme is predominantly dimerized at pH 7.5.[269]

^2H NMR has been used for studying exchange processes in biosynthetic pathways using metabolites isolated from cells, in order to determine the chemical origins of the various molecular substitutions. Such a study was undertaken on griseofulvin.[270]

Downloaded At: 15:58 17 January 2011

Meanwhile, the only ^2H NMR study of *in situ* cell metabolism as yet undertaken (to the author's knowledge) is that on human erythrocytes.[66a] The time course, at 37°C, of lactate production from [1-^{2}H] glucose and [2,3,4,6,6-^{2}H] glucose has been monitored by following the disappearance of the glucose peaks and a rise in the [3-^{2}H] lactate peak. The T_1 of deuterons in the water of muscle has been measured at a few frequencies above 4 MHz,[271,272] and recently over an even broader frequency domain (10^4 to 10^8 Hz) for muscle and brain at several temperatures.[273]

In addition, the T_1 values for protons in the water of these samples with differing proportions of ^2H_2O were measured. The data were interpreted as indicating that the ≈10% of fast-relaxing water protons in brain and muscle relax principally by dipolar interactions between water molecules in the first hydration layer and the protons in the proteins, by the process of spin diffusion (Section IV.B). For ^2H, the fast-relaxing part in the exchange fraction seems to involve only a small portion of the water molecules in the first hydration layer. These water molecules may be those that are more tightly hydrogen bonded to polar groups of the macromolecules.[273]

B. ^{17}O NMR Studies

^{17}O nuclei have been employed in a series of experiments designed to study the physical state of water in biological systems; for this reason the work could have been discussed in Section IV but the results are sufficiently distinct to warrant a separate section.

The relaxation times characterizing the NMR behavior of ^{17}O spins are three orders of magnitude shorter than protons and are some orders of magnitude less than the mean exchange lifetime of water across cell membranes. Table 1 contains some of the characteristics of the ^{17}O nucleus. It should also be noted that with its high spin quantum number, 5/2, electric quadrupolar relaxation is an important and significant spin-lattice relaxation mechanism.

Striated frog muscles were bathed in Ringers' solution enriched with 8 to 14% $H_2{}^{17}O$ for ≈3 hr until the isotopic composition of the cells and bathing medium were identical. The longitudinal relaxation was studied by a pulse method, at 7.55 MHz, and shown to be nonexponential both at 20 to 22°C and at 2 to 3°C.[272,86] This was interpreted as reflecting heterogeneity in the environment of water molecules. On standing for 1 to 2 days, the nonexponential character of the longitudinal relaxation disappeared and eventually could be described by a single T_1.[274] A similar loss of nonexponential longitudinal relaxation was noted in analogous experiments on rat lymphocytes when the cells became necrotic.[275] These studies helped to indicate that the nonexponential longitudinal relaxation behavior seen in muscle was not simply a result of the orientation of myofibrils causing anisotropic effects.

From an analysis of the longitudinal relaxation curves, of viable cells, two relaxation times were determined along with the mole fractions of each compartment (see Section IV.B and Equation 17). Two-thirds of the water was slowly relaxing (T_1, 5.1 msec) and identified with the cell nucleus, whereas the fast-relaxing (T_1, 3.1 msec) fraction was identified with the cytoplasm.[275] Lowering the Larmor frequency (7.72 MHz to 4.36 MHz) by 41% reduced T_1 of the fast component by ≈12% without affecting the slow component. This effect can possibly be attributed to the smaller, lower molecular weight mobile cytoplasmic components having a τ_c nearer to the $1/\omega_o$ used, compared with the large nuclear DNA complexes. Necrosis presumably causes a destruction of the nuclear membrane and thus mixing of the compartments.[275] Also, temperature reduction affected both of the T_1 values by equal proportions suggesting that transmembrane transport exchange is not a significant contribution to relaxation in this system.

^{17}O NMR was used with ^1H NMR to study the relaxation rates for aqueous suspension of dark adapted chloroplasts in the presence of Mn^{2+}.[276] It was shown that the T_1 and T_2 of protons were dependent on the concentration of loosely bound Mn^{2+} in the

Downloaded At: 15:58 17 January 2011

chloroplast membranes. However, $H_2{}^{17}O$ relaxation was a single exponential process and the exchange time of water across the thylakoids was not determined accurately, but given as >1 msec.

^{17}O NMR spectra of suspensions of human erythrocytes equilibrated in 10 to 18% $H_2{}^{17}O$ Ringer showed some different features.[277] Nonexponential longitudinal relaxation was apparent over a wide domain of cytocrit values (0.32 to 0.67). However, the longitudinal relaxation behavior of the supernatant alone, and packed cells alone, was a simple exponential. Thus, the data from suspensions of cells reflected not only intra- and extracellular relaxation, but also the transmembrane exchange process. A theoretical analysis was given in order to extract the exchange rate: 60 and 107 sec^{-1} at 25 and 37°C, respectively.[272] The rate was clearly temperature dependent and gave a linear Arrhenius plot indicating an activation energy for the exchange process of 8.7 ± 1.0 kcal/mol. It should be noted that these measurements required no use of an external paramagnetic ion such as was discussed in Section V.C for ^1H NMR. However, addition of Mn^{2+} to the cell suspension did render the longitudinal relaxation into a single exponential with T_1 equal to that of pelleted cells.

No reports of attempts to incorporate ^{17}O into metabolites and then study metabolism in cells using ^{17}O NMR have yet appeared, although a study has been made of the orientation of $^2H_2{}^{17}O$ water in phospholipid bilayers.[278] It seems likely that the ^{17}O nuclide will be used more for studies of order parameters in membranes and in situations where its rapid relaxation is an advantage than for following the dynamics of chemical reactions, because the resonance lines are too broad to enable good resolution between different substances.

C. ^{15}N NMR Studies

^{15}N nuclei have long correlation times when incorporated in biopolymers. This results in short T_1 values which in turn allow rapid accumulation of FIDs. An interesting property of the ^{15}N nucleus is the negative γ (Table 1) and consequent negative nOe (Equation 9); the latter can significantly influence signal amplitudes in situations where heterocoupled nuclei are irradiated.

The fact that nitrogen atoms are often associated closely with sites of biological activity means that ^{15}N NMR could be a valuable tool in the investigation of enzymes *in situ* as has already been done on isolated pure proteins[279,280] and proteins in general. The range of chemical shifts is greater than for even ^{13}C (Table 1) but until recently the low sensitivity of the nucleus has restricted its use in natural abundance studies. Natural abundance is 0.37% so at natural abundance levels its sensitivity is 3.8×10^{-6} that of protons which means a difference of about 10^{11} in the time required to achieve the same S/N at constant field.[281]

The chemical shift reference usually used is 0.1 M ^2H $^{15}NO_3$ in ^2H_2O (but the absolute reference agreed upon by IUPAC is nitromethane in liquid NH_3), and tabulated data of chemical shifts are available in the literature.[280]

The ability to detect ^{15}N-labeled substances in spectra of biological systems is related to how broad the resonances are and, in proton-decoupled spectra, the magnitude of the nOe (peak area after ^1H decoupling/peak area before decoupling). As noted in Section IV.A, to a first approximation, molecular motion can be related to a single correlation time (τ_c) which describes isotropic tumbling.

The correlation time dependence of line broadening by ^{15}N-^1H dipolar interaction for a N-H group indicates that the ^{15}N resonances of molecules with $\tau_c > 10^{-7}$ sec will be very broad (>200 Hz) and usually not observable. The effect of the τ_c on the nOe suggests that there are three types of resonances to be expected from intact cells: (1) resonances that are enhanced and inverted (nOe = −4) corresponding to molecules with $\tau_c < 10^{-9}$ sec, (2) resonances of molecules with $\tau_c = 5 \times 10^{-9}$ sec will be nulled (nOe = 0) by proton

Downloaded At: 15:58 17 January 2011

decoupling, and (3) resonances that are slightly attenuated (nOe 0.9) corresponding to $\tau_c > 10^{-8}$ sec.[281]

Studies of intact biological systems using ^{15}N NMR have been few, but several important observations have been made on microorganisms and leukemic cells grown in ^{15}N-enriched media.[281,283,284] The majority of resonances observed in whole *E. coli, Bacillius licheniformis,* and baker's yeast were *inverted* and not considered to have originated from small metabolites, but from relatively mobile groups of the cell wall components. The ^{15}N resonances of amino acids and other small nitrogenous molecules with T_1s longer than 1 sec would have been saturated because of the fast repetition rates used in these experiments.

The proton-coupled ^{15}N NMR spectrum of *E. coli* (9.12 MHz, 3 to 6×10^4 FIDs, grown in the presence of 0.1% $^{15}NH_4Cl$) showed a lysine-N_ϵ peak, a protein backbone amide envelope of resonances, and an unassigned amino resonance. Proton decoupling eliminated the protein backbone amides and enabled the assignment of protein *side* chain lysine-N_ϵ, arginine-N_ϵ, arginine-$N_{\omega\omega}$ nitrogens, PE plus some unidentified amide and amino resonances. SDS and chloroform/methanol extraction of cell wall and membranes of *E. coli* enabled the visualization of different ^{15}N resonances and these data contributed to an interpretation of cell wall organization.[284]

The gram-positive bacterium *B. licheniformis* has a thick cell wall consisting of peptidoglycan, teichoic acid, and teichuronic acid, and distinct differences between spectra of these organisms and *E. coli* were noted. The spectra were obtained over a 24-hr period. The lysine and PE resonances were absent and two of the arginine lines were of low intensity. However, an intense envelope of resonances was assigned to N-acetyl glucosamine, N-acetylmuramic acid, and N-acetyl glucosamine of the cell wall.

Friend leukemia cells had a simple spectrum with a predominant lysine peak and a broader peptide envelope. No signal due to cell wall components was seen, owing to their physical absence in these cells.

Staphylococcus aureus cells were grown in a medium containing [^{15}N] glycine and $^{15}NH_4Cl$. The proton-decoupled ^{15}N NMR spectrum showed a single intense inverted resonance (267.8 ppm) assigned to the cell wall peptidoglycan pentaglycine cross bridge. Isolated cell walls gave an identical spectrum. In addition, the chemical shift of the middle glycine of N-acetyl triglycine and unfolded [glycyl-^{15}N] hemoglobin,[280] both of which are random coils, was the same as in whole *S. aureus.*[283] Therefore, it is likely that the pentaglycine bridge is a random coil structure in keeping with the notion that bacterial walls are mobile structures.

The ^{15}N hyperfine shifts of iron-bound $C^{15}N^-$ have been shown to be quite sensitive to the surrounding environment (protein) when bound to heme.[285] In cell-free cyanmethemoglobin the separation of the ^{15}N resonances of $C^{15}N^-$ bound to the α and β chains was quite large, about 70 ppm compared with the corresponding ^{13}CO-hemoglobin experiments[236] (Section VIII.B). Furthermore, the shifts are quite pH dependent. Erythrocytes from humans, rats, rabbits, and beagles were treated with $NaNO_2$ to oxidize the Hb to met-Hb.[286] Addition of $KC^{15}N$ to the dog and human cells yielded two broad ^{15}N resonances with a large downfield shift, from the free $C^{15}N^-$ (−90 ppm from $^{15}NO_3^-$), located at 970 and 1077 ppm; 150K transients were collected at 29°C using 10 KHz spectral width, 4K data points, and a 0.21-sec repetition rate.[286] The extent of the large shift was ascribed to the binding of $C^{15}N^-$ to the paramagnetic hemes and not to other cellular structures such as membranes.

In both human and dog erythrocytes the $C^{15}N$-Hb peaks were separated by 41 and 63 ppm, whereas in rat cells only a single peak was evident, while in rabbit cells three peaks were seen.[286] With respect to the latter case it was suggested that heterogeneity of Hb forms exists. Furthermore, in samples of human erythrocytes the peak separation was pH dependent having the following values for the corresponding extracellular pH: pH

Downloaded At: 15:58 17 January 2011

7.3, 72; pH 7.7, 70; pH 8.1, 65.[286] Thus it was concluded that ^{15}N NMR may be used to study the perturbation of the heme-protein environment by effector ligands such as 23DPG.

The application of the technically difficult method of magic angle spinning in ^{15}N NMR to soy bean seeds, pods, and leaves by Schaefer et al.[287] was the first such study of whole tissues. The procedure enabled a determination of the relative concentrations of amide and amino nitrogens as well as the concentration of a few amino acid residues of proteins in the solid samples. Furthermore, a double-cross polarization (CP) ^{13}C NMR spectrum of a spinning ^{15}N-labeled seed was obtained in which resonances were observed only from those carbons directly bonded to nitrogens. This technique, it was claimed, can lead to an estimate of the amino acid composition of the protein which is complementary to the direct ^{15}N NMR spectrum.

Studies such as this using ^{15}N are valuable because of a dearth of other tracer methods available for nitrogen; since ^{13}N has a half-life of 10 min, radiotracer techniques are extremely difficult to execute. Even so, despite the great deal of information available from the ^{15}N NMR studies so far, the enormously long data accumulation times required would indicate that the information obtained from ^{15}NMR will have to remain structural, rather than kinetic in a metabolic sense.

Downloaded At: 15:58 17 January 2011

D. ^{23}Na NMR Studies

The spin-lattice and spin-spin relaxation times of ^{23}Na in rat gastrocnemius and tibialis anterior muscle were measured using pulse method at 26.45 MHz.[288] The longitudinal relaxation curve followed a single exponential decay, whereas the transverse relaxation was complex and described by at least two exponentials. The state of the Na^+ ions agreed with a model that was characterized by two physical parameters: (1) the average time a Na^+ ion is bound to a macromolecular site and (2) the average distance between the ion and the binding site.

As with other nuclei, all the relaxation times of Na^+ in muscle are less than in free NaCl solution and, in addition, only a single T_2 is evident. The relaxation time shortening was thought to be due to quadrupolar interaction in a restricted environment.[288] It should be noted that quadrupolar effects dominate the relaxation of the ^{23}Na nucleus. It was analyzed according to a theory where electric field gradients fluctuate less rapidly than the Larmor frequency of the $^{23}Na^+$.[289]

Two correlation times, one at 10^{-8} sec and the other at 10^{-11} sec, were calculated from the data. Interestingly, although in the living state the concentration of extracellular Na^+ is tenfold greater than inside the cell, in the metabolically exhausted tissues used in the studies 90% of the Na^+ was inside. Furthermore, the conclusion from the analysis of the quadrupolar relaxation rates was that in the cells most of the Na^+ is adsorbed to macromolecules. The average life time of a given ion-site pair was 10^{-8} to 10^{-5} sec and the average distance between the ion and the site was 0.45 nm, the mean diameter of a water molecule.

Earlier CW ^{23}Na NMR studies on erythrocytes washed in $^{23}NaCl$ showed that all but $\approx$6% of the ^{23}Na was detected by ^{23}Na NMR, and that the whole cells gave a broader peak than with $^{23}NaCl$ added to hemoglobin solution.[290] The reasons for the broadening were, therefore thought not to be paramagnetic but some undefined effect of the membranes, since cell ghosts added to a solution of $^{23}NaCl$ gave rise to broadening. Similar broadening was evident in intact frog muscle, 38 Hz compared with $\approx$20 Hz after the muscle was ashed. However, about 47% of the ^{23}Na was "invisible" to NMR but the findings were consistent with an analysis that suggested that the ions in muscle were partly immobilized.[290]

The physiological implications of the weak Na^+ binding in cells are yet to be evaluated

but it is important to note that the information, of this kind, on *in situ* Na^+ ion behavior, is not obtainable by any other means.

E. ^{19}F NMR Studies

From Table 1 it can be seen that the ^{19}F nucleus, at a given magnetic field, is third only to tritium and hydrogen nuclei in terms of sensitivity. In addition, the coupling constants and chemical shifts are an order of magnitude larger than those of the corresponding hydrogen analogues. These features, together with the high sensitivity and small size (approximately the same size as the —OH group), have enabled its successful use as a chemical shift probe in studies of protein conformation. The chemical shift or line width of ^{19}F incorporated into proteins can be made to change on addition of specific ligands, or ^{19}F-labeled ligands may demonstrate perturbation of their resonances on binding to a specific protein.[32,291]

In some recent work the enhancement of spin-lattice relaxation of $^{19}F^-$ in the presence of the metalloenzyme zinc-copper superoxide dismutase was forwarded as an accurate means of assaying the enzyme.[292] Although the method is not very sensitive, measuring down to $\approx 10^{-8}$ *M*, compared with the direct enzymic assay, it certainly is simple. In another series of experiments the interaction of ^{19}F-substituted sodium trifluoroacetate with pancreatic elastase was monitored by following the chemical shift changes that occurred on the binding of the reagent to the protein.[293]

The previous studies have been conducted on purified protein but, of course, the justification for their inclusion here is that the methods do have potential for the investigation of whole cells. The first report (and only one included here) of ^{19}F NMR studies on whole cells was on platelets (thrombocytes).[294]

Platelets possess two well-defined regions, a cytoplasm and membrane-enclosed vesicles. The cytoplasm is rich in Pi, sugar phosphates, and adenine nucleotides. The vesicles contain high concentrations of 5-hydroxytryptamine (5HT), ADP, ATP, pyrophosphate (PP), and Ca^{2+}. Incubation of platelets with [2-^{19}F] adenosine resulted in accumulation of [2-^{19}F]ATP in the cytoplasm as evidenced by growth of the (broad) assigned peak. It was also stressed that there is little exchange of ATP between mitochondria and cytoplasm in this system so a single compartment was being labeled.

When [4,6-^{19}F] 5HT was incubated with platelets for 60 min, it yielded spectra that showed none of the expected resonances. However, poisoning the cells with 2-deoxyglucose and antimycin A or addition of the ionophore X57A resulted in the appearance of a well-resolved resonance due to [4,6-^{19}F]5HT. It was concluded therefore that the fluorinated 5HT present in the vesicles was very immobile thus resulting in extensive anisotropic signal broadening. Similarly, perchlorate extraction of the [2-^{19}F] adenosine-treated cells gave significant sharpening of the peak.

The possible causes for broadening were discussed, ranging across those mentioned in previous sections: paramagnetic centers, field gradients, and exchange between compartments. However, it was concluded that anisotropy in the highly structured complexes of 5HT, nucleotides, and Ca^{2+} was the likeliest cause.[294] This picture contrasts with the relative mobility of the contents of chromaffin granules as estimated from ^{31}P NMR experiments (Section VII.D).

F. ^{35}Cl, ^{81}Br, and ^{3}H Studies

^{35}Cl NMR (5.88 MHz) has been used to study Cl^- binding to ghosts of human erythrocytes.[295] Anion permeability in erythrocytes is associated with a membrane protein of molecular weight 95,000 called band 3. The measurement of Cl^- binding to the membranes is not feasible by other means because of its low affinity; the K_m for Cl^- transport has been estimated at 67 m*M*.

Downloaded At: 15:58 17 January 2011

The half-width $\Delta\nu_{1/2}$ for 250 m*M* $K^{35}Cl$ was 19 ± 0.6 Hz, but the addition of erythrocyte ghosts (5 mg protein per milliliter) increased $\Delta\nu_{1/2}$ to ≈40 Hz. Triton X100 extracts of the ghosts with enrichment of band 3 also gave rise to broadening ($\Delta\nu_{1/2}$ 52 Hz at 5 mg protein per milliliter). However when the cells were treated with the irreversible anion transport inhibitor 4,4'-diisothiocyano-2,2'-stilbene disulfonic acid (DIDS) prior to the preparation of ghosts, the specific broadening ($\Delta\nu_{1/2}$) of the $^{35}Cl^-$ peak was reduced by 32% for ghosts and 50% for the Triton extract. The line broadening was maximal at pH 7.2, and is thought to arise from *specific* Cl^- binding allowing interaction of the quadrupolar nuclear moments with electric field gradients in the binding site.[295]

The measurement of Cl^- binding in other tissues is clearly possible. Certainly some interesting observations have been made on the binding of ^{35}Cl to purified hemoglobin; the data suggest a specific high affinity site which reduces in affinity on the binding of O_2 onto the molecule.[296]

No biological studies using NMR of the other halogen nuclide, ^{81}Br, have appeared, but the binding of Br^- to pure carbonic anhydrase was followed by observing line broadening in a manner similar to the experiments mentioned above.[297]

Although no work on biological systems using the ^3H nucleus has been published, some promise exists for this highly sensitive nucleus[71] (see Table 1). An obvious drawback is the high radioactivity of the samples which complicates handling,[256] but useful information concerning such properties as kinetic isotope effects in whole cell metabolism using specifically labeled compounds is potentially accessible. Even before such studies could be undertaken, the method would be useful for determining the sites of tritiation of synthetic substrates.[298]

Downloaded At: 15:58 17 January 2011

X. NMR IMAGING TECHNIQUES

A. Introduction

The NMR studies discussed so far in this review have been concerned with nuclear spin properties of the samples averaged over the volume of the sample. However, NMR experiments are capable of being manipulated to yield spatial information, i.e., images.

Investigations into, and development of, NMR imaging techniques are numerous and the field has been usefully reviewed by several authors.[299-305] In addition, Lauterbur has supplied a comprehensive bibliography of the relevant literature up to 1979.[306] The appeal of the method for medical diagnosis is that it is noninvasive, it uses RF radiation which is attenuated little by bone, and is nonionizing.[307] There is no well-documented evidence that high magnetic fields have a detrimental effect on humans, although the biological effects of weak magnetic fields are certainly manifest in the growth and behavior of some plants and animals.[308] Therefore it is worth heeding the cautionary words of Andrew[303] in relation to the use of NMR in medicine.

In general, the formation of a physical image requires that an object interacts with radiation (or matter) whose wavelength is of the same order or less than the smallest features to be resolved; an image is defined here as the graphical representation of the spatial distribution of one or more properties of components of the object.[28] Yet NMR imaging employs radiation (RF) of a wavelength (0.5 to 5.0 m) much greater than the samples themselves. Therefore, because of its novelty it is worth considering here the means whereby the restrictions on wavelength are removed.

In a uniform magnetic field the NMR spectrum of a homogeneous sample, such as pure water, is a single narrow peak. Consider now the schematic NMR apparatus of Figure 14a;[307] if a linear magnetic field gradient along the x-axis is superimposed on the uniform field B_o (in the z-direction), the resonance frequencies at different points along the x-direction will no longer be identical (according to Equation 4), but will be a linear

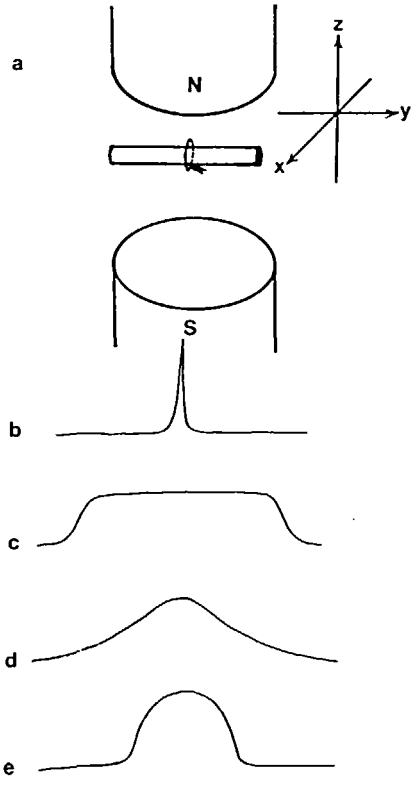

FIGURE 14. NMR signal in the presence of field gradients. A cylindrical sample of water in a NMR spectrometer showing (a) the coordinate system and stylized spectra obtained from it, (b) in the presence of no field gradients, (c) in the presence of a linear field gradient in the x-direction, (d) in the y-direction, and (e) in the z-direction.[307]

function of their x-coordinates. Thus, the original NMR spectrum is transformed into a pattern that is no longer a conventional spectrum, but is a one-dimensional (1-D) distribution function of the x-coordinate, convolved with the shape of the original spectrum.[300] For example, field gradients in either of the x-, y-, and z-directions for a cylindrical sample of water, using ^{1}H NMR, yield the spectra of the form shown in Figure 14c, d, and e.[307] Two- and three-dimensional (3-D) images can be constructed by the mathematically judicious recombination of the projections taken in various orientations.

The interaction of the two fields, B_o and the gradient G, can be considered as being mediated by the sample; hence the commonly accepted term for NMR imaging is zeugmatography (Greek: that which is used for joining together).[28]

B. Imaging Methods

There are basically five different procedures currently used for construction of images using NMR.[300,304,309] They have their own advantages for particular applications and involve a greater or lesser amount of computer processing. Only recently has an objective basis for comparison between the methods been developed which considers computer image processing time, S/N, etc.[310,311] Historically, the first zeugmatographic method

Downloaded At: 15:58 17 January 2011

developed[312] was that which relied on reconstruction of 2-D thin-section image from 1-D images, obtained as described above, with linear field gradients.[28,313] Fairly lengthy reconstruction calculations must be made employing an algorithm (ART: Algebraic Reconstruction Technique) similar to that used in X-ray computerized axial tomography (CAT) scanning.[314] Rotation of the sample or the field gradient is necessary in this procedure and each 1-D projection is obtained by Fourier transformation of the FIDs for each angle of orientation. A schematic diagram of the projections at different angles for a, so-called, phantom test-object with circular cross-sectional symmetry is given in Figure 15a.[304] Such images have been satisfactorily reconstructed, using data from ^1H NMR, from objects with circular symmetry the phantom shown in Figure 15A,[315] a pecan nut, and a live mouse.[304,313]

Kumar et al.[316] developed a method of generating a 2-D image (projection) without the necessity of reconstructing the image from 1-D projections. A $\pi/2$ pulse is applied to the sample followed by a gradient in the x direction (G_x) for time t_x, and a y-gradient (G_y) for the time t_y during which time the signal is detected. The resulting FID is a function of t_x and t_y so that when t_x is varied over a specified range a complete family of FIDs is assembled. The data set is 2-D-Fourier transformed to give a 2-D projection along the z-axis. The theoretical treatment presented addressed also the possibility of 3-D reconstructions using a z-gradient. This technique, called *NMR Fourier zeugamatography,*[316] has not enjoyed wide usage, although it is still being further developed.[317] A disadvantage of the method is the inability to control successfully negative intensities[314] in reconstructed images, and the computational effort is still equivalent to the first method discussed.[311]

The third method is one which does not rely on reconstruction from projections, and is known as *line scan proton spin imaging;*[318] although *proton* is used in the title, as with all these methods they can be applied to other nuclei, e.g., ^{19}F[319] and ^{31}P.[317,320,321] The spatial discrimination is achieved by appropriate preparative RF irradiation of the sample along the y-axis within a field gradient G_y. The gradient direction is then switched to give G_x, and the FID is then acquired.[318,322,323] The preparative irradiation is selective in that it is especially "tailored" to have a narrow distribution of RF field components.[318,322] Consequently, it excites spins in a thin lamina Δy units wide, at an appropriate point in the sample where the field strength satisfies the Larmor equation (Equation 4). Removal of G_y and application of G_x ensures a spreading out of spin frequencies in the original excited lamina. Then, the FID, after Fourier transformation, is a 1-D projection of spin density in the x-direction (Figure 16). In the next cycle another strip is excited, by a newly tailored pulse, or altered G_y, and detected as before so that after repeated application, a 2-D image of the object is built up.

Clearly, in this technique, there is no need for image reconstruction algorithms, such as ART,[318,323] and the image builds up progressively as more slices are selected; this may be time saving, if the image sought appears before the anticipated completion of the experiment.

In the fourth NMR imaging procedure, time-dependent field gradients (i.e., alternating in phase by π) are applied to the sample in such a manner that only one point of the sample experiences a time-independent field. The procedure is known as the *sensitive point method.*[324] The method need not be used exclusively for imaging, but can theoretically be employed to localize study of a sample to a particular point (volume), for example to measure T_1, T_2, D, or flow.[300] For image construction the sensitive point is made to scan throughout the object to sample spin densities at each location, the movement being a consequence of the fact that a particular field strength is the vector sum of the three orthogonal field gradients G_x, G_y, and G_z whose strengths can be independently varied by control of the coil currents.

From the point of view of image construction, the sensitive point method has to date

Downloaded At: 15:58 17 January 2011

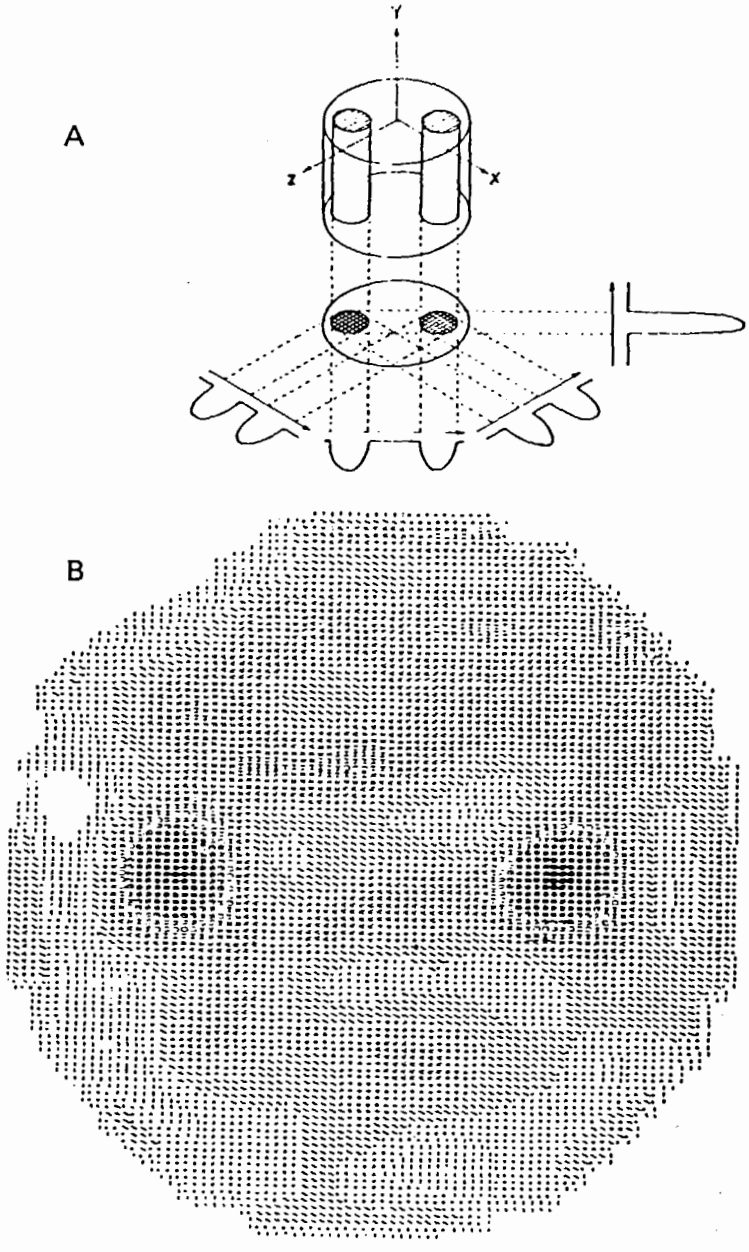

FIGURE 15. Zeugmatography. (A) The relationship between a 3-D object, its 2-D projections along the y-axis, and four 1-D projections at $\pi/4$ intervals in the xz-plane. (B) A proton NMR zeugmatogram of a phantom similar to that in the diagram above; two 1-mm capillaries of water in a 4.2-mm i.d. tube containing a mixture of ^1H_2O and ^2H_2O. (From Lauterbur, P. C., *Nature*, 242, 190, 1973 and Lauterbur, P. C., *Pure Appl. Chem.*, 40, 149, 1974, respectively. With permission.)

proved to be the slowest,[310] but it has several advantages over the other techniques. It has less stringent requirements on the uniformity of the magnetic fields provided the physical location of the null point can be accurately specified, and no computing is required for image formation. The resolution is better than other methods by a factor of 10.[310]

A recent innovation has been the development of the *multiple sensitive point method*

Downloaded At: 15:58 17 January 2011

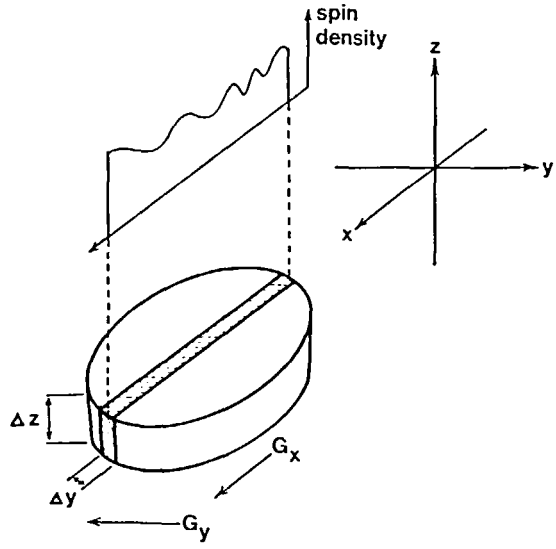

FIGURE 16. Diagram illustrating the principles of line scan proton spin imaging. RF irradiation of the sample occurs in the presence of the magnetic field gradient Gy, then Gx is applied and the FID recorded. It is then Fourier transformed to give the 1-D projection on the x-axis.[323]

Downloaded At: 15:58 17 January 2011

in which two alternating gradients, G_x and G_z, define a line in the y-direction along which is superimposed a static gradient G_y. Detection of the signal follows the procedure that is used in the single point method,[324] steady-state free precession resulting from excitation with a string of coherent equally spaced phase altered pulses. Thus, signals are generated from discrete volume elements along the y-direction. This method clearly dramatically reduces image construction times.[310]

The fifth type of NMR imaging method is a variant of the selective excitation or spin planar mapping procedure and is known as FONAR (Field fOcussing Nuclear mAgnetic Resonance).[326,327] It was in fact the subject of a patent application in 1972.[328] The essential difference is that the static field gradient is nonlinear and the RF pulse is tailored as well so that a large proportion of the excited spins lie in only a small volume, called the *resonance aperture* by the authors.[329] Therefore, as with the sensitive point method, the NMR signal is dependent on the spin density in a small region which can be made to traverse a sample thus enabling the composing of an image.[329]

C. Applications in Biology and Medicine

To date, zeugmatography has been little used for studies on the metabolic status of organs, and the emphasis has been on obtaining better, highly resolved anatomical images more quickly. Straight forward spin density imaging relies for its contrast between various structures, in say the human body, on the different water content in the different tissues. It is clear from Figure 17 why bone is well discriminated from muscle. However, Lauterbur's group has considered the important question as to whether zeugmatography will be capable of detecting ischemia in tissues, the intention being to use the altered relaxation rates of diseased tissues as the spin property that is mapped[302,330-334] (Section IV.D).

In one series of experiments, ligation of the anterior descending coronary artery of the heart of an anaesthetized dog was followed by post-mortem sectioning of the

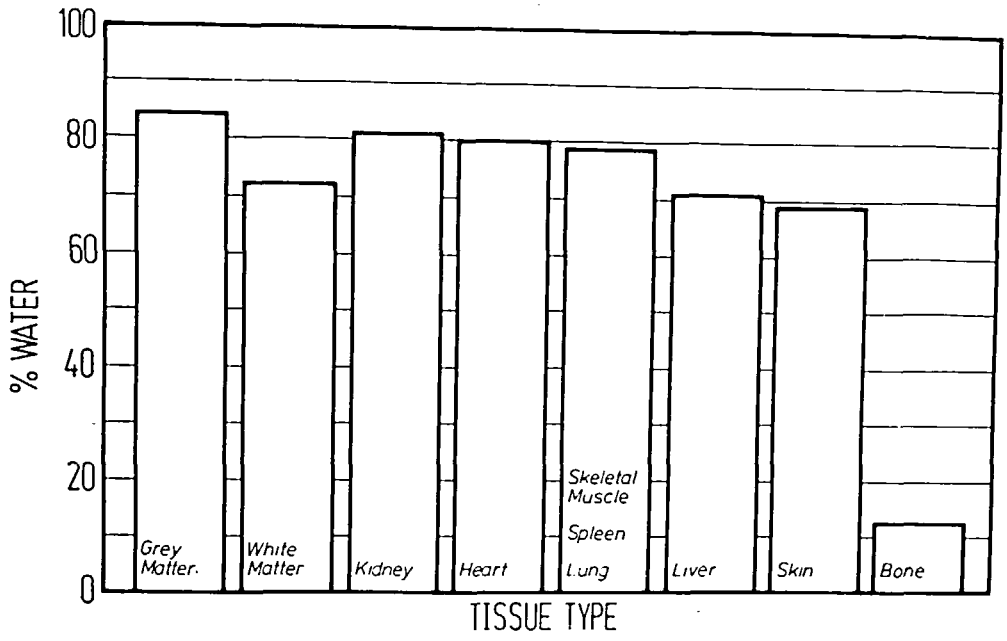

FIGURE 17. The water content of various human tissues. (From Mansfield, P. and Pykett, I. L., *J. Mag. Res.*, 29, 355, 1978. With permission.)

myocardium.[330] The T_1 of water in the tissue distal to the ligation increased by 10 to 20%, and the water content was increased.[332] However, differences between animals were greater than between infarcted and normal myocardium. This led to the use of Mn^{2+} to try and exaggerate the differences between normal and abnormal tissue in this context; 0.1 mmol/g body weight of Mn^{2+} was injected into anaesthetized dogs 60 min after ligation of the coronary artery and allowed to circulate for 30 min. Then T_1 and water contents were measured on small blocks of muscle sectioned from the heart. The mean Mn^{2+} and water contents of the infarcted and normal tissues were 0.058 m*M* 76.6% and 0.191 m*M* 75.8%, respectively.[333] More important, in light of the small differences in water content, was the fact that the respective T_1s for normal and infarcted heart muscle were 0.127 and 0.271 sec. This difference in T_1 was considered to be significant and therefore a useful property to be exploited in the future in zeugmatographic mapping of whole heart *in situ*.[333] Therefore the specific uptake of paramagnetic ions by other tissues and neoplasms may be a useful means of enhancing zeugmatographic contrast.

Steam introduced into the lungs of anaesthetized dogs produces an acute pneumonitis and pulmonary edema.[330,331] Although the water content of lung tissue in one series was increased in the damaged tissue by only 5.6%, the T_1 was increased by 28%.[331] Again, the differences in T_1 between normal and damaged tissue should enable zeugmatography to be used to detect such changes clinically.

As noted in Section IV.D the T_1 of water protons in neoplastic tissues is prolonged.[89] In the first published report of tumor detection, in a whole mouse, a 3-mm "exploring" volume was used with the FONAR technique operating at 10 MHz in a superconducting magnet.[326,327] A second early report was of a mouse with an implanted adenocarcinoma; scans were taken using an 8.15-MHz spectrometer with the field gradient orientated at 15° intervals, and the T_1-dependent image was formed using an ART-type algorithm.[335]

Some of the best published *in vivo* images are those of the human forearm and wrist. Many of the important anatomical structures, muscle, skin, and bone correlated directly with spin density[225] using the multiple sensitive point method. Among other high quality

Downloaded At: 15:58 17 January 2011

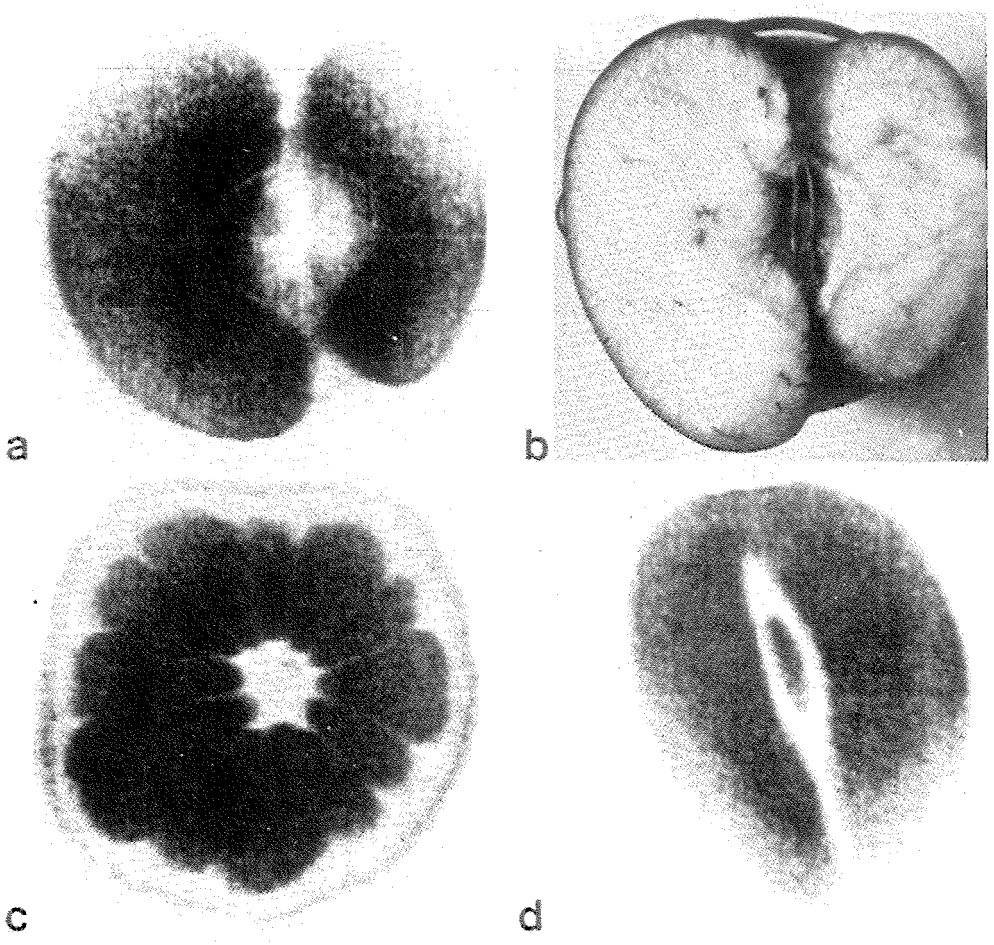

FIGURE 18. Images obtained by NMR zeugmatography using the multiple sensitive point method. Here a, c, and d show thin section NMR images of intact apple, satsuma, and plum, respectively, while b is a subsequent section taken at the level of the imaging plane of the apple. These images demonstrate the resolving power of NMR imaging when applied to biological systems. (From Hinshaw, W. S., Bottomley, P. A., and Holland, G. N., *Experientia*, 35, 1268, 1979. With permission.)

images (16-level color display) were a female rat, 6 cm across,[325] and most recently sections of an apple, a satsuma, and a plum (Figure 18), obtained using the multiple sensitive point method.[336]

D. Other Nuclei

It would be useful to extend the present scope of ^{31}P NMR to include the determination of the spatial distribution of phosphorus metabolites in tissues and to follow changes that occur when organs are stressed. However, a major problem with ^{31}P studies is that the normal spectrum consists of several overlapping peaks so the result of applying a field gradient is to produce an envelope of lines that are virtually impossible to unscramble. The matter has been discussed in some detail, and selective irradiation with consequent peak suppression may be one viable answer to the problem.[320] Studies so far have dealt only with phantoms.[317,320,321] Likewise, two phantoms, one consisting of three parallel tubes and the other a glass star, were filled with fluorocarbon (FC43). The ^{19}F NMR signals obtained by the multiple sensitive point method were used to construct images consisting of a 128×128 array of independent picture elements.[319] Since ^{19}F is 100% abundant

Downloaded At: 15:58 17 January 2011

and naturally occurring fluorides are rare, ^{19}F zeugmatography may in the future be of value in tracing drug localization in the body.

E. Whole Body Imaging

The imaging of the whole human body by NMR is a major objective of several groups,[301,302,337,338] and a significant achievement in this direction has been the development of wide bore superconducting magnets with homogeneous fields.[337,338] However, the field strengths able to be used for large objects are restricted to less than 0.2T, because attenuation and phase-shift-induced distortion occurs with RF fields in excess of 10 MHz.[301] Nevertheless, in a preliminary study, the transverse section of the chest, using FONAR, successfully delineated the lungs, mediastinum, and thoracic wall in a human subject.[338]

The rapid switching of RF and magnetic gradient fields has the potential for inducing eddy currents in the sample[317] (human subject), so caution will clearly have to be exercized in implementing some imaging procedures. The hope is that the new imaging techniques will be a valuable complement to current diagnostic aids such as CAT scanning, but they have the added ability to detect neoplastic and diseased tissues not able to be resolved by any other method — especially since paramagnetic contrast agents hold such promise.[302]

Downloaded At: 15:58 17 January 2011

XI. CONCLUDING REMARKS

From what has been reviewed it must be agreed that in the few years since NMR was first extensively applied in biology and medicine, a vast body of information on cell structure and function, not obtained or obtainable in many cases by other physical means, has been amassed. Such physical characteristics as the tumbling rate of hemoglobin molecules, the viscosity of the intracellular medium, the diffusion coefficient of intracellular water, the transmembrane exchange rate of water and metabolites and the free energy change of the reaction, the Km (affinity) of intracellular enzymes for their substrates, the stereospecificity of intracellular enzymes for their substrates, the first-order rate constants for ATP hydrolysis by membrane-bound ATPase *in situ,* isotope exchange kinetics of substrates, and distribution of labels on metabolites have been measured for the first time *inside* whole cells and organs using NMR. On a more clinical note, NMR has been used to study:

1. The changes in relaxation behavior of water proton spins as hemoglobin aggregates in the sickling process of sickle cell anaemia
2. The measurement of concentration and transport of choline into erythrocytes of patients treated with lithium salts
3. The detection of tumors and discrimination between normal and abnormal tissue on the basis of nuclear spin relaxation times
4. The imaging of organs and the detection of tumors in whole animals

The list is not a complete summary of the contributions made by NMR to our understanding of biological and medical systems but justice has hopefully been done to the rest in the previous 50 or so pages. Arguably, however, these are the most important contributions made by NMR and, as was said before, many of them could not have been made by any other physical techniques known to date. It is expected that many more exciting discoveries will be made in the not too distant future as a greater number of high resolution spectrometers become available or as the problems with large scale high field magnets become solved so that zeugmatographic imaging of organs can improve. After

all, the principal aim of biologists is to understand biochemical and biophysical properties of undisturbed intact cells, tissues, organs, and animals.

ACKNOWLEDGMENTS

It is a pleasure to acknowledge the continuing assistance and collaboration of Dr. Alan J. Jones and likewise to thank Drs. F. F. Brown, I. D. Campbell, and Professor D. L. Rabenstein for collaboration, discussions, and preprint material. Also preprint and other material was kindly supplied by Professors E. R. Andrew and P. C. Lauterbur. Valuable bibliographic and technical assistance was undertaken by Mrs. V. A. Brent, Mrs. P. E. Jarvie, and Mrs. M. G. Kuchel, and the typing was patiently executed by Mrs. E. F. Pearsall. The financial assistance of the Australian National Health and Medical Research Council is gratefully acknowledged.

REFERENCES

1. **Purcell, E. M., Torrey, H. L., and Pound, R. V.,** *Phys. Rev.*, 69, 37 (1946).
2. **Bloch, F., Hansen, W. W., and Packard, M.,** *Phys. Rev.*, 69, 127 (1946).
3. **Odeblad, E., Bhar, B. N., and Lindström, G.,** *Arch. Biochem. Biophys.*, 63, 221 (1956).
4. **Moon, R. B. and Richards, J. H.,** *J. Biol. Chem.*, 248, 7276 (1973).
5. **Hoult, D. I. and Richards, R. E.,** *Proc. R. Soc. London A*, 344, 311 (1975).
6. **Radda, G. K. and Seeley P. J.,** *Ann. Rev. Physiol.*, 41, 749 (1979).
7. **Burt, C. T., Cohen, S. M., and Bárány, M.,** *Ann. Rev. Biophys. Bioeng.*, 8, 1 (1979).
8. **Mathur-DeVré, R.,** *Prog. Biophys. Mol. Biol.*, 35, 103 (1979).
9. **Campbell, I. D. and Dobson, C. M.,** in *Methods of Biochemical Analysis*, Vol. 25, Glick, D., Ed., John Wiley & Sons, New York, 1979, 1.
10. **Wallach, D. F. H.,** *J. Gen. Physiol. London*, 54, 3, (1969).
11. **Ji, T. H. and Urry, D. W.,** *Biochem. Biophys. Res. Commun.*, 34, 404 (1969).
12. **Fisher, A. B., Furia, L., and Chance, B.,** *Am. J. Physiol.*, 230, 1198 (1976).
13. **Moravec, J., Corsin, A., Owen, P., and Opie, L. H.,** *J. Mol. Cell. Cardiol.*, 6, 187 (1974).
14. **Barlow, C. H. and Chance, B.,** *Science*, 193, 909 (1976).
15. **Franke, H., Barlow, C. H., and Chance, B.,** *Am. J. Physiol.*, 231, 1082 (1976).
16. **Chance, B., Barlow, C., Haselgrove, J., Nakase, Y., Quistorff, B., Matschinsky, F., and Mayevsky, A.,** in *The Role of Compartmentation in Metabolic Regulation: Microenvironment*, Srere, P. A. and Estabrook, R. W., Eds., Academic Press, New York, 1978, 131.
17. **Moore, W. J.,** *Physical Chemistry*, 5th ed., Longman, London, 1972.
18. **Lewis, A., Fager, R. S., and Abrahamson, E. W.,** *J. Raman. Spectrosc.*, 1, 465 (1973).
19. **Lewis, A., Spoonhower, J., Bogmolni, R. A., Lozier, R. H., and Stockenius, W.,** *Proc. Natl. Acad. Sci. U.S.A.*, 71, 4462 (1974).
20. **Lewis, A.,** *Fed. Proc.*, 35, 51 (1976).
21. **Schneider, A. S., Middaugh, C. R., and Oldewurtel, M. D.,** *J. Supramol. Str.*, 10, 265 (1979).
22. **Rayleigh ([Lord] J. W. Strutt),** in *Physical Chemistry of Macromolecules*, John Wiley & Sons, New York, 1967.
23. **Tanford, C.,** *Physical Chemistry of Macromolecules*, John Wiley & Sons, New York, 1967, chap. 5.
24. **Joos, G.,** *Theoretical Physics*, Blackie & Son, London, 1941, 430.
25. **Mustacich, R. V. and Ware, B. R.,** *Biophys. J.*, 16, 373 (1976).
26. **Blasie, J. K. and Worthington, C. R.,** *J. Mol. Biol.*, 39, 417 (1969).
27. **Knowles, P. F., Marsh, D., and Rattle, H. W. E.,** *Magnetic Resonance of Biomolecules: An Introduction to the Theory and Practice of NMR and ESR in Biological Systems*, John Wiley & Sons, London, 1976.
28. **Lauterbur, P.C.,** *Nature*, 242, 190 (1973).
29. **Abragam, A.,** *The Principles of Nuclear Magnetism*, Oxford University Press, London, 1961.
30. **Farrar, T. C. and Becker, E. D.,** *Pulse and Fourier Transform NMR: Introduction to Theory and Methods*, Academic Press, New York, 1971.
31. **Shaw, D.,** *Fourier Transform N.M.R. Spectroscopy*, Elsevier, Amsterdam, 1976.
32. **Dwek, R. A.,** *Nuclear Magnetic Resonance in Biochemistry: Application to Enzyme Systems*, Clarendon Press, Oxford, 1973.

Downloaded At: 15:58 17 January 2011

33. **James, T. L.,** *Nuclear Magnetic Resonance in Biochemistry: Principles and Applications,* Academic Press, New York, 1975.
34. **Noggle, J. H. and Schirmer, R. E.,** *The Nuclear Overhauser Effect: Chemical Applications,* Academic Press, New York, 1971.
35. **Pauli, W.,** *Naturwiss,* 12, 741 (1924).
36. **Carver, J. P. and Richards, R. E.,** *J. Mag. Res.,* 6, 89 (1972).
37. **Stejskal, E. O. and Schaeffer, J.,** *J. Mag. Res.,* 14, 160 (1974).
38. **Kuchel, P. W., Roberts, D. V., and Nichol, L. W.,** *Aust. J. Exp. Biol. Med. Sci.,* 55, 309 (1977).
39. **Achs, M. J. and Garfinkel, D.,** *Am. J. Physiol.,* 236, R21 (1979).
40. **Kohn, M. C., Achs, M. J., and Garfinkel, D.,** *Am. J. Physiol.,* 237, R153 (1979).
41. **Paganelli, C. V. and Solomon, A. K.,** *J. Gen. Physiol. London,* 41, 259 (1957).
42. **Viera, F. L., Sha'afi, R. I., and Solomon, A. K.,** *J. Gen. Physiol. London,* 55, 451 (1970).
43. **Hahn, E. L.,** *Phys. Rev.,* 80, 580 (1950).
44. **Carr, H. Y. and Purcell, E. M.,** *Phys. Rev.,* 94, 630 (1954).
45. **Singer, J. R.,** *J. Phys. E. Sci. Instrum.,* 11, 281 (1978).
46. **Rabenstein, D. L.,** *Anal. Chem.,* 50, 1265 (1978).
47. **Rabenstein, D. L. and Nakashima, T. T.,** *Anal. Chem.,* 51, 1465A (1979).
48. **Brindle, K. M., Brown, F. F., Campbell, I. D., Grathwohl, C., and Kuchel, P. W.,** *Biochem. J.,* 180, 37 (1979).
49. **Stejskal, E. O. and Tanner, J. E.,** *J. Chem. Phys.,* 42, 288 (1965).
50. **Reeves, L. W.,** in *Dynamic Nuclear Magnetic Resonance Spectroscopy,* Jackman, L. M. and Cotton, F. A., Eds., Academic Press, New York, 1975, 83.
51. **Freeman, R. and Hill, H. D. W.,** in *Dynamic Nuclear Magnetic Resonance Spectroscopy,* Jackman, L. M. and Cotton, F. A., Eds., Academic Press, New York, 1975, 131.
52. **Packer, K. J., Rees, C., and Tomlinson, D. J.,** *Mol. Phys.,* 18, 421 (1970).
53. **Tanner, J. E. and Stejskal, E. O.,** *J. Chem. Phys.,* 49, 1768 (1968).
54. **Neuman, C. H.,** *J. Chem. Phys.,* 60, 4508 (1974).
55. **Tanner, J. E.,** *J. Chem. Phys.,* 69, 1748 (1978).
56. **Kärger, V. J.,** *Ann. Phys.,* 24, 1 (1969).
57. **Kärger, V. J.,** *Ann. Phys.,* 27, 107 (1971).
58. **Stejskal, E. O.,** *J. Chem. Phys.,* 43, 3597 (1965).
59. **Robertson, B.,** *Phys. Rev.,* 151, 273 (1966).
60. **Callaghan, P. T., Jolley, K. W., and Lelievre, J.,** *Biophys. J.,* 28, 133 (1979).
61. **Andrasko, J.,** *Biochim. Biophys. Acta,* 428, 304 (1976).
62. **Tanner, J. E.,** *Biophys. J.,* 28, 107 (1979).
63. **Webster, D. S.,** A Study of Self-Diffusion in Some Biological Systems Using Pulsed Magnetic Field Gradient NMR Techniques, Ph.D. thesis, University of New South Wales, 1971.
64. **Bunch, W. H. and Kallsen, G.,** *Science,* 164, 1178 (1969).
65. **Andrasko, J.,** *J. Mag. Res.,* 21, 479 (1976).
66. **Jones, A. J. and Kuchel, P. W.,** *Clin. Chim. Acta,* 104, 77, (1980).

66a. **Kuchel, P. W. and Jones, A. J.,** Unpublished data.

67. **Jones, D. W. and Child, T. F.,** in *Advances in Magnetic Research,* Waugh, J. S., Ed., Academic Press, New York, 1976, 123.
68. **Packer, K. J.,** *Mol. Phys.,* 17, 355 (1969).
69. **Grover, T. and Singer, J. R.,** *J. Appl. Phys.,* 42, 938 (1971).
70. **Cooke, R. and Kuntz, I. D.,** *Ann. Rev. Biophys. Bioeng.,* 3, 95 (1974).
71. **Chambers, V. M. A., Evans, E. A., Elvidge, J. A., and Jones, J. R.,** *Tritium Nuclear Magnetic Resonance (TNMR) Spectroscopy,* Review 19, The Radiochemical Centre, Amersham, U.K., 1977.
72. **Eisenberg, D. and Kauzmann, W.,** *The Structure of Water,* Clarendon Press, Oxford, 1969.
73. **Bloembergen, N., Purcell, E. M., and Pound, R. V.,** *Phys. Rev.,* 73, 679 (1948).
74. **Belton, P. S., Packer, K. J., and Sellwood, T. C.,** *Biochim. Biophys. Acta,* 304, 56 (1973).
75. **Knispel, R. R., Thompson, R. T., and Pintar, M. M.,** *J. Mag. Res.,* 14, 44 (1974).
76. **Fung, B. M., Durham, D. L., and Wassil, D. A.,** *Biochim. Biophys. Acta,* 399, 191 (1975).
77. **Glasel, J. A.,** *Proc. Natl. Acad. Sci. U.S.A.,* 58, 27 (1967).
78. **Fung, B. M.,** *Biophys. J.,* 18, 235 (1977).
79. **Hazlewood, C. F., Chang, D. C., Nichols, B. L., and Woessner, D. E.,** *Biophys. J.,* 14, 583 (1974).
80. **Belton, P. S., Jackson, R. R., and Packer, K. J.,** *Biochim. Biophys. Acta,* 286, 16 (1972).
81. **Packer, K. J.,** *J. Mag. Res.,* 9, 438 (1973).
82. **Cope, F. W.,** *Biophys. J.,* 9, 303 (1969).
83. **Outhred, R. K. and George, E. P.,** *Biophys. J.,* 13, 83 (1973).
84. **Outhred, R. K. and George, E. P.,** *Biophys. J.,* 13, 97 (1973).

Downloaded At: 15:58 17 January 2011

85. Fung, B. M., *Biophys. J.*, 18, 235 (1977).
86. Koenig, S. H., Hallenga, K., and Shporer, M., *Proc. Natl. Acad. Sci. U.S.A.*, 72, 2667 (1975).
87. Hallenga, K. and Koenig, S., *Biochemistry*, 15, 4255 (1976).
88. Fung, B. M., *Science*, 190, 800 (1975).
89. Damadian, R., *Science*, 171, 1151 (1971).
90. Hazlewood, F., Nichols, B. L., Chang, D. C., and Brown, B., *Johns Hopkins Med. J.*, 128, 117 (1971).
91. Chang, D. C., Hazlewood, C. F., Nichols, B. F., and Rorscharch, H. E., *Nature*, 235, 170 (1972).
92. Hazlewood, C. F., Chang, D. C., Medina, D., Cleveland, G., and Nichols, B. L., *Proc. Natl. Acad. Sci. U.S.A.*, 69, 1478 (1972).
93. Damadian, R., Zaner, K., Hor, D., DiMaio, T., Minkoff, L., and Goldsmith, M., *Ann. N.Y. Acad. Sci.*, 222, 1048 (1973).
94. Grosch, L. and Noack, F., *Biochim. Biophys. Acta*, 453, 218 (1976).
95. Eisenstadt, M. and Fabry, M. E., *J. Mag. Res.*, 29, 591 (1978).
96. Kalk, A. and Berendsen, H. J. C., *J. Mag. Res.*, 24, 343 (1976).
97. Murayama, M. M., *J. Biol. Chem.*, 228, 231 (1957).
98. Cottam, G. L., Valentine, K. M., Yamaoka, K., and Waterman, M. R., *Arch. Biochem. Biophys.*, 162, 487 (1974).
99. Zipp, A., James, T. L., Kuntz, I. D., and Shohet, S. B., *Biochim. Biophys. Acta*, 428, 291 (1976).
100. Zipp, A., Kuntz, I. D., Rehfeld, S., and Shohet, S. B., *FEBS Lett.*, 43, 9 (1974).
101. Thompson, B. C., Waterman, M. R., and Cottam, G. L., *Arch. Biochem. Biophys.*, 166, 193 (1975).
102. Chuang, A. H., Waterman, M. R., Yamoaka, K., and Cottam, G. L., *Arch. Biochem. Biophys.* 167, 145 (1975).
103. Damadian, R., Zaner, K., Hor, D., and DiMaio, T., *Proc. Natl. Acad. Sci. U.S.A.*, 71, 1471 (1974).
104. Frey, H. E., Knispel, R. R., Kruuv, J., Sharp, A. R., Thompson, R. T., and Pintar, M. M., *J. Natl. Cancer Inst.*, 49, 903 (1972).
105. Inch, W. R., McCredie, J. A., Knispel, R. R., Thompson, R. T., and Pintar, M. M., *J. Natl. Cancer Inst.*, 52, 353 (1974).
106. Hollis, D. P., Saryan, L. A., Eggleston, J. C., and Morris, H. P., *J. Natl. Cancer Inst.*, 54, 1469 (1975).
107. Hazlewood, C. F., Cleveland, G., and Medina, D., *J. Natl. Cancer Inst.*, 52, 1849 (1974).
108. Medina, D., Hazlewood, C. F., Cleveland, G. G., Chang, D. C., Spjut, H. J., and Moyers, R., *J. Natl. Cancer Inst.*, 54, 813 (1975).
109. Beall, P. T., Hazlewood, C. F., and Rao, P. N., *Science*, 192, 904 (1976).
110. Floyd, R. A., Leigh, J. S., Chance, B., and Miko, M., *Cancer Res.*, 34, 89 (1974).
111. Diegel, J. G. and Pintar, M. M., *J. Natl. Cancer Inst.*, 55, 725 (1975).
112. Rabenstein, D. L. and Isab, A. A., *J. Mag. Res.*, 36, 281 (1979).
113. Koutcher, J. A., Goldsmith, M., and Damadian, R., *Cancer*, 41, 174 (1978).
114. Goldsmith, M., Koutcher, J., and Damadian, R., *Cancer*, 183 (1978).
115. Fung, B. M., Wassil, D. A., Durham, D. L., Chestnut, R. W., Durham, N. W., and Berlin, K. D., *Biochim. Biophys. Acta*, 385, 180 (1975).
116. Saryan, L. A., Hollis, D. P., Economou, J. S., and Eggleston, J. C., *J. Natl. Cancer Inst.*, 52, 599 (1974).
117. Eggleston, J. C., Saryan, L. A., and Hollis, D. P., *Cancer Res.*, 35, 1326 (1975).
118. Sinadinović, J., Ratković, S., Krainčonic, M., and Jovanić, M., *Endokrinologie*, 69, 55 (1977).
119. Schara, M., Sentjuric, M., Auersperg, M., and Golough, R., *Br. J. Cancer*, 29, 483 (1974).
120. Swartz, H. M., *J. Mag. Res.*, 29, 393 (1978).
121. Bačic, G., Božović, B., and Ratković, S., *Stud. Biophys.*, 70, 31 (1978).
122. Ratković, S. and Bačic, G., *Stud. Biophys.*, 73, 39 (1978).
123. Valensin, G., Gaggelli, E., Tiezzi, E., Valensin, P. E., and Bianchi Bardinelli, M. L., *Biophys. Chem.*, 10, 143 (1979).
124. Johnson, R. G. and Scarpa, A., *J. Biol. Chem.*, 251, 2189 (1976).
125. Nichols, J. W. and Deamer, D. W., *Biochim. Biophys. Acta*, 455, 269 (1976).
126. Cramer, J. A. and Prestegard, J. H., *Biochem. Biophys. Res. Commun.*, 75, 295 (1977).
127. Prestgard, J. H., Cramer, J. A., and Viscico, D. B., *Biophys. J.*, 26, 575 (1979).
128. Degani, H., *Biochim. Biophys. Acta*, 509, 364 (1978).
129. Hunt, G. R. A., *FEBS Lett.*, 58, 194 (1975).
130. Gent, M. P. N. and Prestegard, J. H., *Biochemistry*, 13, 4027 (1974).
131. Kostelnik, R. J. and Castanello, S. M., *J. Mag. Res.*, 9, 291 (1973).
132. Forster, R. E., *Curr. Top. Membr. Transp.*, 21, 41 (1971).
133. Conlon, T. and Outhred, R., *Biochim. Biophys. Acta*, 288, 354 (1972).
134. Fabry, M. E. and Eisenstadt, M., *J. Membr. Biol.*, 42, 375 (1978).
135. Pirkle, J. L., Ashley, D. L., and Goldstein, J. H., *Biophys. J.*, 25, 389 (1979).

Downloaded At: 15:58 17 January 2011

136. **Fabry, M. E. and Eisenstadt, M.,** *Biophys. J.,* 15, 1101 (1975).
137. **Mildvan, A. S. and Cohn, M.,** *Biochemistry,* 2, 910 (1963).
138. **Chein, D. Y. and Macey, R. I.,** *Biochim. Biophys. Acta,* 464, 45 (1977).
139. **Benga, G. and Morariu, V. V.,** *Nature,* 265, 636 (1977).
140. **Morariu, V. V. and Benga, G.,** *Biochim. Biophys. Acta,* 469, 301 (1977).
141. **McConnell, H. M.,** *J. Chem. Phys.,* 28, 430 (1958).
142. **Woessner, D. E.,** *J. Chem. Phys.,* 35, 41 (1961).
143. **Glasel, J. A. and Lee, K. H.,** *J. Am. Chem. Soc.,* 96, 970 (1974).
144. **Mann, S., Skarnulis, A. J., and Williams, R. J. P.,** *J.C.S. Chem. Comm.,* 825, 1067 (1979).
145. **Daniels, A. J., Krebs, J., Levine, B. A., Wright, P. E., and Williams, R. J. P.,** in *NMR in Biology,* Dwek, R. A., Campbell, I. D., Richards, R. E., and Williams, R. J. P., Eds., Academic Press, New York, 1977, 277.
146. **Brown, F. F., Campbell, I. D., Kuchel, P. W., and Rabenstein, D. L.,** *FEBS Lett.,* 82, 12 (1977).
146a. **Brown, F. F., Campbell, I. D., Emerson, P. M., and Kuchel, P. W.,** unpublished data.
147. **Brown, F. F. and Campbell, I. D.,** *Proc. R. Soc. London B,* 289, 395 (1980).
148. **Campbell, I. D., Dobson, C. M., Jeminet, G., and Williams, R. J. P.,** *FEBS Lett.,* 49, 115 (1974).
149. **Dawson, J., Gadian, D. G., and Wilkie, D. R.,** *J. Physiol. (London),* 267, 703 (1977).
150. **Friedmann, H. and Rapoport, S. M.,** in *Cellular and Molecular Biology of Erythrocytes,* Yoshikawa, H. and Rapoport, S. M., Eds., Urban & Schwarzenberg, München, 1974, 181.
151. **Brewer, G. J.,** in *The Red Blood Cell,* Vol. 1, Surgenor, D. M., Ed., Academic Press, New York, 1974.
152. **Valentine, W. N.,** *Blood,* 54, 549 (1979).
153. **Valentine, W. N. and Tanaka, K. R.,** in *The Metabolic Basis of Inherited Disease,* Stanbury, J. B., Wyngaarden, J. B., and Fredrickson, D. S., Eds., McGraw-Hill, New York, 1978, 1410.
154. **Rapoport, T. A., Heinrich, R., and Rapoport, S. M.,** *Biochem. J.,* 154, 449 (1976).
155. **Heinrich, R., Rapoport, S. M., and Rapoport, T. A.,** *Prog. Biophys. Mol. Biol.,* 32, 1 (1977).
156. **Rapoport, T. A. and Heinrich, R.,** *Biosystems,* 7, 120 (1975).
157. **Heinrich, R. and Rapoport, T. A.,** *Biosystems,* 7, 130 (1975).
158. **Isab, A. A. and Rabenstein, D. L.,** *FEBS Lett.,* 106, 325 (1979).
159. **Brown, F. F., Halsey, M. J., and Richards, R. E.,** *Proc. R. Soc. London B,* 193, 387 (1976).
160. **Beutler, E. and Guinto, E.,** *Blood,* 41, 559 (1973).
161. **Bartlett, G. R.,** in *The Human Red Cell in Vitro,* Greenwalt, T. J. and Jamieson, G. A., Eds., Grune & Stratton, New York, 1974, 5.
162. **Daniels, A., Williams, R. J. P., and Wright, P. E.,** *Nature,* 261, 321 (1977).
163. **Ogino, T., Arata, Y., Fujiwara, S., Shoun, H., and Beppu, T.,** *J. Mag. Res.,* 31, 523 (1978).
164. **Dadok, J. and Sprecher, R. F.,** *J. Mag. Res.,* 13, 243 (1974).
165. **Gupta, R. K., Ferretti, J. A., and Becker, E.,** *J. Mag. Res.,* 13, 275 (1974).
166. **Richards, R. E.,** *Endeavour,* XXXIV, 118 (1975).
167. **Burt, C. T., Glonek, T., and Bárány, M.,** *Science,* 19, 145 (1977).
168. **Shulman, R. G., Brown, T. R., Ugurbil, K., Ogawa, S., Cohen, S. M., and Den Hollander, J. A.,** *Science,* 205, 160 (1979).
169. **Ugurbil, K., Shulman, R. G., Brown, T. R.,** in *Biological Applications of Magnetic Resonance,* Shulman, R. G., Ed., Academic Press, New York, 1979, 537.
170. **Hoult, D. I., Busby, S. J. W., Gadian, D. G., Radda, G. K., Richards, R. E., and Seeley, P. J.,** *Nature,* 252, 285 (1974).
171. **Bárány, M., Bárány, K., Burt, C. T., Glonek, T., and Myers, T. C.,** *J. Supramol. Struct.* 3, 125 (1975).
172. **Seeley, P. J., Busby, S. J. W., Gadian, D. G., Radda, G. K., and Richards, R. E.,** *Biochem. Soc. Trans.,* 4, 63 (1976).
173. **Burt, C. T., Glonek, T., and Bárány, M.,** *J. Biol. Chem.,* 251, 2584 (1976).
174. **Burt, C. T., Glonek, T., and Bárány, M.,** *Biochemistry,* 15, 4850 (1976).
175. **Busby, S. J. W., Gadian, D. G., Radda, G. K., Richards, R. E., and Seeley, P. J.,** *Biochem. J.,* 170, 103 (1978).
176. **Dietrich, M. M. and Keller, R. E.,** *Anal. Chem.,* 170, 103 (1978).
177. **Von Wazer, J. R. and Glonek, T.,** in *Analytical Chemistry of Phosphorus Compounds,* Halman, M., Ed., Interscience, New York, 1972, 151.
178. **Glonek, K. and Von Wazer, J. R.,** *J. Mag. Res.,* 13, 390 (1974).
179. **Labotka, R. J., Glonek, T., Hruby, M. A., and Honig, G. R.,** *Biochem. Med.,* 15, 311 (1976).
180. **Glonek, T., Lunde, M., Mudgett, M., and Myers, T. C.,** *Arch. Biochem. Biophys.,* 142, 508 (1971).
181. **Ugurbil, K., Rottenberg, H., Glynn, P., and Shulman, R. G.,** *Proc. Natl. Acad. Sci. U.S.A.,* 75, 2244 (1978).

Downloaded At: 15:58 17 January 2011

182. **Salhany, J. M., Yamane, T., Shulman, R. G., and Ogawa, S.,** *Proc. Natl. Acad. Sci. U.S.A.,* 72, 4966 (1975).
183. **Seeley, P. J., Sehr, P. A., Gadian, D. G., Garlick, P. B., and Radda, G. K.,** in *NMR in Biology,* Dwek, R. A., Campbell, I. D., Richards, R. E., and Williams, R. J. P., Eds., Academic Press, New York, 1977, 247.
184. **Casey, R. P., Njus, D., Radda, G. K., and Sehr, P. A.,** *Biochemistry,* 16, 972 (1977).
185. **Roos, A.,** *J. Physiol. (London),* 249, 1 (1975).
186. **Aichin, C. C. and Thomas, R. C.,** *J. Physiol. (London),* 267, 791 (1976).
187. **Ogawa, S., Rottenberg, H., Brown, T. R., Shulman, R. G., Castillo, C. L., and Glynn, P.,** *Proc. Natl. Acad. Sci. U.S.A.,* 75, 1796 (1978).
188. **Beutler, E.,** *Red Cell Metabolism. A Manual of Biochemical Methods,* 2nd ed., Grune & Stratton, New York, 1975.
189. **Henderson, T. O., Costello, A. J. R., and Omachi, A.,** *Proc. Natl. Acad. Sci. U.S.A.,* 71, 2487 (1974).
190. **Lam, Y.-F., Lin, A. K.-L. C., and Ho, C.,** *Blood,* 54, 196 (1979).
191. **Duhm, J.,** *Biochim. Biophys. Acta,* 343, 89 (1974).
192. **Kagimoto, T., Hayashi, F., Yamasaki, M., Morino, Y., Akasaka, K., and Kishimoto, S.,** *Experientia,* 34, 1092 (1978).
193. **Rapoport, I., Berger, H., Elsner, R., and Rapoport, S.,** *Eur. J. Biochem.,* 73, 421 (1977).
194. **Benesch, R. and Benesch, R. E.,** *Biochem. Biophys. Res. Commun.,* 26, 162 (1967).
195. **Chanutin, A. and Curnish, R. R.,** *Arch. Biochem. Biophys.,* 121, 96 (1967).
196. **Gupta, R. K., Benovic, J. L., and Rose, Z. B.,** *J. Biol. Chem.,* 253, 6172 (1978).
197. **Ugurbil, K., Holmsen, H., and Shulman, R. G.,** *Proc. Natl. Acad. Sci. U.S.A.,* 76, 2227 (1979).
198. **Salhany, J. M., Yamane, T., Shulman, R. G., and Ogawa, S.,** *Proc. Natl. Acad. Sci. U.S.A.,* 72, 4966 (1975).
199. **Brown, T. R., Ugurbil, K., and Shulman, R. G.,** *Proc. Natl. Acad. Sci. U.S.A.,* 74, 5551 (1977).
200. **Ogawa, S., Schulman, R. G., Glynn, P., Yamane, T., and Navon, G.,** *Biochim. Biophys. Acta,* 502, 45 (1978).
201. **McConnell, H. M. and Thompson, D. D.,** *J. Chem. Phys.,* 26, 958 (1957).
202. **Gupta, R. K. and Redfield, A. G.,** *Science,* 169, 1204 (1970).
203. **Glickson, J. D., Dadok, J., and Marshall, G. R.,** *Biochemistry,* 13, 11 (1974).
204. **Navon, G., Ogawa, S., Shulman, R. G., and Yamane, T.,** *Proc. Natl. Acad. Sci. U.S.A.,* 74, 888 (1977).
205. **Colman, A. and Gadian, D. G.,** *Eur. J. Biochem.,* 61, 387 (1976).
206. **Navon, G., Ogawa, S., Schulman, R. G., and Yamane, T.,** *Proc. Natl. Acad. Sci. U.S.A.,* 74, 87 (1977).
207. **Evans, F. E.,** *Arch. Biochem. Biophys.,* 193, 63 (1979).
208. **Navon, G., Navon, R., Shulman, R. G., and Yamane, T.,** *Proc. Natl. Acad. Sci. U.S.A.,* 75, 891 (1978).
209. **Newsholme, F. A. and Start, C.,** *Regulation in Metabolism,* John Wiley & Sons, New York, 1973.
210. **Schneider, W. C. and Klug, H. W.,** *Cancer Res.,* 6, 691 (1946).
211. **Zaner, K. S. and Damadian, R.,** *Science,* 189, 729 (1975).
212. **Chance, B., Nakase, Y., Bond, M., Leigh, J. S., and McDonald, G.,** *Proc. Natl. Acad. Sci. U.S.A.,* 75, 4925 (1978).
213. **Cohen, S. M., Ogawa, S., Rottenberg, H., Yamane, T., Brown, T. R., and Shulman, R. G.,** *Nature,* 273, 554 (1978).
214. **Radda, G. K.,** *Trans. R. Soc. London,* 272, 159 (1975).
215. **Glonek, T. and Marotta, S. F.,** *Horm. Metab. Res.,* 10, 420 (1978).
216. **Azzi, A.,** *Biochem. Biophys. Res. Commun.,* 37, 254 (1969).
217. **Dawson, M. J., Gadian, D., and Wilkie, D. R.,** *NMR in Biology,* Dwek, R. A., Campbell, I. D., Richards, R. E., and Williams, R. J. P., Eds., Academic Press, New York, 1977, 289.
218. **Chalovich, J. M., Burt, C. T., Danon, M. J., Glonek, T., and Bárány, M.,** *Ann. N.Y. Acad. Sci.,* 317, 649 (1979).
219. **Bárány, M., Burt, C. T., Labotka, R. J., Danon, M. J., Glonek, T., and Huncke, B. H.,** in *Pathogenesis of Human Muscular Dystrophies,* Rowland, L. P., Ed., Excerpta Medica, Amsterdam, 1977, 337.
220. **Gadian, D. G., Hoult, D. I., Radda, G. K., Seeley, P. J., Chance, B., and Barlow, C.,** *Proc. Natl. Acad. Sci. U.S.A.,* 73, 4446 (1976).
221. **Garlick, P. B. Radda, G. K., Seeley, P. J., and Chance, B.,** *Biochem. Biophys. Res. Commun.,* 74, 1256 (1977).
222. **Jacobus, W. E., Taylor, G. J., Hollis, D. P., and Nunally, R. L.,** *Nature,* 265, 756 (1977).
223. **Hollis, D. P., Nunnally, R. L., Jacobus, W. E., and Taylor, G. J.,** *Biochem. Biophys. Res. Commun.,* 75, 1086 (1977).
224. **Salhany, J. M., Pieper, G. M., Wu, S., Todd, G. L., Clayton, F. C., and Eliot, R. S.,** *J. Mol. Cell. Cardiol.,* 11, 601 (1979).

Downloaded At: 15:58 17 January 2011

225. Sehr, P. A., Radda, G. K., Bore, P. J., and Sells, R. A., *Biochem. Biophys. Res. Commun.*, 77, 195 (1977).
226. Doddrell, D., Glushko, V., and Allerhand, A., *J. Chem. Phys.*, 56, 3683 (1972).
227. Lauterbur, P. C., *Appl. Spectrosc.*, 24, 450 (1970).
228. Allerhand, A., Cochran, D. W., and Doddrell, D., *Proc. Natl. Acad. Sci. U.S.A.*, 67, 1093 (1970).
229. Buddenbaum, W. E. and Shiner, V. J., Computation of isotope effects on equilibria and rates, in *Isotope Effects on Enzyme-Catalysed Reactions*, Cleland, W. W., O'Leary, M. H., and Northrop, D. B., Eds., University Park Press, Baltimore, 1976, 1.
230. Matwiyoff, N. A. and Ott, D. G., *Science*, 181, 1125 (1973).
231. Sequin, U. and Scott, A. I., *Science*, 186, 101 (1974).
232. London, R. E., Gregg, C. T., and Matwiyoff, N. A., Science, 188, 266 (1975).
233. Serianni, A. S., Pierce, J., and Barker, R., *Biochemistry*, 18, 1192 (1979).
234. Allerhand, A., in *Methods in Enzymology Enzyme Structure, Part H*, Vol. 61, Hirs, C. H. W. and Timasheff, S. N., Eds., Academic Press, New York, 1979, chap. 19.
235. Matwiyoff, N. A. and Neadham, T. E., *Biochem. Biophys. Res. Commun.*, 49, 1158 (1972).
236. Moon, R. B. and Richards, J. H., *J. Am. Chem. Soc.*, 94, 5093 (1972).
237. Barnikol, W. K. R. and Burkhard, O., *J. Physiol. (London)*, 284, 139P (1978).
238. Cerami, A. and Peterson, C. M., *Sci. Am.*, 232, 44 (1975).
239. Yeagle, P. L. and Martin, B. M., *Biochem. Biophys. Res. Commun.*, 69, 775 (1976).
240. Kitamura, K., Kishino, T., and Hozumi, K., *Chem. Pharm. Bull.*, 27, 1264 (1979).
241. Eakin, R. T., Morgan, L. O., Gregg, C. T., and Matwiyoff, N. A., *FEBS Lett.*, 28, 259 (1972).
242. Kainosho, M., Ajisaka, K., and Nakazawa, H., *FEBS Lett.*, 80, 385 (1977).
243. Schaefer, J., Stejskal, E. O., and Beard, C. F., *Plant Physiol.*, 55, 1048 (1975).
244. Ugurbil, K., Brown, T. R., Den Hollander, J. A., Glynn, P., and Shulman, R. G., *Proc. Natl. Acad. Sci. U.S.A.*, 75, 3742, (1978).
245. Cohen, S. M., Ogawa, S., and Shulman, R. G., *Proc. Natl. Acad. Sci. U.S.A.*, 76, 1603 (1979).
246. Lee, Y. P., Takamari, A. E., and Lardy, H., *J. Biol. Chem.*, 234, 3051 (1959).
247. Cohen, S. M., Shulman, R. G., and McLaughlin, A. C., *Proc. Natl. Acad. Sci. U.S.A.*, 76, 4808 (1979).
248. Fung, B. M., *Biophys. J.*, 19, 315 (1977).
249. London, R. E., Hildebrand, C. E., Olson, E. S., and Matwiyoff, N. A., *Biochemistry*, 15, 5480 (1976).
250. Williams, E., Hamilton, J. A., Jain, M. K., Allerhand, A., and Cordes, E. H., *Science*, 181, 869 (1973).
251. Stoffel, W. and Bister, K., *Biochemistry*, 14, 2841 (1975).
252. Stoffel, W., Bister, K., Schreiber, C., and Tunggal, B., *Hoppe-Seylers' Z. Physiol. Chem.*, 357, 905 (1976).
253. Schaefer, J. and Stejskal, E. O., *J. Am. Chem. Soc.*, 98, 1031 (1976).
254. Pines, A., Gibby, M. G., and Waugh, J. S., *J. Chem. Phys.*, 59, 569 (1973).
255. Andrew, E. R., *Prog. Nucl. Mag. Res. Spectrosc.*, 8, 1 (1971).
256. Diehl, P., in *Nuclear Magnetic Resonance of Nuclei Other Than Protons*, Axenrod, T. and Webb, G. A., Eds., John Wiley & Sons, New York, 1974, chap. 18.
257. Smith, I. C. P., Saito, H., and Schreier-Muccillo, S., *Varian Appl. Note*, NMR-73-2, 1 (1973).
258. Montsch, H. H., Saito, H., and Smith, I. C. P., *Prog. Nucl. Mag. Res. Spect.*, 11, 211 (1977).
259. Stockton, G. W., Polnaszek, D. F., Tulloch, A. P., Hasan, F., and Smith, I. C. P., *Biochemistry*, 15, 954 (1976).
260. Stockton, G. W., Polnaszek, C. F., Leitch, L. C., Tulloch, A. P., and Smith, I. C. P., *Biochem. Biophys. Res. Commun.*, 60, 844 (1974).
261. Davis, J. H., *Biophys. J.*, 27, 339 (1979).
262. Saito, H., Schreier-Muccillo, S., and Smith, I. C. P., *FEBS Lett.*, 33, 281 (1973).
263. Oldfield, E., Chapman, D., and Derbyshire, W., *Chem. Phys. Lipids*, 9, 68 (1975).
264. Stockton, G. W., Johnson, K. G., Butler, K. W., Polnaszek, C. F., Cyr, R., and Smith, I. C. P., *Biochim. Biophys. Acta*, 401, 535 (1975).
265. Oldfield, E., Meadows, M., and Glaser, M., *J. Biol. Chem.*, 251, 6147 (1976).
266. Arvidson, G., Lindblom, G., and Drakenberg, T., *FEBS Lett.*, 54, 249 (1975).
267. Matthews, H. R., Matthews, K. S., and Opella, S. J., *Biochim. Biophys. Acta*, 497, 1 (1977).
268. Oster, O., Neireiter, G. W., Clause, A. O., and Gurd, F. R. N., *J. Biol. Chem.*, 250, 7990 (1975).
269. Wooten, J. B. and Cohen, J. S., *Biochemistry*, 18, 4188 (1979).
270. Sato, Y., Oda, T., Miyata, E., and Saito, H., *FEBS Lett.*, 98, 271 (1979).
271. Fung, B. M., Durham, D. L., and Wassil, D. A., *Biochim. Biophys. Acta*, 399, 191 (1975).
272. Civan, M. M. and Shporer, M., *Biophys. J.*, 15, 299 (1975).
273. Fung, B. M., *Biophys. J.*, 18, 253 (1977).
274. Civan, M. M. and Shporer, M., *Biochim. Biophys. Acta*, 343, 399 (1974).
275. Shporer, M., Haas, M., and Civan, M., *Biophys. J.*, 16, 601 (1976).

Downloaded At: 15:58 17 January 2011

276. **Wydrzynski, T. J., Marks, S. B., Schmidt, P. G., Govindjee, and Gutowsky, H. S.,** *Biochemistry,* 17, 2155 (1978).
277. **Shporer, M. and Civan, M.,** *Biochim. Biophys. Acta,* 385, 81 (1975).
278. **Tricot, Y. and Niederberger, W.,** *Biophys. Chem.,* 9, 195 (1979).
279. **Gust, D., Moon, R. B., and Roberts, J. D.,** *Proc. Natl. Acad. Sci. U.S.A.,* 72, 4696 (1975).
280. **Lapidot, A. and Irving, C. S.,** *J. Am. Chem. Soc.,* 99, 5488 (1977).
281. **Lapidot, A. and Irving, C. S.,** *Proc. Natl. Acad. Sci. U.S.A.,* 74, 1988 (1977).
282. **Witanowski, M., Stefaniak, L., and Januszewski, H.,** in *Nitrogen NMR,* Witanowski, M. and Webb, G. A., Eds., Plenum Press, New York, 1973, 163.
283. **Llinas, M., Wurthrich, K., Schwatzer, W., and Von Philipsborn, W.,** *Nature,* 257, 817 (1975).
284. **Irving, C. S. and Lapidot, A.,** *Biochim. Biophys. Acta,* 470, 251 (1977).
285. **Morishima, I., Inubushi, T., Neya, S., Ogawa, S., and Yonezawa, T.,** *Biochem. Biophys. Res. Commun.,* 78, 739 (1977).
286. **Morishima, I. and Inubushi, T.,** *Biochem. Biophys. Res. Commun.,* 80, 199 (1978).
287. **Schaefer, J., Stejskal, E. O., and McKay, R. A.,** *Biochem. Biophys. Res. Commun.,* 88, 274 (1979).
288. **Chang, D. C. and Woessner, D. E.,** *J. Mag. Res.,* 30, 185 (1978).
289. **Hubbard, P. S.,** *J. Chem. Phys.,* 53, 985 (1970).
290. **Yeh, H. J. C., Brinley, F. J., and Becker, E. D.,** *Biophys. J.,* 13, 56 (1973).
291. **Roberts, G. C. K., Feeney, J., Birdsall, B., Kimber, B., Griffiths, D. V., King, R. W., and Burgen, A. S. V.,** in *NMR in Biology,* Dwek, R. A., Campbell, I. D., Richards, R. E., and Williams, R. J. P., Eds., Academic Press, New York, 1977, 93.
292. **Rigo, A., Viglino, P., Argese, E., Terenzi, M., and Rotilio, G.,** *J. Biol. Chem.,* 254, 1759 (1979).
293. **Winninger, C., Lestienne, P., Dimicole, J.-L., and Bieth, J. G.,** *Biochim. Biophys. Acta,* 526, 227 (1978).
294. **Costa, J. L., Dobson, C. M., Kirk, K. L., Poulsen, F. M., Valeri, C. R., and Vecchione, J. J.,** *FEBS Lett.,* 99, 141 (1979).
295. **Shami, Y., Carver, J., Ship, S., and Rothstein, A.,** *Biochem. Biophys. Res. Commun.,* 76, 429 (1977).
296. **Norne, J.-E., Chiancone, E., Forsén, S., Antonini, E., and Wyman, J.,** *FEBS Lett.,* 94, 410 (1978).
297. **Ward, R. L. and Whitney, P. L.,** *Biochem. Biophys. Res. Commun.,* 51, 343 (1973).
298. **Elvidge, J. A., Jones, J. R., and Mane, R. B.,** *J. Lab. Comp. Radiopharm.,* 5, 141 (1978).
299. **Lauterbur, P. C.,** in *NMR in Biology,* Dwek, R. A., Campbell, I. D., Richards, R. E., and Williams, R. J. P., Eds., Academic Press, New York, 1977, 323.
300. **Lai, C. -M., House, W. V., and Lauterbur, P. C.,** Paper 2, in Proc. IEEE Electro/78 Conf., Session 30, Technology for Non-Invasive Monitoring of Physiological Phenomena, May 25, 1978.
301. **Andrew, E. R.,** *Phil. Trans. R. Soc. B,* 289, 471 (1980).
302. **Lauterbur, P. C.,** *Phil. Trans. R. Soc. B,* 289, 483 (1980).
303. **Andrew, E. R.,** in *Medical Imaging,* Keel, L., Ed., HM & M Publishers, Aylesbury, U.K., 1979, chap. 7.
304. **Mansfield, P.,** *Contemp. Phys.,* 17, 553 (1976).
305. **Mansfield, P. and Pykett, I. L.,** *J. Mag. Res.,* 29, 355 (1978).
306. **Lauterbur, P. C.,** *IEEE Trans. Nuc. Sci.,* NS-26, 2808 (1979).
307. **Lauterbur, P. C.,** in Proc. 1st Int. Conf. Stable Isotopes Chem., Biol. Med., AEC, CONF-730525, May 9 to 11, 1973.
308. **Barnothy, M. F.,** *Biological Effects of Magnetic Fields,* Plenum Press, New York, 1964.
309. **Andrew, E. R.,** *Phys. Bull.,* 323 (1977).
310. **Bottomley, P. A.,** *J. Mag. Res.,* 36, 121 (1979).
311. **Brunner, P. and Ernst, R. R.,** *J. Mag. Res.,* 33, 83 (1979).
312. **Lauterbur, P. C.,** *Bull. Am. Phys. Soc.,* 18, 86 (1972).
313. **Lauterbur, P. C.,** *Pure Appl. Chem.,* 40, 149 (1974).
314. **Gordon, R., Herman, G. T., and Johnson, S. A.,** *Sci. Am.,* 233, 56 (1975).
315. **Lauterbur, P. C., Kramer, D. M., House, W. V., and Chen, C. N.,** *J. Am. Chem. Soc.,* 97, 6866 (1975).
316. **Kumar, A., Welti, D., and Ernst, R. R.,** *J. Mag. Res.,* 18, 69 (1975).
317. **Hoult, D. I.,** *J. Mag. Res.,* 33, 183 (1979).
318. **Mansfield, P. and Maudsley, A. A.,** *Phys. Med. Biol.,* 21, 847 (1976).
319. **Holland, G. N., Bottomley, P. A., and Hinshaw, W. S.,** *J. Mag. Res.,* 28, 133 (1977).
320. **Bendel, P., Lai, C.-M., and Lauterbur, P. C.,** *J. Mag. Res.,* 38, 343 (1980).
321. **Hoult, D. I.,** *J. Mag. Res.,* 26, 165 (1977).
322. **Garroway, A. N., Grannell, P. K., and Mansfield, P.,** *J. Phys. C: Solid State Phys.,* 7, L457 (1974).
323. **Mansfield, P. and Maudsley, A. A.,** *Br. J. Radiol.,* 50, 188 (1977).
324. **Hinshaw, W. S.,** *J. Appl. Phys.,* 47, 3709 (1976).
325. **Andrew, E. R., Bottomley, P. A., Hinshaw, W. S., Holland, G. N., Moore, W. S., and Simaroj, C.,** *Phys. Med. Biol.,* 22, 971 (1977).

Downloaded At: 15:58 17 January 2011

326. **Damadian, R., Minkoff, L., Goldsmith, M., Stanford, M., and Koutcher, J.,** *Physiol. Chem. Phys.,* 8, 61 (1976).
327. **Damadian, R., Minkoff, L., Goldsmith, M., Stanford, M., and Koutcher, J.,** *Science,* 194, 1430 (1976).
328. **Damadian, R.,** Apparatus and Method for Detecting Cancer in Tissue, U.S. Patent 3,789,832, 1972.
329. **Damadian, R., Goldsmith, M., and Minkoff, L.,** *Physiol. Chem. Phys.,* 9, 97 (1977).
330. **Frank, J. A., Feiler, M. A., House, W. V., Lauterbur, P. C., and Jacobson, M. J.,** *Clin. Res.,* 24, 217A (1976).
331. **Lauterbur, P. C., Frank, J. A., and Jacobson, M. J.,** *Phys. Can.,* 32, 33.9 (1976).
332. **Lauterbur, P. C.,** in *Medical Imaging Techniques,* Preston, K., Taylor, K. J. W., Johnson, S. A., and Ayers, W. R., Eds., Plenum Press, New York, 1979, 209.
333. **Lauterbur, P. C., Dias, M. H. M., and Rudin, A. M.,** in *Frontiers of Biological Energetics,* Vol. 1, Dutton, P. L., Leigh, J. S., and Scarpa, A., Eds., Academic Press, New York, 1978, 752.
334. **Lauterbur, P. C., House, W. V., Simon, H. E., Dias, M. H. M., Jacobson, M. J., Lai, C.-M., and Bendel, P.,** in *Stereodynamics of Molecular Systems,* Sarm, R. H., Ed., Pergamon Press, Elmsford, N.Y., 1979, 453.
335. **Lauterbur, P. C., Lai, C.-M., Frank, J. A., and Dulcey, C. S.,** *Phys. Can.,* 32, 33.11 (1976).
336. **Hinshaw, W. S., Bottomley, P. A., and Holland, G. N.,** *Experientia,* 35, 1268 (1979).
337. **Minkoff, L., Damadian, R., Thomas, T. E., Hu, N., Goldsmith, M., Koutcher, J., and Stanford, M.,** *Physiol. Chem. Phys.,* 9, 101 (1977).
338. **Goldsmith, M., Damadian, R., Stanford, M., and Lipkowitz, M.,** *Physiol. Chem. Phys.,* 9, 105 (1977).

Downloaded At: 15:58 17 January 2011